

**NOVEL REGULATORY MECHANISMS BY WHICH LARGE T ANTIGEN
COORDINATES THE MERKEL CELL POLYOMAVIRUS LIFE CYCLE**

Jason Diaz

A DISSERTATION

in

Cell and Molecular Biology

Presented to the Faculties of the University of Pennsylvania

in

Partial Fulfillment of the Requirements for the

Degree of Doctor of Philosophy

2015

Supervisor of Dissertation

Jianxin You, Ph.D.
Associate Professor of Microbiology

Graduate Group Chairperson

Daniel S. Kessler, PhD.
Associate Professor of Cell and Developmental Biology

Dissertation Committee

Matthew D. Weitzman, Ph.D.
Associate Professor of
Pathology and
Laboratory Medicine

Erle S. Robertson, Ph.D.
Professor of Microbiology

Paul M. Lieberman, Ph.D.
Professor of Microbiology

Nigel W. Fraser, Ph.D.
Professor of Microbiology

**NOVEL REGULATORY MECHANISMS BY WHICH LARGE T ANTIGEN
COORDINATES THE MERKEL CELL POLYOMAVIRUS LIFE CYCLE**

COPYRIGHT

2015

Jason Diaz

This work is licensed under the
Creative Commons Attribution-
NonCommercial-ShareAlike 3.0
License

To view a copy of this license, visit

<http://creativecommons.org/licenses/by-nc-sa/3.0/>

DEDICATION

This work is dedicated to my parents, Teo and Millie Diaz. Both my father and my mother's parents immigrated to the USA in the hopes of providing a brighter future for their own children. The privilege of completing this work and earning my degree was made possible only by the incredible sacrifices given and challenges overcome by my parents and my family. It is an honor to pay tribute to their dedication with the work presented here.

ACKNOWLEDGMENTS

They say “it takes a village to raise a child,” and this is no less true for a graduate trainee. It is impossible for me to thank every single person and organization that made my training possible, but I shall endeavor to at the very least highlight those who bear special recognition. I apologize in advance for any omission and am extremely grateful to all who impacted my time at Penn in any way.

I would first like to thank my advisor and advocate, Jianxin You. As I was one of her first students, my graduate training was very much a team effort as we both learned and adapted to each other’s mentoring and learning styles. Jian not only demanded excellence and hard work, but also recognized my strengths and weaknesses and made sure to encourage me and redirect my focus when necessary. Above all, I value the honest communication we developed over the years, and am continuously humbled by her advocacy.

My thesis committee, comprised of Drs. Matthew Weitzman, Erle Roberston, Paul Lieberman, and Nigel Fraser, was similarly instrumental to my success. Their critique, encouragement and high standards pushed me to be the best I could be, and I would not have completed this work without their guidance.

I owe special thanks to our long-standing collaborator at the NCI, Dr. Chris Buck. Our lab’s work with MCPyV would not be possible if not for the incredibly generous

gifts of reagents, technical expertise and discussions Chris provided. The scientific endeavor is a communal one, more so now than ever before, and collaborations such as these are the life blood of exemplary research.

The Penn Biomedical Graduate Studies program in general, and the Cell and Molecular Biology program specifically, provided an outstanding environment for graduate training. A special thank you goes to the curriculum coordinators for making any and all logistical issues painless. I want to also recognize the amazing outreach and mentoring efforts made by Dr. Bob Doms, chair of the Department of Microbiology through 2012. His charisma and mentorship during the first half of my graduate training were instrumental to my success and happiness as a graduate student. His energy and dedication to students was a major motivation for me to make the decision to come to Penn for my graduate training.

My lab became a second family, and I certainly benefited from a very friendly and supportive working environment. I thank all lab members, past and present, for their hard work and dedication not just to their own success but to others' as well. A special thank you goes to my fellow graduate students Christie Gifford and Sabrina Tsang; they were the first to witness every high and low over the past five and a half years, and were my constant companions on the often tortuous path of graduate work. I could not have asked for more caring, supportive, and ultimately incredibly talented coworkers.

Similarly, if my lab became my family, the second floor of Johnson Pavilion was my

extended family. I am fortunate to have been surrounded by so many fun and supportive students, technicians, post docs and trainees.

The pursuit of science, so often rife with set backs and failure, can at times feel like a slow approach towards madness; I owe my sanity and well-being to an incredibly diverse group of friends who were instrumental in helping me balance the stress and difficulty of graduate training with humor and encouragement. It would be impossible to name them all, but I do wish to highlight a few key individuals who made graduate school a truly enjoyable experience. Sam Minot, Hilary DeBardeleben, and Nate Snyder (along with their respective spouses) were amongst my very first companions at Penn and ignited within me a passion for both board games and cats. Erin Krock made me feel a part of the O’Doherty lab long after I had finished my rotation and was the senior graduate student I would always consult for advice. A special thank-you goes to all the members of the “Wednesday Night” crew, past and present, including: Joe Zinski, Sam Falk, Fred Melhuish, Charlie Mo, Scott Ashley, Alex Klattenhoff, Janelle Spinazzola, Seth Johnson, Vasu Kameswaran, Inny Lekova, Wen Lin, Julie Chen, Lee Dietterich, Celine Santiago, Tina Ho, Amanda Hay, Michael Herriges, Alex Rohacek, and Will Towler. It astounds me that a group of incredibly busy people such as ourselves has been able to maintain this weekly movie/gaming night going for over four years now. I can’t imagine what my Wednesdays will be like when this eventually comes to an end.

Although already highlighted, Sam Falk, Alex Rohacek and Will Towler bear special mentioning as very dear friends who not only bore the brunt of full force of my

especially difficult moments, but also lifted me up when I had fallen, assured me when I was doubtful, and were in all ways integral to my social and mental well-being as a graduate student. They are true companions, and I could not imagine getting through my training without their unyielding love and support.

Finally, I would like to thank my family – my parents Teo and Millie as well as my brothers David and Carlos – who were constant sources of encouragement and support throughout these five and half years. Their presence throughout my time at Penn helped provide the stability required for pursuing the very difficult endeavor of producing new knowledge. As always, I owe any success I might have to them.

ABSTRACT

NOVEL REGULATORY MECHANISMS BY WHICH LARGE T ANTIGEN COORDINATES THE MERKEL CELL POLYOMAVIRUS LIFE CYCLE

Jason Diaz

Dr. Jianxin You

Due to its association with Merkel cell carcinoma (MCC), a substantial effort has been made to better understand how Merkel cell polyomavirus (MCPyV) proteins drive oncogenesis; however, our understanding of the early steps of MCPyV infection remains poor. The polyomavirus Large Tumor antigen (LT) is a highly multi-functional protein with a wide range of activities, including: stimulation of cellular proliferation through its interaction with retinoblastoma protein and DnaJ heatshock protein family members; arrest of the cell cycle through a poorly understood activity localized to the C-terminal region; and regulation of the initiation of viral DNA replication. LT proteins also play important roles in regulating viral transcription. How these various functions are regulated to ensure an orderly progression of events conducive for the viral life cycle has not been well established.

In this study, I show how phosphorylation of MCPyV LT plays an important role in regulating its many functions. I identify threonines 297 and 299 as key phospho-sites which regulate LT's ability to initiate replication. T297 phosphorylation inhibits LT binding to the viral origin of replication and acts as an "off" switch, while phosphorylation of T299 is required to stimulate LT-mediated replication of viral

genomes. This study was the first to identify phosphorylation sites of LT and link them to important protein functions.

Cross-reactivity to a phospho-specific antibody revealed yet another phosphorylation site on MCPyV LT as S816. We discovered that this phosphorylation event is mediated by ATM kinase, and may play a role in the MCPyV LT C-terminal domain's ability to arrest the cell cycle. This study helps to further elucidate MCPyV's association with the host DNA Damage Response (DDR) and provides some rationale for the recruitment of these factors to viral replication centers.

Finally, studies of the viral non-coding control region (NCCR) reveal a surprising interaction between LT and sT on the late promoter. MCPyV LT is able to robustly stimulate the late promoter only in the context of an intact Ori and sT co-expression. Using phosphomutant LTs and mutant Ori sequences, I highlight the importance of LT binding to the Ori and stimulation of replication as key factors in LT-mediated activation of the late promoter in the context of sT co-expression. LT alone actually represses the late promoter and requires sT coexpression to efficiently stimulate the late promoter after replication. This study therefore reveals an important dependence on sT expression for the regulation of transcription that has not yet been reported with other polyomaviruses.

In sum, this study demonstrates multiple mechanisms of regulation including protein phosphorylation, protein-DNA interactions, and co-expression of key viral proteins as regulators of LT function. These studies may help elucidate critical factors required for establishing a robust cellular infection system which is greatly needed to further our understanding of the basic virology of this important human tumor virus.

TABLE OF CONTENTS

| | |
|--|-------------|
| DEDICATION..... | iii |
| ACKNOWLEDGMENTS..... | iv |
| ABSTRACT..... | viii |
| LIST OF TABLES..... | xiii |
| LIST OF FIGURES..... | xiv |
| CHAPTER 1: INTRODUCTION..... | 1 |
| 1.1: Merkel Cell Carcinoma and Merkel Cell Polyomavirus..... | 1 |
| 1.1.1: Merkel Cell Carcinoma..... | 1 |
| 1.1.2: Merkel Cell Polyomavirus and Cancer..... | 2 |
| 1.2: Merkel Cell Polyomavirus Virology..... | 5 |
| 1.2.1: MCPyV Genes and Genome Organization..... | 5 |
| 1.2.2: Large T Antigen..... | 6 |
| 1.2.3: MCPyV Small T Antigen..... | 8 |
| 1.2.4: Additional Early Gene Products..... | 9 |
| 1.2.5: MCPyV Late Genes..... | 10 |
| 1.2.6: Natural Infection of MCPyV..... | 11 |
| 1.3: Polyomavirus Genome Replication..... | 12 |
| 1.3.1: LT-mediated Initiation of Replication..... | 12 |
| 1.3.2: Regulation of Viral Replication..... | 14 |
| 1.3.3: MCPyV Genome Replication..... | 15 |
| 1.4: Regulation of Polyomavirus Transcription..... | 16 |
| 1.4.1: SV40 Gene Regulation..... | 16 |
| 1.4.2: MCPyV Gene Regulation..... | 17 |
| 1.5: Scope of My Work..... | 17 |
| | |
| CHAPTER 2: PHOSPHORYLATION OF LARGE T ANTIGEN REGULATES MERKEL CELL POLYOMAVIRUS REPLICATION..... | 18 |
| 2.1: Chapter Summary..... | 20 |
| 2.2: Introduction..... | 21 |
| 2.3: Results..... | 24 |
| 2.3.1: Mass Spectrometry Identifies T271, T297 and T299 as Phosphorylation Sites on MCPyV LT..... | 24 |
| 2.3.2: MCPyV LT Phosphorylation Affects the Formation of Viral Replication Centers..... | 27 |
| 2.3.3: MCPyV LT Phospho-mutant Proteins Have Altered Replication Capacities..... | 28 |

| | |
|--|-----------|
| 2.3.4: T297A and T299A Phospho-mutant LT Proteins Bind the Viral Ori with Altered Affinity..... | 30 |
| 2.3.5: MCPyV Phospho-mutant LT Proteins Exhibit Similar Unwinding and Helicase Activities..... | 32 |
| 2.4: Discussion..... | 34 |
| 2.5: Figures..... | 40 |
| | |
| CHAPTER 3: PHOSPHORYLATION OF MERKEL CELL POLYOMAVIRUS LARGE T ANTIGEN AT SERINE 816 BY ATM KINASE INDUCES APOPTOSIS IN HOST CELLS..... | 55 |
| 3.1: Chapter Summary..... | 56 |
| 3.2: Introduction..... | 57 |
| 3.3: Results..... | 60 |
| 3.3.1: MCPyV LT is Phosphorylated at S816..... | 60 |
| 3.3.2: Activation of ATM Stimulates MCPyV LT S816 Phosphorylation..... | 62 |
| 3.3.3: Inhibition of ATM Prevents MCPyV LT S816 Phosphorylation..... | 63 |
| 3.3.4: ATM Kinase Binds and Phosphorylates MCPyV LT at S816 <i>In Vitro</i> | 64 |
| 3.3.5: Prevention of MCPyV LT S816 Phosphorylation Partially Rescues the MCPyV LT Growth Inhibition Effect..... | 65 |
| 3.3.6: MCPyV LT S816A Induces Less Apoptosis Than Wild-Type MCPyV LT..... | 67 |
| 3.4: Discussion..... | 69 |
| 3.5: Figures..... | 73 |
| | |
| CHAPTER 4: MERKEL CELL POLYOMAVIRUS LT AND ST COOPERATIVELY REGULATE THE VIRAL LATE PROMOTER..... | 86 |
| 4.1: Chapter Summary..... | 87 |
| 4.2: Introduction..... | 88 |
| 4.3: Results..... | 91 |
| 4.3.1: The MCPyV Late Promoter is Activated by Coexpression of Both LT and sT in the Context of an Intact NCCR | 91 |
| 4.3.2: Increased LT Expression Alone Does Not Account for Activation of the Late Promoter... .. | 93 |
| 4.3.3: Replication of the NCCR Reporter Partially Contributes to Late Promoter Activation..... | 94 |
| 4.3.4: A Phosphomutant LT With a Defective Replication Phenotype Still Robustly Activates the Late Promoter..... | 95 |
| 4.3.5: MCPyV LT Silences the Late Promoter in the Absence of Ori Sequences..... | 97 |
| 4.4: Discussion..... | 98 |

| | |
|--|------------|
| 4.5: Figures..... | 103 |
| | |
| CHAPTER 5: CONCLUSIONS AND FUTURE DIRECTIONS..... | 111 |
| 5.1: Regulation of MCPyV LT Function by Phosphorylation | 111 |
| 5.1.1: Regulation of Protein Function by Phosphorylation..... | 111 |
| 5.1.2: Regulation of MCPyV Replication by Phosphorylation of LT T297 and T299..... | 112 |
| 5.1.3: Phosphorylation of MCPyV LT by ATM Kinase at S816..... | 115 |
| 5.1.4: Uncovering the Function of MCPyV LT T271 Phosphorylation..... | 116 |
| 5.2: Regulation of Viral Transcription..... | 117 |
| 5.3: Current Obstacles in Basic MCPyV Research..... | 118 |
| 5.4: Concluding Remarks | 119 |
| | |
| CHAPTER 6: MATERIALS AND METHODS..... | 120 |
| | |
| REFERENCES..... | 137 |

LIST OF TABLES

| | |
|--|----|
| Table 2.1: Phosphorylated peptides Identified by mass spectrometry..... | 41 |
|--|----|

LIST OF FIGURES

| | |
|--|-----|
| Figure 1.1: Organization of the MCPyV genome..... | 5 |
| Figure 1.2: Organization of polyomavirus origins of replication..... | 12 |
| Figure 2.1: Identification of MCPyV LT phosphorylation sites..... | 42 |
| Figure 2.2: Modeling MCPyV LT's interaction with DNA..... | 44 |
| Figure 2.3: MCPyV LT phospho-mutant proteins form viral replicaiton foci at altered efficiencies..... | 45 |
| Figure 2.4: MCPyV phospho-mutant LT proteins recruit cellular factors to the same degree..... | 47 |
| Figure 2.5: MCPyV LT phospho-mutant proteins replicate plasmids containing the viral Ori to differing degrees..... | 48 |
| Figure 2.6: MCPyV LT phospho-mutants bind the viral Ori with different affinities..... | 50 |
| Figure 2.7: MCPyV LT phospho-mutants have similar unwinding and helicase activities..... | 52 |
| Figure 2.8: Unwinding assay performed with a helicase mutant LT and a mutated Ori probe..... | 54 |
| Figure 3.1: Anti phospho-Chk1 S345 antibody cross-reacts with MCPyV LT..... | 74 |
| Figure 3.2: MCPyV LT is phosphorylated at S816..... | 76 |
| Figure 3.3: ATM kinase phosphorylates MCPyV LT at S816..... | 78 |
| Figure 3.4: ATM can bind and phosphorylate LT <i>in vitro</i> | 80 |
| Figure 3.5: C33A cells stably expressing MCPyV LT S816A form more colonies than cells stably expressing wild-type LT..... | 82 |
| Figure 3.6: MCPyV LT induces more apoptosis than LT S816A..... | 84 |
| Figure 4.1: The MCPyV Non-coding Regulatory Region..... | 104 |

Figure 4.2: MCPyV LT and sT cooperate within the NCCR to activate the late promoter.....105

Figure 4.3: LT protein level alone does not explain late promoter activation.....107

Figure 4.4: An intact origin of replication is required for late promoter activation.....108

Figure 4.5: A MCPyV LT replication-defective mutant can still activate the late promoter.....109

Figure 4.6: MCPyV LT represses the late promoter when the viral origin is absent.....110

CHAPTER 1: INTRODUCTION

1.1: Merkel Cell Carcinoma and Merkel Cell Polyomavirus

1.1.1 Merkel Cell Carcinoma

Merkel cell carcinoma (MCC) was first described in 1971 by Cyril Toker as a trabecular tumor of the dermis (1). MCC is thought to arise from Merkel cells, a unique cell type of the skin, which transmit fine-touch sensation and have characteristics of both epithelial and neurosecretory cells (2). MCC was long regarded to be a rare cancer, with an incidence of around 2 cases per million in 1984, but this rate has tripled over subsequent decades. Old age, immune suppression, and UV exposure are the major risk factors for MCC disease (3,4). Although rare, MCC is a very aggressive cancer, with a mortality rate as high as 30% (5).

Risk of MCC increases dramatically at older ages, and is also increased with immunosuppression (4). These factors led Chang and Moore to investigate whether MCC was associated with an infectious agent. Using Digital Transcriptome Subtraction, they identified a unique transcript expressed at extremely high levels in these tumors, which did not match known human transcripts; sequence analysis showed that it was homologous to the major viral protein of polyomaviruses, the Large Tumor (LT) antigen. Using PCR and sequencing techniques, they were then able to identify a novel polyomavirus clonally integrated within the genomes of the four tumor samples they analyzed. They named this new polyomavirus Merkel cell Polyomavirus (MCPyV) for its association with MCC (6). Subsequent analysis of MCC tumors have shown that

MCPyV sequences can be found in at least 80% of all MCC cases examined, although more recent advances in detection methods has shown an association as high as 97% (7). MCPyV is the first human polyomavirus that has been associated with a human cancer and has generated a lot of interest in the tumor virology field.

1.1.2 Merkel Cell Polyomavirus and Cancer

Polyomavirus associated cancers are generally driven by the expression of LT (8). The N-terminal half of LT can bind to many cellular proteins, including DnaJ family members and pRb, to drive host cell proliferation. The C-terminal half of LT is important for initiating replication from the viral origin, and includes an origin binding domain (OBD) and a helicase domain. Interestingly, LT was found to be expressed in a truncated form in almost every MCPyV-associated MCC tumor analyzed (9). While the truncations were unique to every tumor, they universally deleted the C-terminal half of the protein required for viral replication while retaining the N-terminal half, which could still inhibit key tumor suppressors like pRb. This led Chang and Moore to initially hypothesize that viral replication of the integrated MCPyV genome was antithetical to tumor progression, a theme shared with papillomavirus associated cancers. In support of this hypothesis, they described a unique MCC tumor that retained wild-type expression of LT, but had a mutated origin of replication (Ori350), rendering the integrated sequence replication incompetent (9,10). These observations bear a striking resemblance to papillomavirus associated cancers, where deletion of the major regulatory protein E2 decreases replication from the viral origin and induces overexpression of the viral oncogenes (11,12). Since that initial hypothesis, further study of the C-terminal domain

has also revealed a growth-inhibitory property linked to the activation of a host cell DNA Damage Response (DDR), and it has been hypothesized that this region of LT is therefore negatively selected during oncogenesis (13,14).

Since its discovery in 2008, many reagents and tools have been developed to study MCPyV prevalence. Generation of a monoclonal antibody against MCPyV LT allowed investigators to screen MCC tumors for presence of the viral antigen, while production of viral particles allowed studies of viral infection to be performed in cell culture and provided a capture method for screening human sera for antibodies against MCPyV (15-20). Serological studies indicate that MCPyV seroconversion occurs early in childhood and that most adult individuals harbor antibodies against MCPyV (16,18,19). In agreement with this finding, Rolling Circle Amplification and deep sequencing of DNA obtained from skin tissue gave evidence of chronic shedding of MCPyV in healthy human donors (21,22). These observations suggest that MCPyV establishes an early, persistent, subclinical infection, and that a rare few individuals go on to develop MCPyV related cancer.

Given its early and ubiquitous infection in human skin, it is vital to understand basic MCPyV virology and how viral infection leads to cancer. Extensive study of the prototypical polyomavirus, Simian Virus 40 (SV40) has given the field a strong foundation for understanding MCPyV associated oncogenesis, but this framework has only taken us so far. Many key differences unique to MCPyV have already been described. Phylogenetically, MCPyV is more closely grouped with murine polyoma

virus instead of SV40; this is in contrast to the better described human polyomaviruses JK and BC virus (6,8,23). Additionally, MCPyV LT bears two important differences from its SV40 counterpart. The first is the existence of an N-terminal 200 amino acid stretch of peptide flanking the pRb binding site not found in any other polyomavirus LT; this region has been termed the MCPyV Unique Region (MUR) (24,25). The second major difference is that MCPyV LT does not appear to bind the key tumor suppressor p53 (or binds with extremely low affinity), a finding that challenges conventional understanding of polyomavirus-associated oncogenesis (26). MCPyV sT also appears to act differently than its SV40 homologue: MCPyV sT plays a much more dominant role in tumorigenesis, and interacts with its key cellular target, PP2A phosphatases, in ways distinct from SV40 sT (27). Finally, the non-coding control region (NCCR) of the viral genome, which bisects the circular genome into an early and late region, is organized more similarly to mouse polyomavirus genome architecture than the more extensively studied SV40 NCCR (10,28). Regulation of both gene expression and replication through the NCCR may be different for MCPyV than SV40; indeed, recruitment and assembly of the origin binding domains of MCPyV LT around the viral origin has already been shown to be unique (28). The focus of my work has been to further our understanding of how MCPyV LT's multiple functions are regulated through post-translational modifications. I have also sought to better elucidate how viral transcription from both the early and late promoters is regulated, which will both shed new light on MCPyV persistent infection and might also explain how expression of viral oncogenes during tumorigenesis is regulated.

1.2 Merkel Cell Polyomavirus Virology

1.2.1 MCPyV Genes and Genome Organization

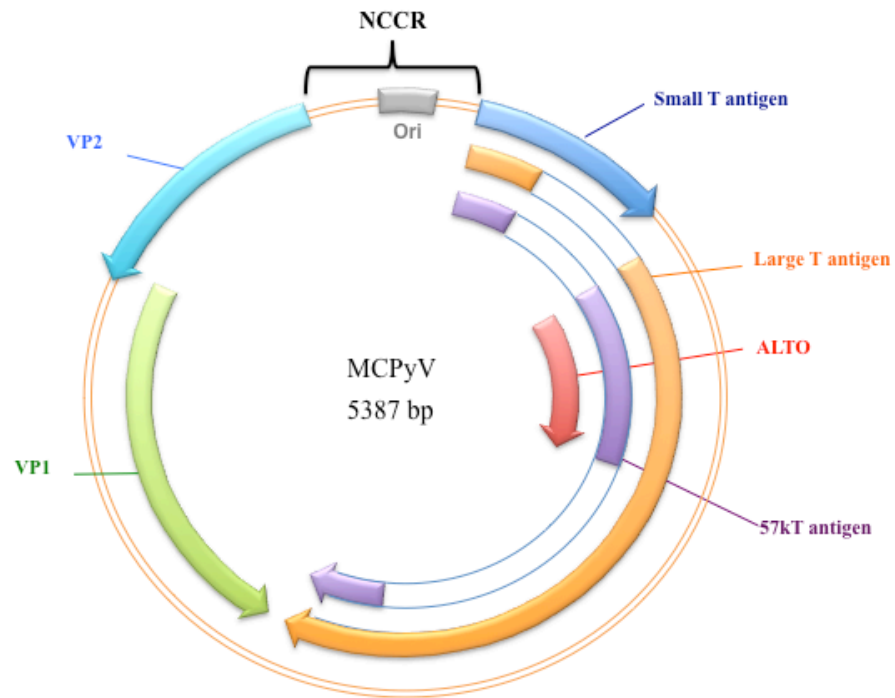


Figure 1.1 Organization of the MCPyV genome. The genome is bisected into two regions by a central non-coding control region (NCCR) which contains the promoters for the early and late genes, as well as the viral Origin of Replication (Ori). The Tumor Antigen is expressed early in infection, and is multiply spliced into many proteins, including Large T antigen (LT), small T antigen (sT), antigen of 57 kDa (57kT), and Alternate frame of the Large T Open reading frame (ALTO). The capsid proteins VP1 and VP2 are expressed following genome replication.

MCPyV is a double-stranded DNA virus with a circular genome of about 5.3kb protected by an icosohedral capsid. The genome is divided into two regions by an NCCR housing the origin of replication (Ori) and promoter sequences (Figure 1.1). The early and late regions flank this NCCR in opposite directions. The Tumor-antigen open reading frame is expressed from the early promoter and multiply spliced into mRNAs expressing four products: Large T antigen (LT), small T antigen (sT), 57kDa T antigen (57kT), and Alternate frame of the Large T Open reading frame (ALTO). These nonstructural genes primarily manipulate the host cell and are also responsible for replication of the viral genome. From the late promoter, two capsid proteins (VP1 and VP2) are expressed which package viral genomes into nascent virions. Of these viral proteins, both MCPyV LT and sT proteins have been found expressed in MCPyV related tumors and have therefore been the most extensively studied thus far (6,8,23).

1.2.2 Large T Antigen

Like other polyomavirus LT proteins, MCPyV LT can bind pRb and DnaJ family members, which drives host cell proliferation; the domains responsible for these functions generally remain intact in virus-associated MCC as well, and are likely a driving force for proliferation of these tumors (9). Classically, polyomavirus LTs bind and inhibit the tumor suppressor p53; the dual inhibition of pRb and p53 is a common feature of oncogenic DNA viruses like papillomaviruses and certain herpesviruses (29). Association of p53 with MCPyV LT has only recently been reported, but this interaction was weak and concluded to be indirect (26); additionally, the p53 binding domains of SV40 LT lie within the helicase domain, which in most MCPyV associated tumors is

deleted from LT due to nonsense mutations in the LT gene (9). MCPyV may be unique among polyomaviruses for lacking a direct interaction with p53; in fact, LT expression may actually activate p53 downstream signaling indirectly through activation of the host DDR (14). Further investigation is required to better understand MCPyV's relationship with this key tumor suppressor.

MCPyV LT encodes a 200 amino acid stretch flanking the LXCXE pRb binding motif which is not found in any other polyomavirus LT. The function of this MUR remains largely unknown. A host protein involved in the fusion of lysosomes, Vam6p, was identified as a LT binding partner in cells which associated with the MUR, but the functional relevance of this interaction in relation to the viral life cycle has not been elucidated (24). Finally, like other polyomaviruses, MCPyV LT is necessary and sufficient for the initiation of replication from the viral Ori in the NCCR (10), which will be reviewed in depth below (1.3) and will be the focus of the work presented in Chapter 2.

In SV40, LT is necessary and sufficient for transforming cells in culture, while sT plays a lesser role in transformation (30,31). In contrast, expression of MCPyV LT alone is not sufficient to transform any cells studied thus far. In fact, expression of wild type LT commonly leads to growth arrest, a feature that has been localized to an activity intrinsic to the C-terminal domain, which is commonly deleted in MCPyV associated tumors (13,14). This growth arresting activity requires wild type p53 activity and a host DNA damage response instigated by the C-terminal portion of LT, and likely explains

why MCPyV LT has poor transformation activity when expressed alone (14). Truncated LT's with this inhibitory activity deleted may still play an important role in tumorigenesis, however, as mouse xenograph transplant experiments have demonstrated a requirement for tumor-derived LT in MCPyV associated MCC tumors (32).

1.2.3 MCPyV Small T Antigen

MCPyV sT has emerged as a key player in MCPyV associated oncogenesis. Early studies of sT confirmed that its expression can transform rat cells, and it is commonly expressed in many MCPyV associated tumors (27,33,34). Like other polyomaviruses, MCPyV sT shares its N-terminal DnaJ domain with LT, while its C-terminal half encodes a PP2A phosphatase binding domain. SV40 sT's contribution to oncogenesis has been linked to its ability to bind and inhibit PP2A phosphatases, thereby preventing the dephosphorylation of Akt, rendering it constitutively active (35-37). MCPyV sT, in contrast, acts further downstream of Akt, and is able to induce hyperphosphorylation of 4E-BP1, thereby releasing eIF4E to stimulate cap-dependent translation, independently of PP2A binding (27). The PP2A binding domain of MCPyV sT is not dispensable, however; this domain allows it to bind the adaptor protein NEMO, possibly in complex with certain PP2A or PP4A subunits, to disrupt host cell inflammatory signaling mediated by NF- κ B (38). Additionally, PP2A binding by MCPyV sT was shown to destabilize microtubules by dysregulating phosphorylation of stathmin, a key microtubule binding protein (39). This destabilization led to increased cell migration and invasion, and may explain why MCC tumors are prone to rapid metastases (39).

MCPyV sT has also been shown to stabilize the expression of MCPyV LT through its inhibition of the E3 ubiquitin ligase SCF^{Fbw7} (40). This stabilization of LT is unique to MCPyV, as other sT proteins generally don't affect the protein levels of their cognate LT proteins. LT-mediated replication of viral origins is greatly enhanced when sT is also expressed, once again highlighting sT's more prominent role in MCPyV (10,40).

1.2.4 Additional Early Gene Products

The other two viral proteins, 57kT and ALTO, are much less understood. 57kT is an alternatively spliced T-antigen of 432 amino acids (9,41). It shares the first 332 amino acids of LT, including the DnaJ and pRb binding sites, the MUR and a nuclear localization signal, but lacks LT's origin binding domain and the majority of the helicase domain. It similarly shares its C-terminal 100 amino acids with LT. Robust expression of 57kT appears to require viral replication but its function remains unknown. It is sometimes compared to SV40's 17kT, a small protein which similarly shares sequences with its cognate LT, and which appears to behave both independently and in concert with other T-antigens to control cellular proliferation (42,43). Given that 57kT retains both tumor suppressor (DnaJ, pRb) binding domains and the C-terminal region of LT shown to inhibit growth, it will be interesting to study this protein's role in cell cycle manipulation and investigate what role(s) it plays during natural infection.

The overprinting gene, ALTO was discovered as a cryptic reading frame within the T-antigen locus that is evolutionarily related to the murine polyomavirus middle T

antigen (44). Its expression can be detected in cells carrying MCPyV molecular clones but its role during infection remains to be elucidated (44).

1.2.5 MCPyV Late Genes

The late region of MCPyV encodes two capsid proteins, VP1 and VP2. A third capsid gene, VP3, is predicted by sequence analysis but has never been shown to be expressed; indeed, attempts to express this capsid have failed (17). These proteins are expressed after replication and encapsidate newly replicated viral genomes into nascent virions. The major capsid protein, VP1, is necessary and sufficient for the production of pseudovirions. VP2 is a minor capsid protein which is required for efficient infection of a number of cell lines, although its precise mechanism of action remains to be fully explored (19,41,45,46). Initial reports identified sialic acid as the major attachment factor for MCPyV, similar to other polyomaviruses (47). Subsequent studies have uncovered a more nuanced process where binding to sulfated glycosaminoglycans, especially heparin sulfate, was required in addition to sialic acid for efficient entry (46). The crystal structure of VP1 confirmed a sialic acid binding pocket, but mutation of this domain did not inhibit initial attachment of virions to target cells, supporting a model where heparin sulfate acts as an initial attachment factor with subsequent binding of sialic acid required for internalization into the target cell (48). This dual-receptor paradigm is novel among polyomaviruses, once again highlighting MCPyV's novelty.

1.2.6 Natural Infection of MCPyV

Thus far the natural host cell of MCPyV has not yet been identified. Merkel cells are post-mitotic and do not support robust infection of MCPyV, and are thought to be a dead-end host cell. The lack of a robust *in vitro* system for propagating the virus has hampered our ability to thoroughly study MCPyV's life cycle, so research efforts have thus far studied various aspects of the virus life cycle in isolation. For example, pseudovirions composed of the viral capsids encapsidating either an MCPyV molecular clone or a reporter construct have been useful in better understanding viral entry (46-48). Similarly, ectopic expression of viral proteins alone or in combination allowed for the discovery of many of the functions described for LT and sT in sections 1.2.2 and 1.2.3 above. Additionally, identification of cell lines that support replication of the viral Ori have allowed for an in-depth exploration of this key step of the viral life cycle (10,17,41,49,50).

To date, a significant portion of MCPyV research has focused on the oncogenic properties of both LT and sT. Regulation of key processes such as genome replication and transcription remains to be thoroughly explored. A better understanding of how these early events are regulated during natural infection can provide clues for understanding how these processes might then be altered during oncogenesis, and may even point to therapeutic targets in MCPyV associated tumors.

1.3 Polyomavirus Genome Replication

1.3.1 LT-mediated Initiation of Replication

SV40 replication has been an essential model for understanding eukaryotic replication (51). This section will review the formation of the polyomavirus replication initiation complex, directed by LT, followed by mechanisms of regulation in section 1.3.2. A discussion of our current understanding of MCPyV replication will be the focus of section 1.3.3.

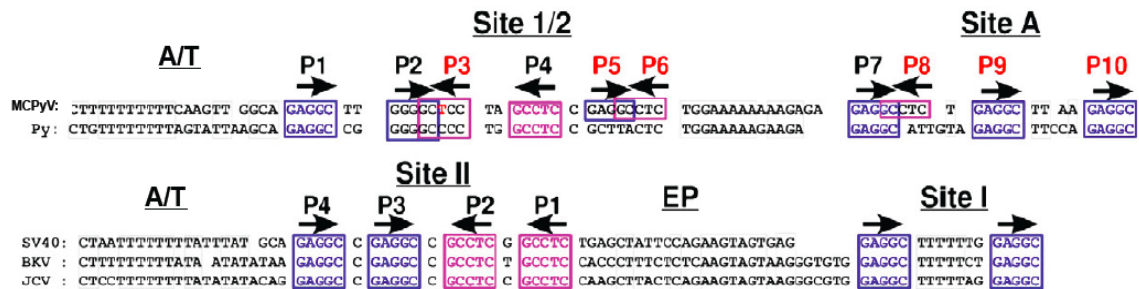


Figure 1.2 Organization of polyomavirus origins of replication. Pentanucleotide sequences (GAGGC) which are recognized by LT are denoted with a “P” and highlighted in blue, while inverted complimentary binding sites (CTCCG) are highlighted in magenta. Arrows denote the orientation of bound LT. The A/T rich tract (A/T) and Early Palindrome (EP) are also indicated. Py – murine polyomavirus. Adapted from Harrison *et al.*, 2011 (28).

The SV40 Ori is located at the center of the NCCR, and is flanked on both ends by the early and late promoters. The Ori is comprised of three functional domains (see Figure 1.2, bottom). The central domain, Site II, contains four GAGGC pentanucleotide repeats which serve as LT binding sites. Site II is flanked on the early side by the Early Palindrome (EP) and on the late side by an A/T rich tract (A/T), both of which are easily

melted and serve as the initial sites of unwinding and recruitment of the DNA replication machinery (51).

SV40 LT binds the viral origin and forms hexameric complexes to initiate replication. LT contains two domains critical for replication: an OBD and a helicase domain. The OBD specifically recognizes the GAGGC pentanucleotide repeats of Site II, and additionally make contacts with the other OBD of adjacent LT molecules during hexamer formation (52,53). The helicase domain makes non-specific interactions with DNA, especially single stranded DNA, and helps stabilize LT recruitment to the Ori. The helicase domain also contains an ATPase domain required for unwinding activity; this activity can be stimulated by single stranded DNA (54-56). In addition to forming a viral helicase required for unwinding of the genome, LT recruits key cellular replication factors including RPA70, RFC1 and DNA Polymerases to the viral origin (51,57).

LT is the only viral protein required for initiating replication of the genome. Biochemical analysis of a variety of LT mutants, as well as extensive structural analyses, have allowed for a deep understanding of the initial events of replication initiation, which will be briefly summarized. The OBD recruits LT specifically to the viral Ori, where the arrangement of the GAGGC pentanucleotides causes a head-to-head configuration of LT molecules (53). These LT proteins then recruit additional LT molecules to form two hexameric complexes at the Ori (58). During hexamer formation, the OBDs release the Ori DNA and form contacts with each other to stabilize the hexamer, while the non-specific DNA interactions from the helicase domains keep the complexes localized to the

viral genome (53). The ATPase activity of the helicase domains are then activated and the hexameric complexes begin unwinding the viral genome at the A/T and EP domains flanking Site II. After initial unwinding of the DNA, the LT helicase continues to unwind the genome as the cellular replication machinery, recruited by LT, begins replicating the viral genome. *In vitro* replication studies have shown that magnesium and ATP are required to stimulate helicase activity, while initial hexamer formation of LT requires ATP binding but not hydrolysis, as non-hydrolyzable analogues can still stimulate hexamer formation (53,58-70).

1.3.2 Regulation of Viral Replication

In addition to orchestrating replication of the viral genome, LT has many other important functions which are required for manipulating the host cell to drive proliferation, as has been outlined above. Initiation of replication must be timed to occur when the host cell is most permissive to replication. This switch is mediated by phosphorylation of LT at threonine 124 (T124) (71,72). Phosphorylation at T124 is required for LT to be replication competent, and is thought to stimulate interactions between both hexamers at the Ori which lead to initiation of unwinding (73). Cyclin dependent kinases have been shown to phosphorylate LT at this site *in vitro*, but have not been definitively proven to perform this function *in vivo* (71). In addition to T124, phosphorylation at serines 120 and 123 plays an indirect role in regulating replication. Specifically, S120/123 phosphorylation is required for efficient nuclear import of LT but diminishes LT's ability to initiate replication. These phosphorylation marks must be removed prior to replication, likely by PP2A phosphatases. The kinase(s) responsible for

phosphorylating S120/123 remains to be confirmed, but these phosphorylation events can be simulated *in vitro* with casein kinase (74-79).

Many DNA viruses have been shown to manipulate the host DDR for their replication. SV40 has been shown to recruit DDR factors to viral replication foci (80). Additionally, ATM kinase, a key regulator of double-strand break repair, has been shown to phosphorylate LT directly, and this activity was required for replication (81). While the interaction between SV40 and the host DDR has been well documented, the functional/mechanistic role(s) of these DDR proteins still requires exploration.

1.3.3 MCPyV Genome Replication

MCPyV genome replication follows the SV40 model to a large extent. MCPyV LT is the only protein required for initiating replication, although co-expression of sT can boost LT's activity by stabilizing LT protein expression (10). MCPyV LT recognizes the viral Ori through its OBD; neither SV40 nor MCPyV LT can recognize the other's Ori at a level that allows for replication (28). Interestingly, the MCPyV Ori is organized more similarly to the murine polyomavirus Ori (Figure 1.2, top): it lacks a true early palindrome region and instead has two A/T tracts that flank the central pentanucleotides. Additionally, instead of having a symmetrical set of four GAGGC pentanucleotides at the center of the Ori, MCPyV contains ten GAGGC repeats within the NCCR, eight of which are relevant to replication; LT binds four of these repeats in an asymmetric fashion (P1, P2, P4 and P7) which has been shown to be similar to murine polyomavirus LT's origin binding architecture (10,28,82). Notably, crystal structures predict that MCPyV LT

OBDs make more extensive contacts with each other on the viral origin compared to SV40 LT (28). Novel to MCPyV replication is LT's ability to recruit the host protein Brd4 to replication foci, which in turn recruits Replication Factor C; this activity was not seen with SV40 LT, but has been shown to be relevant to papillomavirus replication (50,83). Similar to SV40, however, is the recruitment of host DDR proteins to actively replicating MCPyV viral genomes (49). The recruitment of these proteins appears to be necessary for efficient replication of the viral genomes in cells, although the detailed mechanisms by which these DDR proteins assist replication remain to be elucidated (49). Recruitment and manipulation of the host DDR has emerged as a common theme among DNA viruses, and MCPyV LT expression alone can elicit a robust DDR in cells, even in the absence of viral genomes (14).

Important questions remain for MCPyV replication. The role(s) played by DDR proteins at replication foci remains to be elucidated. Additionally, contribution from sT beyond its stabilization of LT has yet to be explored in the context of replication. Finally, whether MCPyV LT is phosphorylated as a means of controlling the replication process has not yet been described.

1.4 Regulation of Polyomavirus Transcription

1.4.1 SV40 Gene Regulation

Regulation of both early and late promoters for SV40 has been well described. The early promoter contains binding sites for many cellular transcription factors, including Sp1, Sp2, AP-1, AP-4 and NFAT (84-87). A TATA box targets the

transcription machinery to the correct start site (88). As expression of LT increases during early infection, the early promoter becomes inactivated. During and especially after LT has initiated replication of viral genomes, the early promoter is shut down while the late promoter is activated to express the capsid proteins (87). LT directly mediates the repression of the early promoter and activation of the late promoter; sT's involvement in either event has not been well established, although one report shows that sT can help complement the activity of a sub-optimal level of LT expression (89).

1.4.2 MCPyV Gene Regulation

Regulation of MCPyV transcription has thus far not been studied. Only a few cell lines support expression of viral proteins from their natural promoters, and the few reports on the topic are largely observational. Expression of viral proteins from native MCPyV genomes is highly restricted in all cell lines tested thus far (14,41,45,46,49,90); the mechanism(s) regulating viral MCPyV transcription remains unexplored. A better understanding of how the viral promoters, especially the early promoter, are regulated is vital for understanding viral oncogene expression in MCPyV associated cancers as well as in naturally infected cells.

1.5 Scope of My Work

My work has focused on early events of MCPyV infection, including replication and transcription, and has also explored how post-translational modifications regulate LT function. In Chapter 2, I identify three novel phosphorylation sites on MCPyV LT and go on to describe how they regulate LT-mediated replication of viral genomes. In

Chapter 3, I identify a fourth phosphorylation site on the extreme C-terminus of LT and demonstrate how this phosphorylation event, mediated by ATM kinase, may contribute to the growth-inhibitory properties of the C-terminal region of LT. Finally, in Chapter 4 I offer a preliminary analysis of MCPyV transcription from both early and late promoters. I describe how replication is tied to transcriptional activation and demonstrate a unique dependence of LT on sT co-expression for upregulation of the viral late promoter.

CHAPTER 2: PHOSPHORYLATION OF LARGE T ANTIGEN REGULATES MERKEL CELL POLYOMAVIRUS REPLICATION

I was the principal investigator who designed and performed the experiments in this chapter, and prepared the associated manuscript published in *Cancers*. Jing Jiao prepared the LT sample for mass spectrometry analysis, which was performed by the School of Medicine Proteomics Core (Figure 2.1A), while I performed the protein alignment (Figure 2.1B). Dr. Jianxin You assisted in modeling the extended OBD of LT in contact with DNA (Figure 2.2). Sabrina Tsang assisted in performing the replication assay in Figure 2.5. Dr. Xin Wang was of great assistance in performing the *in vitro* biochemical assays to probe the LT phosphomutants for their ability to bind and unwind the viral origin (EMSA in Figure 2.6, Unwinding Assay and Helicase assays in Figure 2.7 and 2.8).

This research was originally published in *Cancers*. Jason Diaz, Xin Wang, Sabrina H. Tsang, Jing Jiao, and Jianxin You. Phosphorylation of Large T Antigen Regulates Merkel Cell Polyomavirus Replication. *Cancers* (2014) **6**(3): 1468-86

2.1: CHAPTER SUMMARY

Polyomavirus Large T antigen (LT) is a multifunctional protein which manipulates the host cell and regulates replication of the viral genome as well as transcription of both the early and late promoters. These multiple functions must be closely regulated to ensure each step of the viral life cycle is executed correctly. Phosphorylation is a major regulator of protein function, but no studies have yet been performed for MCPyV LT. Using mass spectrometry, I identified three phosphorylation sites in MCPyV LT: T271, T297 and T299. T299 is homologous to a highly conserved threonine found in all the major polyomavirus LTs I examined; phosphorylation of the homologous threonine in SV40 LT stimulates its ability to initiate viral replication. Using the tools already developed in our lab for studying MCPyV replication, I showed by immunofluorescence and southern blotting that alanine mutants of MCPyV LT T297 and T299 dramatically affected viral replication without affecting recruitment of replication factors: T297A stimulated replication well over levels seen by wild-type LT, while T299A was replication defective, as was predicted by homology to SV40 LT. Further biochemical analyses showed that the MCPyV LT T297A mutant could bind the origin of replication with increased affinity, while the T299A mutant had reduced binding, compared to wild-type. The unwinding and helicase activities of LT were unaffected by these mutations. These results showed that phosphorylation at two sites in MCPyV LT dramatically regulates its ability to replicate, and identified a third, novel site at T271 in a unique region of MCPyV LT that warrants further investigation.

2.2: INTRODUCTION

MCPyV is the first human polyomavirus to be linked to a human cancer MCC (3,6,8). Since its discovery in 2008, this virus has been found clonally integrated in a majority of MCC tumors. In most MCPyV related MCC tumors the major viral protein, LT, has been mutated such that it is expressed in truncated forms (9). These tumor-derived truncated LT proteins retain their binding sites for pRb and DnaJ family heatshock proteins, thereby driving proliferation (3,9). Indeed, at least one study has shown that tumors with knocked-down LT protein regress rapidly in a xenograft model (32). Both LT and the splice variant sLT have been shown to have oncogenic properties (10,32,33,91), although the precise contribution of each protein to the process of tumorigenesis is still unclear.

MCPyV appears to be a natural resident of the skin microflora, and is acquired early in life (19,21,22). While considerable efforts have been made to better understand MCPyV's oncogenic potential, especially in MCC tumors, comparatively little work has been done to better understand this virus's basic life cycle. The lack of a relevant cell culture system for propagating virus has made investigations of its basic virology difficult; however, ectopic expression of MCPyV LT in cell lines such as HEK 293, C33A and U2OS has been valuable in enhancing our understanding of MCPyV's interaction with host cells (14,41,50,92).

Our lab has previously characterized MCPyV LT's interaction with the host cell to stimulate replication (50). In that study we showed by immunofluorescent staining (IF), fluorescent *in situ* hybridization (FISH) and BrdU staining that MCPyV LT proteins form large nuclear foci which contain actively replicating plasmids carrying the viral Ori. We also showed that several cellular factors colocalize to these foci, including: the double bromodomain protein, Brd4, the PCNA loading protein replication factor 1 (RFC1), and the single-stranded DNA binding protein RPA70. In another study we demonstrated that full length MCPyV LT activates host DNA damage response (DDR) pathways and dramatically alters the host cell cycle (14). Additionally, members of the DDR pathway were seen to colocalize with nuclear foci containing actively replicating viral genomes, potentially contributing to viral replication (49). While it is still unclear whether DDR activation and recruitment upon LT expression is a side-effect of active viral replication and/or LT helicase activity, or if this activation is being actively subverted and manipulated by MCPyV, the link between MCPyV LT expression and DDR activation is well established. This DDR activity, coupled with LT's ability to dramatically alter the host cell cycle, may provide enough low-level genomic instability to lead to integration of the MCPyV genome into the host cell genome, which appears to occur in the majority of MCPyV-related MCC tumors (7).

Merkel cells may not represent the natural host cell of MCPyV and may predispose MCPyV to randomly integrate its genome. Indeed, the prototypical polyomavirus SV40 has a transforming phenotype in cell lines that are non-permissive for viral replication (30); Merkel cells may similarly represent a non-permissive host for

MCPyV. A better understanding of how MCPyV replication is regulated would provide a clearer framework for understanding how infection may be altered in Merkel cells and lead to integration of the mutated viral genome.

SV40 LT has been a model for understanding eukaryotic replication for decades (51). SV40 LT is recruited to the viral Ori through its OBD, which recognizes GAGGC pentanucleotide repeats arranged symmetrically within the Ori. LT then oligomerizes into two hexameric protein complexes arranged in a head-to-head fashion. The C-terminal helicase domains make non-specific contacts with an extended palindrome and an A/T rich tract flanking the central pentanucleotide repeats; these become the initial sites of unwinding. SV40 LT then acts as a helicase to unwind the viral genome and recruits cellular factors to begin replication (51,57).

Phosphorylation has been a well established mechanism by which SV40 LT replication is regulated (93). T124 was identified as a critical residue for regulating SV40 LT-mediated viral replication; removal of this phosphorylation either biochemically or genetically abrogated replication (71,94-96). Intensive biochemical studies demonstrated that this phosphorylation plays an important role in mediating interactions between both hexamers at the Ori. Alanine mutants are defective in forming double-hexamer complexes and unwinding the viral origin (68,73).

Somewhat paradoxically, early biochemical analyses of purified SV40 LT seemed to indicate that phosphatase treatment could actually stimulate viral replication *in vitro*

(75,78). It was later clarified that, in addition to phosphorylation at T124, there are serine phosphorylation modifications nearby which have an inhibitory effect on viral replication (74). These phosphorylation events seem to accumulate throughout the course of infection (97). These observations led to a model where T124 phosphorylation stimulates replication, while subsequent phosphorylation at neighboring serines dampen this effect, potentially altering LT's activity on the viral genome to favor transcription of the capsid genes (93).

No such analysis of MCPyV LT phosphorylation has yet been reported. We sought to provide an initial framework for understanding the regulation of MCPyV LT's functions by performing a proteomic analysis to search for relevant phosphorylation sites. Our studies identify three phosphorylation marks on MCPyV LT; T271, T297 and T299. We found that T271 had no effect on replication, while T297 and T299 phosphorylation had antagonistic effects. Both T297 and T299 altered the binding affinity of MCPyV for the viral Ori while leaving unwinding and helicase functions largely intact. Taken together, our data reveal a dynamic interplay between multiple phosphorylation sites, which together regulate MCPyV LT's ability to initiate replication at the viral Ori.

2.3: RESULTS

2.3.1: Mass Spectrometry Identifies T271, T297 and T299 as Phosphorylation Sites on MCPyV LT

Polyomavirus LT proteins perform a large variety of functions in infected cells to establish a replicative niche; these functions include manipulation of the host cell cycle

through its DnaJ domain and pRb binding domain, regulation of viral transcription, and initiation of viral genome replication by acting as the viral helicase (8,31,93).

Phosphorylation of LT has been well established as a mechanism of regulating its function, especially as a replication initiator protein.

To date, no analysis of MCPyV LT phosphorylation has been performed. To get a broad view of MCPyV LT phosphorylation, we performed a mass spectrometry analysis to identify potential LT phosphorylation sites. MCPyV LT was first affinity tagged with two IgG binding domains from *S. aureus* Protein A and a Tobacco Etch Virus (TEV) Protease cleavage site. This construct was then ectopically expressed in HEK 293 cells. The protein was affinity purified on IgG-Sepharose beads, separated by SDS-PAGE and stained with Coomassie blue (Figure 2.1A). The visible band corresponding to MCPyV LT was excised and analyzed by mass spectrometry.

Trypsin-digested peptides from LT were purified and analyzed by LC/MS/MS. The peptides covered 45% of MCPyV LT and identified two unique peptides with a shift of 80 daltons over the predicted size, indicating a potential phosphorylation modification at T271 and T299. We repeated this analysis using a titanium oxide column to enrich for negatively charged peptides, such as those with phosphorylated residues. The peptides from this purification covered 25% of MCPyV LT and identified potential phosphorylation at T271 and T297 (Table 2.1).

To better understand how these phosphorylation modifications may regulate MCPyV LT function, we aligned the amino acid sequence of various representative polyomavirus LT proteins (Figure 2.1B). T271 localized to the serine rich unique region of MCPyV LT spanning amino acids 95-290. Of the polyomavirus LT proteins analyzed, only murine polyomavirus contains such a tract; however, it is not well conserved with MCPyV LT. Although the lack of homology prevented us from making functional predictions of T271 phosphorylation, it is interesting to note this threonine was identified by multiple peptides in both mass spectrometry purification schemes (Table 2.1), giving us high confidence that this site is phosphorylated when LT is expressed in cells.

Threonine 297 is not well conserved amongst polyomavirus LT proteins. Its function was not readily apparent to us based on homology, although its close proximity to the OBD led us to predict that it might have some impact on viral replication. Modeling of the OBD (aas 308-433) using the structure published by Harrison and colleagues (Figure 2.2A) (28), and extending their structure to include this threonine supported this hypothesis; T297 appears to face the protein/DNA interface and might even make direct contacts with DNA (Figure 2.2B). In contrast to the two threonines discussed above, T299 is a highly conserved site found in all polyomavirus LT proteins analyzed. The homologous site in SV40 LT, T124, has been well established as a key regulator of LT mediated DNA replication. Phosphorylation of this threonine in SV40 is thought to regulate double-hexamer interactions on the viral origin to stimulate unwinding and melting of the DNA. Alanine substitutions of this site in SV40 LT completely abolish LT-mediated DNA replication. Our modeling of the OBD showed

that this threonine does not directly face the protein/DNA binding interface and likely plays a role in protein-protein interactions between LT monomers and/or hexamers (Figure 2.2C). The crystal structure of the MCPyV OBD was solved in complex with DNA; since this structure did not include the T299 residue, we cannot rule out the possibility that T299 may interact with DNA in steps prior to hexamer assembly on the origin.

The sequence analysis and modeling led us to believe that phosphorylation of at least a subset of the threonines identified would play a role in viral DNA replication. Our lab has previously studied MCPyV LT-mediated replication in C33A cells, an HPV-negative cervical cancer cell line; we therefore took advantage of this system to probe the potential roles of these threonines in viral DNA replication.

2.3.2: MCPyV LT Phosphorylation Affects the Formation of Viral Replication Centers

To begin elucidating the role(s) these phospho-sites might play in replication, we generated alanine point mutants at each threonine identified by the mass spectrometry analysis. We then co-transfected these constructs with a plasmid containing the MCPyV Ori into C33A cells and stained these cells for LT and various replication factors, as has been described in our previous study (50). We assessed these mutants for their ability to form viral replication centers, which appear as nuclear foci, in transfected nuclei by IF. We also assessed their ability to recruit factors known to co-localize with MCPyV replication foci, including Brd4, RFC1 and RPA70.

As has been shown previously, wild-type (WT) LT formed punctate foci in nuclei when co-transfected with a construct containing the MCPyV Ori. Our previous studies have confirmed that under these transfection conditions these foci contain the MCPyV Ori plasmid (as shown by FISH) and are actively replicating (assessed by incorporation of BrdU) (49). Both the T271A and T297A mutants formed replication foci while T299A completely failed to assemble replication foci (Figure 2.3A-C). The T271A and T297A mutant LT proteins formed replication foci at altered rates. Compared to WT LT, which formed replication foci in about 15% of LT positive nuclei, the T271A mutant had a small decrease in the frequency of replication focus formation (about 10%) (Figure 2.3D). This difference, however, was not statistically significant in a one-way ANOVA test. In contrast, the T297A mutant exhibited twice as many LT-positive nuclei with replication foci. For constructs which formed replication foci, recruitment of cellular factors did not seem to be affected; WT, T271A and T297A LT proteins all recruited Brd4, RFC1 and RPA70 proteins at similar rates. Colocalization with T299A, which did not form replication foci, was not evident (Figures 2.3 and 2.4). As has been seen previously, replication foci came in a variety of sizes, and nuclear swelling was often evident, especially in cells expressing T297A LT, possibly to accommodate rapidly replicating plasmids.

2.3.3: MCPyV LT Phospho-mutant Proteins Have Altered Replication Capacities

Our IF studies indicated that at least a subset of the threonines identified in our proteomic analysis affect viral genome replication. To more rigorously examine these mutants' ability to replicate plasmids containing the viral Ori, we performed Southern

blotting experiments to detect replicated plasmids. C33A cells were co-transfected with a MCPyV LT construct and a plasmid containing the viral Ori. Two days after transfection, cells were harvested and divided into two fractions. Whole genomic DNA extracts were prepared from one fraction while proteins were collected from the other fraction. Whole genomic DNA was then digested with BamHI to linearize the plasmids. The DNA was then detected with ³²P-labeled MCPyV Ori plasmid as a probe. The LT expression construct is made from the same vector backbone as the MCPyV Ori plasmid, and is therefore detected as a second, higher molecular weight band in our Southern blot. Additionally, the vector control for MCPyV LT is almost identical in size to the MCPyV Ori plasmid, so these two plasmids co-migrate as one band in our blots (Figure 2.5A, bottom). Whole genomic DNA was also digested with DpnI to reveal newly replicated DNA (Figure 2.5A, top).

The Southern blotting results complemented what was seen by IF (Figure 2.3 and 2.4). Compared to WT MCPyV LT, the T271A mutant replicated the MCPyV Ori plasmid almost as well. In contrast, the T297A mutant, which had twice as many nuclei with replication foci as WT (Figure 2.3D), had a robust replication phenotype that was well over that seen for WT. This was especially striking given that both the amount of MCPyV Ori input plasmid and the protein level of T297A LT was less than WT (Figure 2.5). Finally, the T299A mutant, which failed to form replication foci as seen by IF, was unable to replicate Ori plasmids at a level detectable by Southern blot (compare Figure 2.5A, top panel, Vector and T299A lanes). This agrees with what was seen in SV40, where the homologous mutant, T124A, failed to replicate viral genomes.

2.3.4: T297A and T299A Phospho-mutant LT Proteins Bind the Viral Ori with Altered Affinity

Our studies up to this point confirmed that the T297A and T299A mutants had greatly altered replication phenotypes; T271A by contrast showed a modest effect on replication. To get a firmer understanding of the molecular basis for the replication phenotypes we observed, we next sought to examine the binding, unwinding and helicase activities of these mutants. We focused our analyses on the T297A and T299A mutants, which had dramatic replication phenotypes.

Polyomavirus LT binding of the viral Ori is mediated by its OBD, which recognizes GAGGC pentanucleotide repeats in the Ori. The MCPyV Ori more closely resembles that of murine polyomavirus; it contains eight perfect GAGGC pentanucleotides and two imperfect pentanucleotides, with two A/T rich regions interspersed between these repeats (Figure 2.6A) (10,28,82). Previous studies have shown that pentanucleotides 1, 2, 4 and 7 are essential for replication (10).

To test origin binding, we performed electromobility shift assays (EMSA). Affinity tagged MCPyV LT constructs were transfected into HEK 293 cells. Forty-eight hours later, LT proteins were immunopurified and cleaved with TEV protease (Figure 2.6B). Various amounts of purified proteins were then incubated with a ³²P-labeled PCR product encompassing all ten pentanucleotides and one of the two A/T tracts (Figure 2.6A, EMSA probe). Previous work with the SV40 Ori demonstrated that using Ori probes that lacked either the A/T rich tract or early palindrome region of the Ori revealed

a defect in double hexamer formation for T124A mutants (73). We predicted that the T299A mutant would exhibit a similar double hexamer defect in similarly altered Ori probes; however, given that one of the key pentanucleotides required for MCPyV replication (#7) lies outside one of the two A/T rich tracts of the MCPyV Ori, it was impossible to directly copy the unique architecture of the artificial probes generated in that study (10,73,98). Following these observations, we chose to omit one A/T tract but retain all ten pentanucleotide repeats in the hopes of seeing this phenotype. In addition, the ATP analogue AMP-PNP was included to stimulate hexamer formation but inhibit ATPase activity, which would unwind the double-stranded probe (62). Protein/DNA complexes were resolved on a non-denaturing polyacrylamide gel in TBE.

All mutant MCPyV LT proteins were able to bind the probe, albeit with different affinities. The WT LT showed robust binding beginning at 1 μ g purified protein; probe binding was further enhanced when more LT was added (Figure 2.6C). In contrast, the T297A mutant achieved maximal probe binding at 0.5 μ g, indicating a more robust affinity for this probe than WT. This phenotype agrees with the previous observation that this mutant replicates plasmids with the MCPyV Ori to a high degree (Figures 2.3 and 2.5). On the other hand, the T299A mutant exhibited an attenuated affinity for the EMSA probe; only at the highest dose (1.5 μ g) was binding evident, and still not to the level of either WT or T297A LT proteins. Our EMSA studies with T299A did not reveal single hexamers, which would migrate faster than the double hexamers binding our probe. It is possible that T299A does not have a double hexamer defect like its SV40 homologue, or that the probe used in our study was not sufficiently small to reveal such a phenotype.

Native PAGE analyses of these proteins was unable to resolve this question (data not shown). The technical limitations of our assay therefore preclude making any statements about the ability of these mutants to form single or double hexameric complexes. The attenuated binding phenotype for the T299A mutant, however, agrees with the observation that this mutant fails to replicate plasmids containing the viral Ori (Figures 2.3 and 2.5) and agrees with what has been reported for SV40 LT T124A binding (99).

2.3.5: MCPyV Phospho-mutant LT Proteins Exhibit Similar Unwinding and Helicase Activities

After initial binding of the viral Ori, polyomavirus LT proteins form two hexameric complexes that then untwist and unwind the origin DNA to form an initial bubble of single-stranded DNA (61,64,69). To test these mutants for their ability to unwind a double-stranded Ori sequence, we generated a probe that contained both A/T tracts and the first eight pentanucleotide repeats (Figure 2.7A, Unwinding Probe). This probe was generated by annealing two oligonucleotides which form a duplex with a four nucleotide overhang; this overhang was filled in with the Klenow fragment of DNA Polymerase and ³²P-labeled dCTP, generating a double stranded probe with one labeled strand. This probe was then incubated with purified MCPyV LT in conditions that promote ATPase activity. Reactions were then stopped with the addition of SDS and EDTA, and the DNA was resolved on a non-denaturing polyacrylamide gel. All LT constructs were able to unwind the probe (Figure 2.7B). This result was helicase dependent, because an MCPyV LT mutant, E627A, that we have previously described

failed to unwind our probe (Figure 2.8) (14). The T297A mutant, which showed a high affinity for the Ori (Figure 2.6C) showed unwinding activity similar to WT LT; because WT LT's activity was close to maximal unwinding in this assay (compare Boiled Control lane with WT LT lanes, Figure 2.7B) we are unable to say whether this mutant might have increased unwinding activity over WT activity. We also tested whether MCPyV LT could unwind a mutated Ori sequence. We introduced the Ori350 point mutation to pentanucleotide 7 in our assay; this mutation was reported by our lab and others to have partially abrogated replication due to reduced binding of LT to the origin (Figure 2.8) (10,92). LT was still able to unwind this mutant sequence; this is likely because either the amount of LT protein used in our *in vitro* settings, or the extended reaction time (1hr) compared to the EMSA (20min) can compensate for the reduced binding of LT to this mutant Ori.

Following unwinding of the viral Ori, hexameric LT complexes then function as a DNA helicase that translocates along DNA to separate double stranded DNA (100). To test this function, we employed a helicase assay that has been previously reported from our lab (14). This assay uses a circular, partially duplex DNA substrate as a probe for LT helicase activity. The probe does not contain MCPyV Ori sequences; DNA binding is mediated by non-specific interactions in the helicase domain. The reaction is carried out with affinity purified LT proteins still immobilized to the affinity resin. After washing bound proteins, half of the resin with bound LT protein was boiled in sample buffer and western blotted to detect protein levels (Figure 2.7C). The other half of the resin was incubated with the ³²P labeled probe in reaction buffer. Helicase activity separates the

labeled oligonucleotide from the circular template, allowing the probe to migrate faster during electrophoresis (Figure 2.7D).

Our results show that the mutant MCPyV LT proteins had similar helicase activity as WT LT (Figure 2.7D). In the conditions used, WT LT was able to maximally unwind the labeled probe; therefore we cannot conclude whether either of the mutants had enhanced helicase activity from this assay. Interestingly, the T299A mutant, which failed to replicate the viral origin (Figure 2.5) did not have attenuated helicase activity in this experiment. This has been previously reported for the T299A homologue in SV40 LT, indicating that this mutant's helicase functions remain intact, and the block to replication is primarily due to an inability to bind the origin efficiently (Figure 2.6C) (94). In contrast, the T297A mutant likely replicates to a high degree solely due to an increased affinity for the origin, as its unwinding and helicase activities were not markedly different from WT LT. Taken together, our data indicate that T297 phosphorylation plays a direct role in binding of the origin, while T299 phosphorylation affects both origin recognition and possibly initial unwinding of the origin DNA, similar to its function in SV40 LT.

2.4: DISCUSSION

Merkel Cell Polyomavirus is the first human polyomavirus linked to a human cancer. As such, it has garnered a considerable amount of interest, especially with regards to its oncogenic potential and its causative role in MCC. Much of the basic virology of MCPyV, in contrast, has been lacking, in large part due to the difficulty in propagating the virus and the lack of a natural host cell line. Previous work from our lab

has established that MCPyV LT interacts with the host DNA damage response machinery, potentially to regulate viral genome replication (92). Understanding how polyomavirus replication is regulated will be critical for understanding the very early steps of MCPyV-induced transformation and oncogenesis.

Phosphorylation has been a well-established mechanism of regulation for SV40 LT activities, especially for genome replication. In addition, MCPyV LT has a unique stretch of amino acids that is rich in serines and threonines, offering many new potential phosphorylation sites and therefore mechanisms of regulation. To search for relevant sites in a relatively unbiased fashion, we performed a proteomic analysis of ectopically expressed MCPyV LT (Figure 2.1 and Table 2.1). This analysis identified three threonines that are likely phosphorylated when MCPyV LT is expressed: T271, T297 and T299. We generated alanine substitutions of these sites to probe their function.

T271 was immediately interesting to us for a variety of reasons. It was independently identified in multiple peptides in both standard and titanium oxide purifications (Table 2.1), providing us with a high degree of confidence that this site is phosphorylated in cells. More intriguing, this site is located in the unique region of MCPyV LT (aa 95-290). It does not have any homologies to other polyomavirus LT proteins analyzed (Figure 2.1B). We anticipate phosphorylation at this site may represent a novel function that MCPyV has acquired. Efforts thus far, however, have not revealed what those functions may be. The T271A mutant's ability to bind Brd4 and activate the host DDR is similar to that seen for WT LT (data not shown). Additionally, this mutant

was able to form replication foci and replicate plasmids containing the Ori almost as well as WT (Figures 2.3 and 2.5). Additional experiments will be performed to identify its role in MCPyV infection.

T299, in contrast, is highly conserved among all polyomavirus LT proteins analyzed (Figure 2.1B). This site is homologous to T124 in SV40 LT, which has been extensively studied for its role in regulating SV40 LT-mediated DNA replication. Alanine substitution of this site in SV40 LT completely abrogated replication. Biochemical analysis of T124A mutants showed that it had somewhat impaired double-hexamer interactions and unwinding activity (68,73). More importantly, its ability to unwind duplex Ori DNA was abrogated while basic helicase activity remained unperturbed (68). In line with these findings, T299A in MCPyV LT also failed to replicate plasmids containing the viral Ori (Figure 2.5) and did not form replication foci (Figure 2.3). This mutant had a reduced capacity to bind the viral Ori in EMSA experiments (Figure 2.6). Although studies of the homologous LT mutant, T124A, in SV40 demonstrated that unwinding of the origin was attenuated, we were unable to reproduce this finding in our studies (94). While it is possible that MCPyV LT behaves differently from other polyomavirus LT's, we believe technical limitations in our hands are more likely responsible for not seeing this phenotype in MCPyV T299A LT. Its helicase activity remained identical to wild-type (Figure 2.7D), which has been reported for T124A LT in SV40 (94). Our EMSA studies did not indicate an attenuated double-hexamer phenotype as shown by Barbaro and colleagues for SV40 LT (73), and the unwinding phenotype we observe is extremely subtle. It is possible our experimental

conditions are not conducive for revealing these phenotypes, or (less likely) that T299 phosphorylation behaves in a slightly different biochemical manner than T124 in SV40 LT. We conclude that phosphorylation of T299 is required for MCPyV LT to initiate replication of its genome in ways similar to T124 phosphorylation in SV40.

T297 was not well conserved among the polyomavirus LT proteins analyzed. Modeling of this site seemed to indicate that this residue might face and even interact with DNA when the LT OBD engages the viral genome (Figure 2.2B). We speculated this site might have an impact on DNA replication. Indeed, the T297A mutant had twice as many LT-positive nuclei exhibiting replication foci as WT LT (Figure 2.3D). Supporting this observation, Southern blotting of *in cellulo* replication products showed that this mutant replicated plasmids containing the viral origin to a very high degree (Figure 2.5). Biochemical analyses revealed a strikingly robust affinity for the viral Ori (Figure 2.6), while unwinding and helicase activities remained largely unaffected (Figure 2.7). These data indicate that phosphorylation of this site would dramatically decrease LT's capacity to bind the viral Ori, which would presumably limit its ability to initiate viral replication. These observations are in line with our structural model (Figure 2.2) predicting that this site faces the OBD/DNA binding interface. The negative charge of a phosphate moiety at this site would presumably clash with the negatively charged phosphate-backbone of DNA, leading to reduced DNA binding. SV40 has also been reported to have phosphorylation sites that negatively impact replication. Phosphorylation at serines 120 and 123 was shown to have a negative effect on replication (74). Threonine 297 may provide a similar regulatory function for MCPyV

LT. It is possible that phosphorylation at a site neighboring the stimulatory threonine (124 for SV40 LT, 299 for MCPyV LT) may be a general feature of polyomavirus LT proteins to limit Ori recognition and to provide a brake for viral replication.

We attempted to generate phosphomimetic mutants (threonine to aspartate or glutamate) of these sites to probe these dynamics more closely; however, these mutants behaved just like alanine substitutions (data not shown). Interestingly, a MCPyV LT expression construct containing both T297A and T299A mutations matched the T299A phenotype completely: it failed to form replication foci or replicate plasmids with viral Ori's (data not shown). The T297A mutation would allow for enhanced binding of the origin (Figure 2.6), but the T299A mutation, which likely acts at steps after Ori binding during initiation of replication, completely abrogated replication of this double mutant (data not shown).

Taken together, our data support a model where T299 and T297 phosphorylation act as antagonistic ON and OFF switches for replication, respectively. We would hypothesize that T299 is first phosphorylated to stimulate viral replication, while subsequent phosphorylation at threonine 297 would abrogate Ori recognition and presumably reduce viral genome replication, possibly in favor of late gene expression and/or packaging. Phosphatases may also play a role, either removing phosphates from T299 to halt replication or from T297 to allow replication to continue. Without antibodies specific for phosphorylation at these sites, it is difficult to track when these sites become phosphorylated during infection or to begin searching for the kinases that

add these marks during infection. Analysis of the amino acid sequences of these sites offer some clues. For SV40, cdc2/CDK1 was shown *in vitro* to be responsible for phosphorylation at T124, the homologue to MCPyV LT T299 (71). The residues surrounding both MCPyV LT T299 and SV40 LT T124 (TPPK for both viruses, see Figure 2.1B) exhibit a classic cdc2/CDK1 consensus sequence (S-P-X-basic residue) (101). Although it was not directly tested here, it is likely that cdc2/CDK1 plays a role in phosphorylating T299 during MCPyV infection. Casein kinase II was also shown to phosphorylate nearby serine residues in SV40 LT *in vitro*, which played a role in SV40 LT nuclear import (102-105). Finally, ATM kinase has been shown to phosphorylate SV40 LT in this region as well, contributing to LT-mediated replication (81). The threonines T271 and T297 identified in this study do not exhibit homologies to the known consensus sequence of either of these kinases, indicating that other kinases are likely involved. Finally, other MCPyV viral proteins, like sT antigen, 57kT antigen and ALTO (44), may affect when, where and how LT is phosphorylated during the viral life cycle. These questions should be explored further as more reagents and cell lines become available for MCPyV studies.

One of the hallmark features of MCPyV LT in MCC is that the protein frequently becomes mutated such that it is expressed in a truncated fashion (9). These truncations almost always delete the helicase domain and the OBD. Interestingly, the three phosphorylation sites identified in this study are almost always omitted from the truncated proteins as well. It has been hypothesized that LT becomes truncated to avoid replicating the integrated viral genome, which would presumably cause genomic

instability (3). In line with this reasoning, at least one MCPyV related MCC tumor has been identified with a full-length LT protein but the integrated viral genome contains a mutated Ori that fails to support viral replication (9,10). Given that mutation of T299 completely abolishes LT's capacity to replicate the viral origin, it is interesting to note that this mutation has never been observed in any of the MCC cases studied thus far. It is possible that the OBD, helicase domain and/or extreme C-terminal domain contain additional activities beyond replication that are negatively selected out during MCC progression. Our previous studies have indicated that the C-terminal half of MCPyV LT interacts with the p53 pathway to maintain cells in a stalled S-phase, which may be conducive to viral genome replication but antithetical to tumorigenesis (14). Others have similarly postulated that the C-terminal domain contains activities beyond replication that are negatively selected during MCC oncogenesis (13). Further investigation of this region of the protein may provide a broader and more comprehensive understanding of how MCPyV LT manipulates the host cell, and how these activities become disrupted during MCC tumorigenesis.

2.5: FIGURES

TABLE 2.1

| Peptide Purification | Peptide Sequence | Probability | Amino Acid | Modification |
|-----------------------------|------------------------------------|--------------------|-------------------|---------------------|
| Standard | (R)SSASSASSAS F TSTPPKPK(K) | 95% | Thr 297 | Phospho (+80) |
| | (R)SSSF T TPKTPPPFSR(K) | 95% | Thr 271 | Phospho (+80) |
| | (R)SSSF T TPKTPPPFSR(K) | 95% | Thr 271 | Phospho (+80) |
| Titanium Oxide | (R)SSASSASSAS F TSTPPKPK(K) | 95% | Thr 299 | Phospho (+80) |
| | (R)SSASSASSAS F TSTPPKPK(K) | 95% | Thr 299 | Phospho (+80) |
| | (R)SSSF T TPKTPPPFSR(K) | 95% | Thr 271 | Phospho (+80) |
| | (R)SSSF T TPKTPPPFSR(K) | 95% | Thr 271 | Phospho (+80) |
| | (R)SSSF T TPKTPPPFSR(K) | 95% | Thr 271 | Phospho (+80) |

TABLE 2.1: Phosphorylated peptides Identified by mass spectrometry. Shown are the reconstructed peptides isolated by both the standard purification and titanium oxide enrichments after trypsin digest. Confidence in identification is given as a probability. The residues in bold are the ones identified as having a mass value 80 daltons higher than predicted, indicating a phosphorylation modification.

FIGURE 2.1

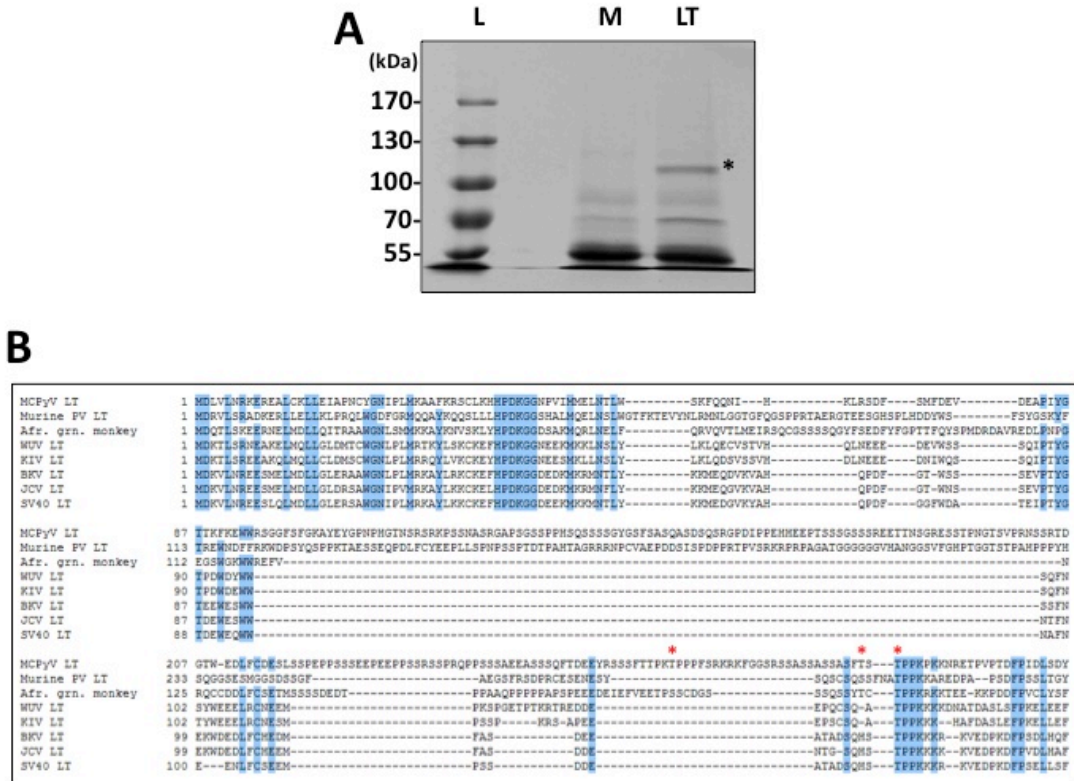


Figure 2.1: Identification of MCPyV LT phosphorylation sites. (A) Affinity-tagged MCPyV LT was transfected into HEK 293 cells. Forty-eight hours post transfection, lysates from transfected (LT) or untransfected (Mock, M) cells were purified with IgG-Sepharose beads. Bound proteins were cleaved from beads with TEV protease, separated by SDS-PAGE and stained with Coomassie brilliant blue. The band corresponding to MCPyV LT (*) was excised and analyzed by mass spectrometry. L – Protein Marker ladder. (B) Alignment of the N-terminal portion of various polyomavirus LT proteins. The three phosphorylated threonines identified by the proteomic analysis in (A) are indicated by the red asterisks (*). Conserved residues are highlighted in blue (60% conservation).

FIGURE 2.2

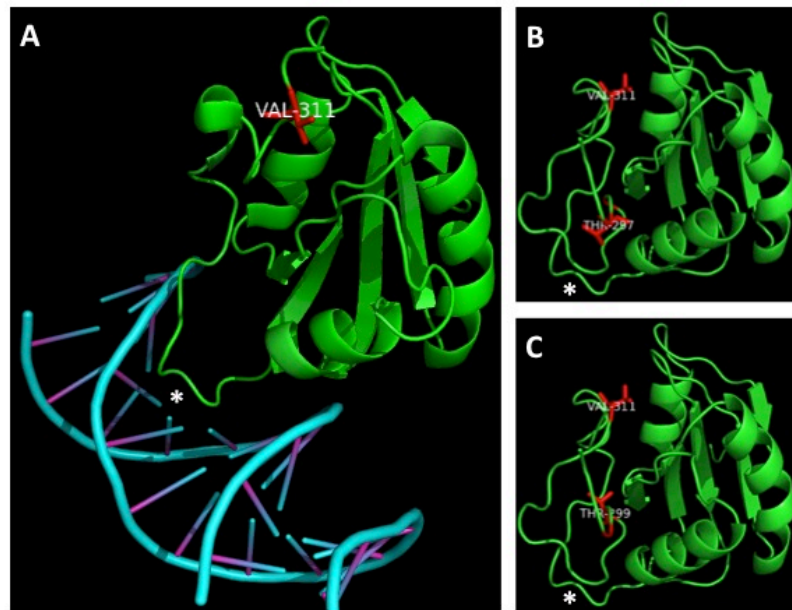


Figure 2.2: Modeling MCPyV LT's interaction with DNA. (A) Phyre2 and PyMOL software was used to model the MCPyV LT protein origin binding domain (OBD) contacting DNA as reported by Harrison and colleagues (28). The asterisks indicate the loop of the OBD that makes contacts with DNA. (B) The structure modeled in (A) was extended to aa 290 and modeled using Phyre2 and PyMOL software. The model was rotated to match the orientation of the structure in (A). T297 is highlighted in red and appears to face – and possibly contact – DNA. (C) The same model in (B) was labeled to show T299, which appears to face away from DNA, possibly to interact with adjacent LT monomers or hexamers. Valine 311 is labeled in all three structures to aid in comparison.

FIGURE 2.3

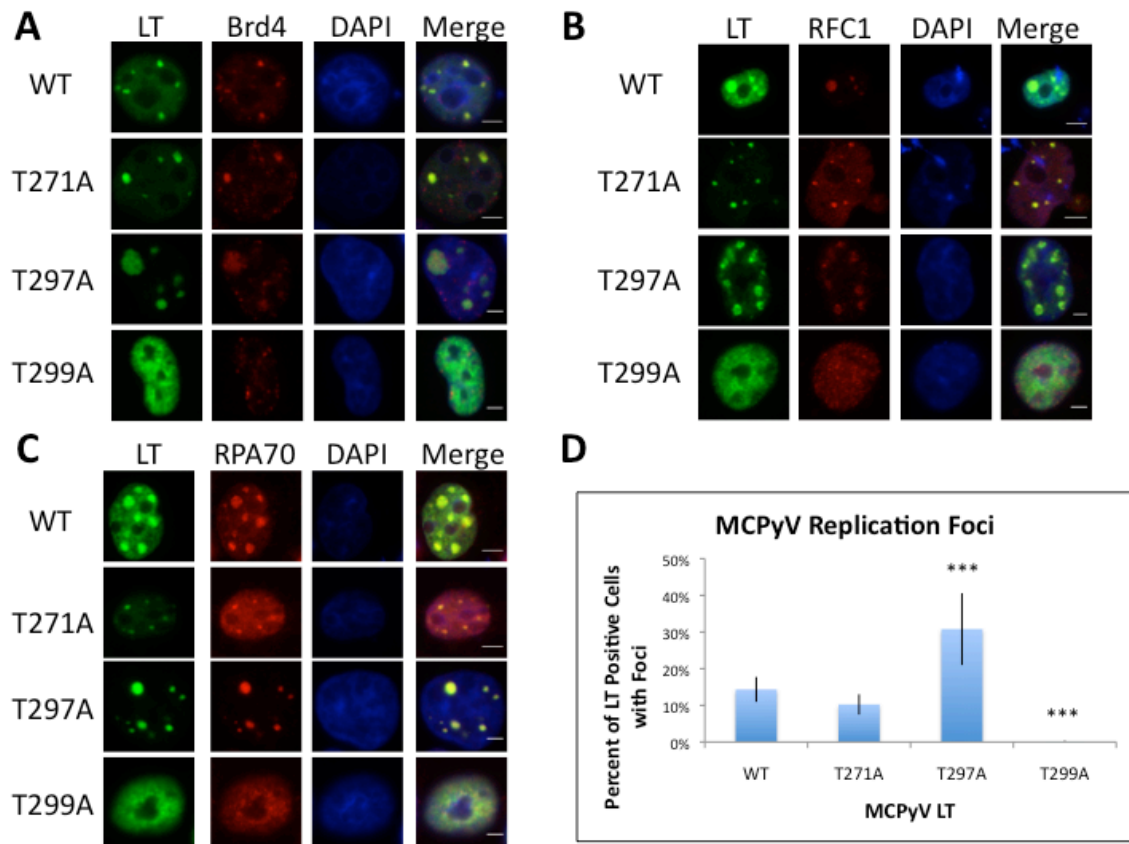


Figure 2.3: MCPyV LT phospho-mutant proteins form viral replication foci at altered efficiencies. (A-C) C33A cells were co-transfected with an MCPyV Ori plasmid and the indicated MCPyV LT phospho-mutant. Forty-eight hours post transfection, cells were fixed and stained for LT (green) and the indicated cellular factor (Red). Nuclei were counterstained with DAPI. Bar = 3 μ m. (D) Nuclei stained positively for LT as shown in (A-C) were scored for the presence of viral replication foci (at least 150 LT positive nuclei were counted in triplicate per transfection). Bar indicates standard deviation from the mean from at least three independent experiments. Statistical significance was calculated against WT LT using a one-way ANOVA (***) $p < 0.0001$).

FIGURE 2.4

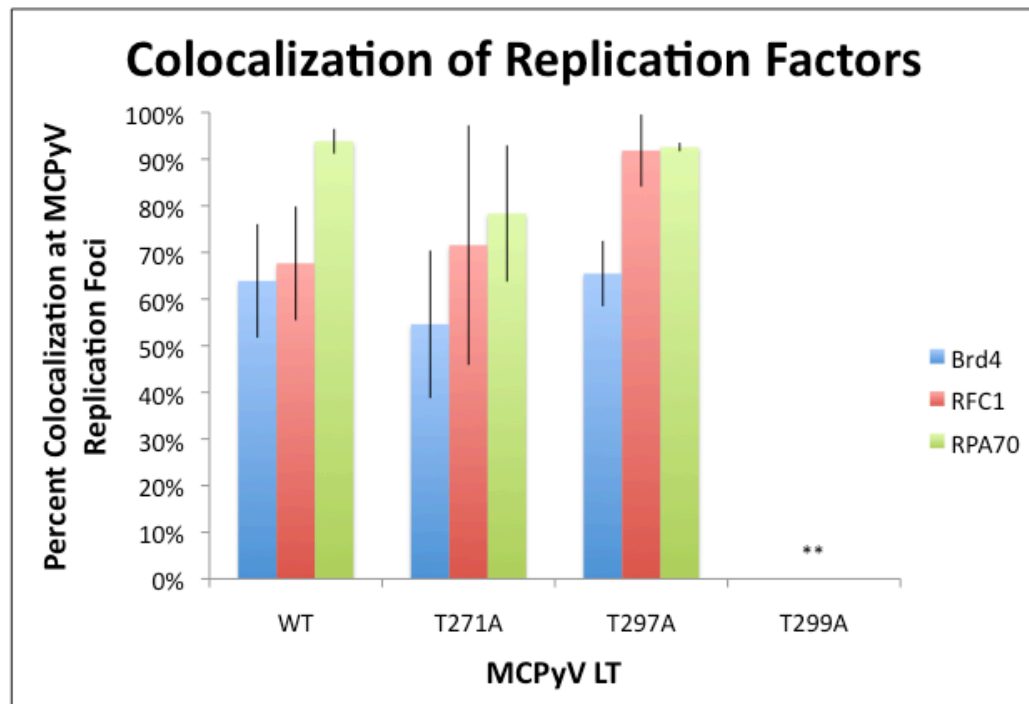


FIGURE 2.4: MCPyV phospho-mutant LT proteins recruit cellular factors to the same degree. Replication foci scored in Figure 2.3 A-C were assessed for colocalization of the indicated cellular factors. Bar indicates standard deviation from the mean from three independent experiments. A one-way ANOVA was performed to determine significance (** $p < 0.001$).

FIGURE 2.5

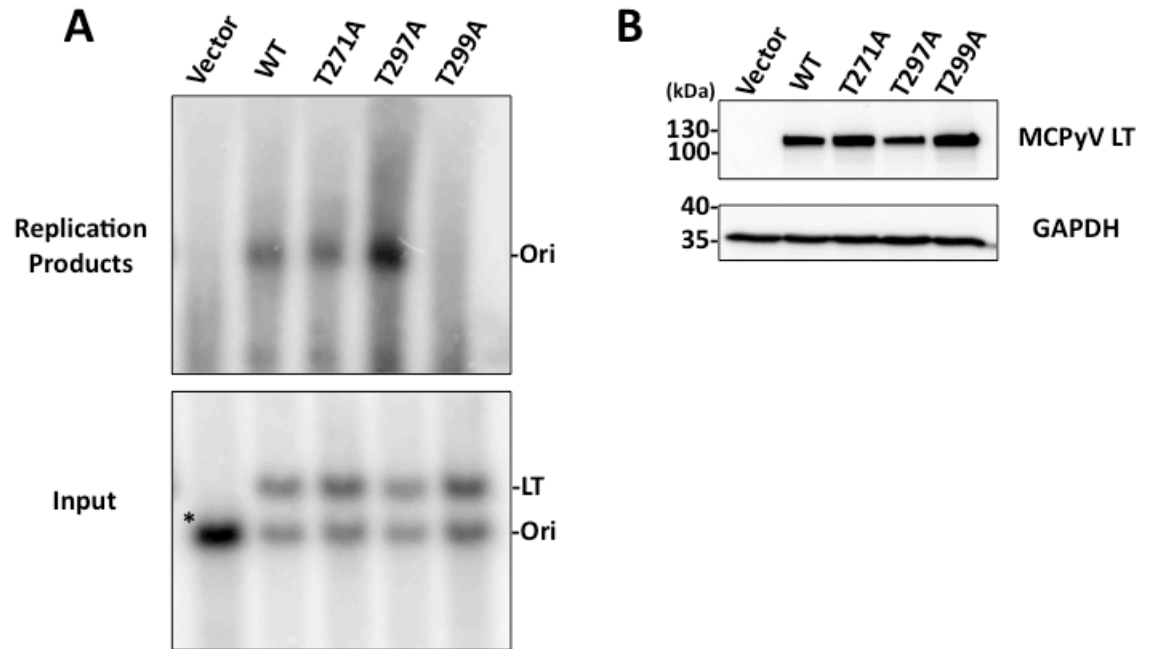


Figure 2.5: MCPyV LT phospho-mutant proteins replicate plasmids containing the viral Ori to differing degrees. C33A cells were co-transfected with a MCPyV Ori plasmid and the indicated MCPyV phospho-mutant LT. Forty-eight hours post transfection cells were split and extracted for total cellular DNA or total proteins. **(A)** Southern blotting of whole genomic DNA. Both the MCPyV Ori and MCPyV LT plasmids use the same vector backbone and are both recognized by the Southern blot probe. 15 μ g of DNA was digested with BamHI and DpnI to detect replicated origin plasmid (Replicated Products, top); replicated Ori plasmid is indicated. 2 μ g of DNA was digested with only BamHI to show equal loading (Input, bottom); Ori and LT plasmids are indicated. The vector control plasmid for LT is almost identical in size to the Ori plasmid, causing both plasmids to co-migrate in the blot (asterisk, first lane, bottom panel). **(B)** Total protein extracts were Western blotted to detect MCPyV LT and GAPDH. Southern and Western blots are representative of at least three experiments.

Figure 2.6: MCPyV LT phospho-mutants bind the viral Ori with different affinities.

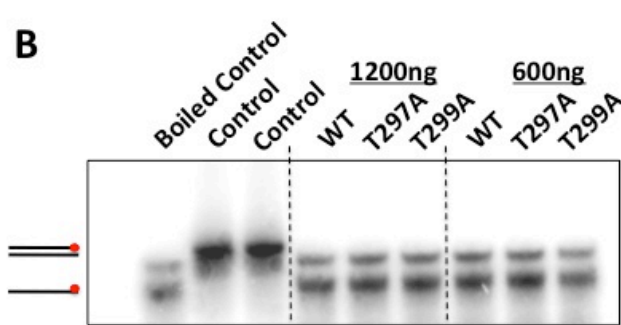
(A) Schematic of the MCPyV Ori and the EMSA Probe. Only one strand of DNA is shown for clarity. The MCPyV Ori sequence was cloned from the R17a isolate of MCPyV into a pcDNA4c vector (50). This origin was used for replication assays (Figure 2.3, 2.4, and 2.5). Consensus GAGGC pentanucleotide repeats which are recognized by the OBD of LT are marked with arrows and numbered as was reported by Kwun *et al.* (10). Arrows with dashed lines indicate imperfect pentanucleotides. The EMSA Probe was generated by PCR amplification of the indicated region of the MCPyV Ori. This PCR product was 5' end-labeled with [³²P-γ] ATP using T4 polynucleotide kinase (indicated by red asterisk). **(B)** Western blot of purified MCPyV proteins (0.25μg) used in EMSA. The buffer control contained residual TEV protease (also in LT samples). **(C)** Electromobility shift assays were performed with the EMSA probe in (A) and increasing amounts of MCPyV wild type or phospho-mutant LT affinity purified from HEK 293 cells. Reactions with buffer and residual TEV protease served as a negative control (first lane). Positions of free probe and LT bound probe are indicated. Data in (B) and (C) are representative of at least three experiments.

FIGURE 2.7

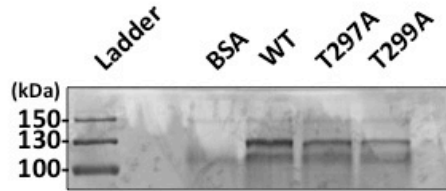
A



B



C



D

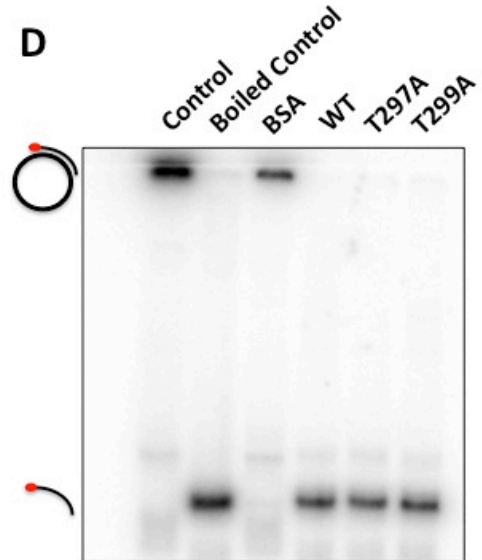


Figure 2.7: MCPyV LT phospho-mutants have similar unwinding and helicase activities. (A) Schematic of the Unwinding Probe. The Unwinding Probe was generated by annealing two complimentary oligonucleotides spanning the indicated sequence. The duplexed oligo contains a four-nucleotide overhang that was filled in by Klenow and [³²P- α] dCTP so that only one strand was labeled. The filled-in nucleotides are marked in bold, and the radiolabeled dCTP is indicated by an asterisk. The MCPyV Ori sequence depicted in Figure 2.6A is shown for reference. (B) Unwinding assays were performed with varying amounts of affinity purified MCPyV LT (wild-type or phospho-mutant). Samples without purified protein served as a negative control. One sample was boiled to show the migration of unbound probe. Data are representative of three independent experiments. (C, D) Constructs expressing affinity tagged MCPyV wild-type or phospho-mutant LT were transfected into 293 cells. Proteins were harvested 48 hrs post-transfection and LT was immunopurified on IgG-conjugated beads. Half of the beads with bound LT were boiled in sample buffer and resolved on an SDS-PAGE followed by Coomassie staining (C) while the remaining beads were used in the helicase assay (D). Beads incubated with 1% bovine serum albumin served as a negative control (BSA). Helicase reaction mix incubated at room temperature (Control) or at 95°C for 5min (Boiled Control) served as controls for partially duplex and unwound substrate, respectively. Data shown are representative of at least three independent experiments.

FIGURE 2.8

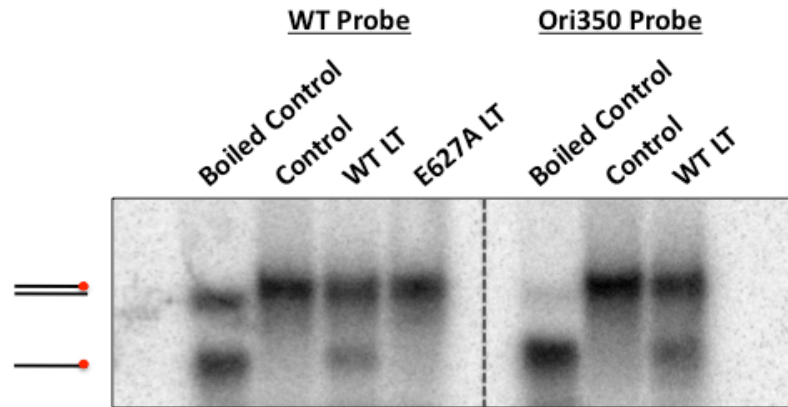


FIGURE 2.8: Unwinding assay performed with a helicase mutant LT and a mutated Ori probe. Unwinding assays were performed with both wild-type LT and the E627A mutation, which abolishes helicase activity. In parallel, an origin probe with a mutation in the seventh pentanucleotide repeat which abolishes origin-dependent replication (Ori350) was also tested using wild-type MCPyV LT. Data shown are representative of two repeats.

**CHAPTER 3: PHOSPHORYLATION OF MERKEL CELL POLYOMAVIRUS
LARGE T ANTIGEN AT SERINE 816 BY ATM KINASE INDUCES APOPTOSIS
IN HOST CELLS**

Dr. Jing Li was the primary investigator for this project, and was responsible for the design and execution of most of the experiments. I assisted in screening various LT truncation and point mutants to show that the C-terminal half of LT was recognized by the phospho-Chk1 antibody (Figure 3.1 and data not shown). I also designed and performed the CIP experiment to show that this cross-reactive antibody recognized a true phosphorylation mark, and helped confirm that S816 was the phosphorylation site (Figure 3.2). I later assisted in testing whether S816E was a phosphomimetic. Dr. Xin Wang assisted in performing the *in vitro* phosphorylation assay, while Sabrina Tsang assisted with the ATM pulldown experiment (Figure 3.4). All other experiments were performed by Jing. I prepared the manuscript and made major contributions to the experimental design of the manuscript.

Jing Li, Jason Diaz, Xin Wang, Sabrina H. Tsang, and Jianxin You. Phosphorylation of Merkel Cell Polyomavirus Large T Antigen at Serine 816 by ATM Kinase Induces Apoptosis in Host Cells. *Journal of Biological Chemistry* 2014; Epub Ahead of print DOI: 10.1074/jbc.M114.594895 © the American Society for Biochemistry and Molecular Biology

3.1: CHAPTER SUMMARY

During the preparation of an earlier manuscript (Jing Li *et al.*, *Journal of Virology* (2013) **87**: 9173-88), we noticed that an antibody raised against phosphorylated serine 345 of the cellular kinase Chk1 had cross reactive bands identical in size with ectopically expressed MCPyV LT constructs specifically retaining the C-terminus. We showed that this cross-reactivity was through a true phosphorylation mark sensitive to phosphatase treatment, and screened a number of candidate point-mutants to finally localize this mark to serine 816 of LT. Since the cross-reactive antibody targeted a kinase involved in the DDR, we asked whether phosphorylation of S816 was mediated by DDR pathways. Pharmacological treatment to activate and suppress various arms of the DDR, coupled with *in vitro* binding and kinase assays, indicated that the double-strand break repair kinase ATM was likely the cellular kinase for S816 phosphorylation. The c-terminal region of LT has been shown to have a growth-inhibitory effect, so we asked whether S816 phosphorylation contributed to this activity. A clonogenic assay showed that the alanine mutant S816A LT partially rescued the growth arresting properties of MCPyV LT. Analysis of molecular markers for apoptosis also showed less cell death with S816A. This study uncovered a novel phosphorylation site for MCPyV LT and identified a candidate cellular kinase responsible for this modification while also implicating growth arrest and apoptosis as functional consequences of this activity.

3.2: INTRODUCTION

Merkel cell polyomavirus (MCPyV) is a recently identified polyomavirus that is associated with a highly aggressive skin cancer MCC (6,8). MCPyV is associated with approximately 80% of MCC cases (6,9,106). MCC metastasizes rapidly. It is one of the most aggressive skin cancers with an extremely high mortality rate of 33%, exceeding the rate of melanoma (107), and less than 45% five-year survival rate (108). The incidence of MCC has increased from 1.5 to 6 per million people between 1986 and 2006, and approximately 1500 new cases of MCC are diagnosed each year in the United States (109,110). Epidemiological surveys of MCPyV antibodies and sequencing analyses of healthy human skin have indicated that MCPyV may represent a natural component of the human skin micro-flora (19,21,22).

Like other polyomaviruses, MCPyV encodes a single early gene, the Tumor antigen. The MCPyV Tumor antigen is multiply spliced into the Large Tumor antigen (LT), small Tumor antigen (sT), 57 kT, and ALTO (41,44). Similar to other polyomaviruses, the multi-functional MCPyV LT protein is involved in a variety of processes, including viral genome replication and host cell cycle manipulation (14,50,111).

MCPyV LT contains conserved features of other polyomavirus LT proteins, such as conserved region 1 (CR1), a DnaJ domain which interacts with Heat shock protein 70 (Hsc70) family members, an LXCXE pRb binding motif, an OBD, and a helicase/ATPase domain required for viral DNA replication (9,41). The T antigens from

several polyomaviruses have oncogenic activity. Notably, the simian virus 40 (SV40) large and small T antigens can transform a variety of rodent and human cells (31,112). In addition, LT from SV40 as well as the human polyomaviruses JCV and BKV can bind to pRb and p53 tumor suppressor proteins (113-116). MCPyV LT can bind specifically to pRb (9,32). While there are two potential p53 binding motifs on the MCPyV LT C-terminal domain, there appears to be no direct interaction between MCPyV LT and p53 (13,26). Interestingly, the MCPyV genome is commonly clonally integrated into MCC tumor cell genomes. Almost all MCPyV LTs expressed from the integrated MCPyV genomes harbor non-sense mutations, which result in expression of a truncated large T that retains the N-terminal pRb binding motif but deletes the C-terminal DNA binding and helicase domains (9).

It has been postulated that these truncated LT proteins arise because replication of the integrated viral genome by full-length MCPyV LT may instigate a debilitating amount of DNA damage due to abortive replication at the integrated viral origin (9). The identification of a tumor with intact, full length LT but a mutated viral origin sequence supports this hypothesis (10). Later studies have since suggested that the C-terminal helicase domain may contain other functions that oppose tumorigenesis (13,14). Our previous work indicates that expression of full-length MCPyV LT activates a dramatic DDR that is antagonistic to tumorigenesis; this activity activates p53 and induces a growth-inhibition phenotype (14). Additionally, Cheng *et al.* reported that expression of the C-terminal 100 residues of MCPyV LT could inhibit the growth of several different cell types (13). These studies support a model where the C-terminal domain must be

deleted in tumor cells to both limit viral replication from the integrated viral genomes, and eliminate growth-arresting properties intrinsic to the C-terminal domain of LT. How the MCPyV C-terminal 100-residues accomplishes this growth-arresting function is not clearly understood.

In addition to being stimulated by MCPyV LT expression, work from our lab has shown that components of the host DDR are recruited to viral replication centers (49). These factors were necessary for supporting MCPyV genome replication (49), but their mechanism of action was not understood. Protein phosphorylation of serines (S), threonines (T), and tyrosines is one of the most common methods for regulating protein function. Phosphorylation of SV40 LT on both serine and threonine residues plays an important role in regulating LT antigen function. Phosphorylation of SV40 LT S120 and S123 inhibits viral replication, while phosphorylation of T124 enhances replication by activating the DNA binding domain and stimulating double-hexamer activity (71,72,81,117,118). Phosphorylation of T701 is required for binding to the host FBW7 gamma isoform, which regulates SV40 LT protein stability (119). The studies presented in Chapter 2 identified T271, T297 and T299 as phosphorylation sites on MCPyV LT. In that study, we demonstrated that phosphorylation of T297 and T299 regulates MCPyV LT-mediated replication of the viral DNA. In this current study, we identify a novel MCPyV LT phosphorylation site at S816. We demonstrate that this site is phosphorylated by ataxia telangiectasia mutated (ATM) kinase, a key component of the host DDR primarily activated by dsDNA breaks (DSBs) (120). Activation of ATM kinase by etoposide increases MCPyV LT phosphorylation at S816. In contrast, Ataxia-

telangiectasia and Rad3 related (ATR) kinase was unable to robustly phosphorylate MCPyV LT. Expression of wild-type MCPyV LT inhibits cell proliferation and also induces several cell lines to undergo apoptosis. Expression of the serine to alanine substitution mutant MCPyV LT S816A partially rescues this growth inhibition and also inhibits the induction of apoptosis. This report reveals that MCPyV LT is a substrate of ATM kinase, and that phosphorylation at S816 contributes to the regulation of host cell proliferation and apoptosis.

3.3: RESULTS

3.3.1: MCPyV LT is Phosphorylated at S816

In our previous study, we found that either MCPyV infection or transfection of MCPyV genomes into cells activated both ATM and ATR kinases, while ectopic expression of just MCPyV LT primarily induced the ATR-Chk1 DDR pathway in U2OS cells (14). Interestingly, in these immunoblotting experiments we also discovered that the anti phospho-Chk1 S345 antibody not only detected phospho-Chk1 S345 but also recognized protein bands with molecular weights that match those of transfected LT 1-817, LT 212-817, GFP-LT 441-817 or GFP-LT 1-817, respectively (Figure 3.1A and B, bands with an arrow). This cross-reactivity was observed for all MCPyV LT truncation mutants retaining the carboxyl terminal ~400 amino acids (Figure 3.1A and B). These cross-reactive bands were also detected in C33A and HeLa cells (data not shown). This antibody also recognized another cross-reactive band of about 120 kD in all samples, regardless of LT expression (Figure 3.1B, band marked with an asterisk). SV40 LT also activated phospho-Chk1 S345 in U2OS cells (14), but there were no cross-reactive bands

detected in the SV40 LT sample (Figure 3.1A). Since the cross-reactive bands (marked with an asterisk) had similar molecular weights as the ectopically expressed LTs in those samples, we suspected that the anti-pChk1 S345 antibody specifically cross-reacts with MCPyV LT.

To confirm that this cross-reaction was mediated by a true phosphorylation modification, lysates from U2OS cells transfected with pcDNA4C-MCPyV LT were treated with or without calf-intestinal alkaline phosphatase (CIP) for 30 minutes, and analyzed by Western blot. As shown in Figure 3.2A, expression of LT 1-817 activates a robust phospho-Chk1 S345 signal in U2OS cells, and there is again a cross-reactive band with a molecular weight around 110 kD that matches the size of full-length MCPyV LT. Treatment with CIP significantly diminished both the phospho-Chk1 and the 110 kD cross-reactive signal (marked with an arrow) in the cell lysate (Figure 3.2A). Interestingly, the other cross-reactive band of about 120 kD (marked with an asterisk) was also diminished. This result suggests that the phospho-Chk1 S345 antibody recognizes a true phosphorylation modification on both the 110 kD and 120 kD cross-reactive bands.

Chk1 is phosphorylated by ATR kinase at S345 in a canonical S/T-Q epitope that is commonly targeted by ATM and ATR kinases. Assuming the cross-reactive band similar to transfected LT was indeed MCPyV LT, the data from Figure 3.1 suggested that the phosphorylation site was within the C-terminal 400 amino acids. We compared the epitope recognized by the phospho-Chk1 S345 antibody with the C-terminal sequence of

MCPyV LT and generated alanine substitutions of several potential phosphorylation sites. These point mutants were transfected into U2OS cells and immunoblotted with the pChk1 S345 antibody. Out of all the sites analyzed, we found that mutagenesis of S816 alone abolished MCPyV LT cross reactivity with the phospho-Chk1 S345 antibody (Figure 3.2B and data not shown). The 120 kD cross-reactive band was unaffected when cells were transfected with this mutant LT. Taken together, these data demonstrate that MCPyV LT is phosphorylated at S816, and that this phosphorylation is specifically recognized by the pChk1 S345 antibody. The 120 kD band (marked with an asterisk) is likely a cellular phospho-protein that is also recognized by this antibody; however, we chose to focus the remainder of our study on the phosphorylation of MCPyV LT at S816.

3.3.2 Activation of ATM Stimulates MCPyV LT S816 Phosphorylation

Having identified S816 as a phosphorylation site of MCPyV LT, we next sought to determine which kinase(s) or kinase pathway(s) was responsible for this modification. Our previous data showed that MCPyV virus infection and MCPyV genome transfection activate both ATM and ATR DNA damage response pathways. In contrast, ectopic expression of MCPyV LT alone predominantly activates ATR and only weakly activates ATM (14,49). Additionally, we have reported that components of the host DDR pathways are recruited to viral replication centers, and that their activity is required for efficient replication (49). We wondered whether components of these DDR pathways could be responsible for LT S816 phosphorylation.

We first used etoposide or UV light to activate either ATM or ATR pathways, respectively, and tested whether phosphorylation of LT was altered. U2OS cells were transfected with pcDNA4C (Vec) or pcDNA4C-MCPyV LT. Forty-four hours post transfection, cells were treated with either 4 μ M etoposide for another 4 hours or treated with 10 J UVC light. The cells were then harvested for Western blot analysis. As shown in Figure 3.3A, expression of LT induced a mild activation of both ATM S1981 phosphorylation and Chk1 S345 phosphorylation, a surrogate of ATR activation (compare lane 4 to lane 1 in Figure 3.3A). Etoposide treatment, which primarily activates ATM kinase, induced dramatic activation of ATM S1981 phosphorylation as well as LT phosphorylation at S816 (Figure 3.3A, lane 5). In contrast, UV light treatment, which predominantly activates ATR, caused a much smaller degree of ATM phosphorylation and very little activation of LT S816 phosphorylation compared to DMSO treatment (Figure 3.3A, compare lane 6 to lane 4). These results demonstrated that activation of the host ATM DDR pathway could stimulate phosphorylation of MCPyV LT at S816. Robust phosphorylation of Chk1 S345 was seen with both etoposide and UV treatments, indicating either that ATR was activated in both settings, or that the robust activation of ATM during etoposide treatment allowed it to phosphorylate Chk1 through cross talk (121-124).

3.3.3: Inhibition of ATM Prevents MCPyV LT S816 Phosphorylation

We next sought to determine which component(s) of the host DDR was responsible for phosphorylating MCPyV LT. We tested a panel of chemical inhibitors to screen for the possible kinases that phosphorylate MCPyV LT at S816. U2OS cells were

transfected with pcDNA4C (Vec) or pcDNA4C-MCPyV LT. Forty-four hours later, cells were treated with DMSO, Wortmannin, NU 6027, NU 7441, KU 55933, AZD 7762, or caffeine for another six hours. The cells were harvested for Western blot analysis. As shown in Figure 3.3B, the expression level of LT is constant with different drug treatments. MCPyV LT transfected cell lysates show phosphorylated MCPyV LT S816 bands at around 110 kD; however, the band density changes with various drug treatments (Figure 3.3B). Caffeine, which inhibits both ATM and ATR, reduced phosphorylation of LT S816 to a small extent (Figure 3.3B). Wortmannin, which acts as a broad PI3K inhibitor that inhibits DNA-PK, ATM, and ATR, efficiently inhibited MCPyV LT S816 phosphorylation (Figure 3.3B). On the other hand, the ATR inhibitor NU 6027, the DNA-PK inhibitor NU 7441, and the Chk1 inhibitor AZD 7762, did not affect LT phosphorylation (Figure 3.3B). These results suggest that the ATM pathway was likely important for the LT S816 phosphorylation. Further supporting this notion, the ATM inhibitor KU 55933 caused dramatically reduced LT S816 phosphorylation (Figure 3.3B). These experiments were repeated in C33A cells with similar results (data not shown). Taken together, these data suggest that ATM is likely the kinase that phosphorylates MCPyV LT at S816.

3.3.4: ATM Kinase Binds and Phosphorylates MCPyV LT at S816 In Vitro

We then performed *in vitro* phosphorylation experiments to more directly confirm that ATM kinase phosphorylates MCPyV LT at S816. An IgG-IgG-TEV (IIT) affinity tag, comprising two IgG binding domains and a tobacco etch virus (TEV) cleavage site, was subcloned in-frame with wild type and S816A mutant MCPyV LT for affinity

purification (See Materials and Methods and (50)). IIT affinity tagged wild type MCPyV LT or S816A LT was purified from 293 cells and treated with CIP to remove phosphorylation modifications. In parallel, U2OS cells were stimulated with etoposide to activate the host DDR, and either ATM or ATR kinases were immunoprecipitated from nuclear extracts (Figure 3.4A). ATM or ATR was then immunoprecipitated and immobilized on sepharose beads and incubated with radiolabeled ATP and equal amounts of either wild type LT or LT S816A protein in kinase reaction buffer. Only wild type LT incubated with immunopurified ATM demonstrated significant phosphorylation; incubation with ATR did not show detectable activity above background (Figure 3.4A). This was true when the *in vitro* phosphorylation reaction was performed either at room temperature or at 37°C. The S816A LT was not phosphorylated by either ATM or ATR kinases, regardless of temperature (Figure 3.4A). We also confirmed that LT could interact with ATM by pulling down ATM kinase from U2OS nuclear extracts using immobilized, bacterially derived LT (Figure 3.4B). This binding was clearly evident even with a relatively small amount of LT (Figure 3.4B, compare GST with GST-LT in the CBB stain). These data, together with the kinase inhibitor screen shown in Figure 3.3B, strongly suggest that ATM is the major kinase that phosphorylates MCPyV LT at S816.

3.3.5: Prevention of MCPyV LT S816 Phosphorylation Partially Rescues the MCPyV LT Growth Inhibition Effect

We next sought to better understand the physiological function of the ATM-mediated MCPyV LT S816 phosphorylation. We were unable to find defects in genome

replication or viral gene transcription for MCPyV LT S816A (data not shown). Our previous study demonstrated that the C-terminal portion of LT activates p53 and promotes growth inhibition (14). Cheng *et al.* also reported that the C-terminal 100 amino acids of MCPyV LT have a cell growth inhibition effect (13). The underlying mechanism of these findings was not completely established. Since the C-terminal domain of MCPyV LT was sufficient for DDR activation (14), and because S816 lies within the C-terminal 100-amino acids region of MCPyV LT, we asked whether S816 phosphorylation played a role in the cellular growth inhibition function of the MCPyV LT C-terminus. We generated C33A cells stably expressing wild type MCPyV LT, S816A LT, or Cherry-LacI as a negative control. Using these cell lines, we performed a clonogenic assay to detect the long-term effect of MCPyV LT and MCPyV LT S816A on cellular proliferation. The same number of C33A stable cells were seeded in 6-well dishes and cultured for 10 days under puromycin selection. As shown in Figure 3.5, the Cherry-LacI stable cell line forms a large number of colonies. As reported previously (14), expression of wild type MCPyV LT caused a significant inhibition of cell growth, resulting in drastically reduced colony number after selection (Figure 3.5). S816A LT partially reversed this LT growth inhibition phenotype, allowing more colonies to be formed after the extended culture period (Figure 3.5). This result suggests that blocking MCPyV LT S816 phosphorylation can partially rescue the LT growth inhibition activity, demonstrating the impact of MCPyV LT S816 phosphorylation on cellular proliferation.

3.3.6: MCPyV LT S816A Induces Less Apoptosis Than Wild-Type MCPyV LT

We consistently observed that transfection of the MCPyV LT S816A construct led to less cell death than the wild-type MCPyV LT construct. The results of the clonogenic assay also suggested that S816A LT might induce less cell death than wild type MCPyV LT. We therefore tested both proteins for their ability to induce apoptosis. We performed Annexin V staining to detect cells that express phosphatidylserine (PS) on the cell surface, which is an early marker of apoptosis (125). GFP tagged MCPyV LT or MCPyV LT S816A was transfected into C33A cells. The transfected cells were stained with PE conjugated Annexin V at 24 hours post transfection. Cells were then fixed and nuclei were counterstained with DAPI. At this time point, about 0.2% of vector transfected cells have Annexin V staining, while 6.5% of MCPyV LT transfected cells show positive Annexin V staining; however, only 3.8% of MCPyV LT S816A transfected cells were Annexin V positive (Figure 3.6A and B). This result shows that MCPyV LT S816A has decreased ability to induce cell death than MCPyV LT. Flow-cytometry analysis also detected slightly more apoptotic cells with sub-G1 fraction in wild type MCPyV LT transfected cells than in LT S816A samples (data not shown). These results are consistent with the observation that MCPyV LT can more potently inhibit cell proliferation than S816A LT (Figure 3.5).

To examine the differential activation of cell death by wild type MCPyV LT and S816A LT at the molecular level, we performed Western blotting analyses to detect the apoptotic marker Caspase-3 and Poly (ADP-ribose) polymerase 1 (PARP1). Caspase-3 is activated in both the extrinsic (death ligand) and intrinsic (mitochondrial) apoptotic

pathways (126,127). In the intrinsic activation pathway, cytochrome-c from the mitochondria works in combination with caspase-9, apoptosis-activating factor 1 (Apaf-1), and ATP to process pro-Caspase-3 (128-130). Proteolytic processing of the inactive zymogen into p17 and p12 fragments activates Caspase-3. PARP1 is involved in the repair of DNA damage by adding poly (ADP-ribose) polymers onto a variety of substrates in response to various cellular stresses (131). PARP1 is also a substrate for caspases; during the execution phase of apoptosis, PARP1 is specifically proteolyzed by Caspase-3 to produce a 24 kD N-terminal DNA binding domain (DBD) and a 89 kD C-terminal catalytic fragment (132). Cleavage of PARP1 by caspases is considered to be a hallmark of apoptosis (133,134).

We transfected either C33A or HeLa cells with pcDNA4C (Vector), pcDNA4C-MCPyV LT, or pcDNA4C-MCPyV LT S816A. Cells were harvested at 30 hours post transfection and analyzed by Western blotting. As shown in Figure 3.6C and D, expression levels of LT and LT S816A are similar. Vector transfected cells did not exhibit cleaved Caspase-3 and only showed background level of cleaved PARP1, indicating little apoptosis in these conditions (Figure 3.6C and D). Wild type LT transfected cells have less intact PARP1, but more cleaved PARP1 as well as more cleaved Caspase-3 than the empty vector samples, confirming the induction of apoptosis (Figure 3.6C and D). In contrast, the levels of cleaved PARP1 and cleaved Caspase-3 in the MCPyV LT S816A transfected cells were reduced to nearly the vector control level (Figure 3.6C and D). These results are consistent with the observation that MCPyV LT-positive cells are more likely to undergo apoptosis than MCPyV LT S816A-positive cells

(Figure 3.6A and B). These results support the rescue of cell growth inhibition phenotype seen in the clonogenic assay (Figure 3.5). We also tested whether the S816E mutant would act as a phosphomimetic, and presumably induce more apoptosis. Unfortunately, LT S816E behaved identically to the alanine mutant and therefore was not a viable phosphomimetic (data not shown); this phenomenon has occasionally been reported for other phosphoproteins, including SV40 LT and MCPyV LT at other phosphosites (135,136). Taken together, these data suggest that phosphorylation of LT at S816 contributes to growth-arrest and apoptotic induction mediated by the C-terminal domain.

3.4: DISCUSSION

Most MCPyV-related MCC tumors examined thus far contain clonally integrated MCPyV genomes, which express truncated LT proteins that omit the C-terminal domain (9). This observation suggests a strong selective pressure to eliminate the C-terminal region of MCPyV LT during MCC tumor development. These tumor specific mutations do not affect LTs pRb binding domain or DnaJ domain (6). In fact, these LT mutants even have an increased affinity for pRb (26). Work from our lab and others suggest that the C-terminal domain of MCPyV LT might be negatively selected during tumorigenesis to eliminate growth inhibitory properties encoded in this region (13,14).

Our previous report shows that inhibition of cellular proliferation by the C-terminal half of MCPyV LT is linked to its ability to activate the host DDR pathways (14). In those experiments, we consistently detected cross-reactivity of the monoclonal anti-pChk1 S345 antibody when MCPyV LT constructs were expressed. In this report,

we explored the nature of this cross-reactivity. The cross-reactive bands correlated with the sizes of ectopically expressed full-length MCPyV LT or LT C-terminal mutants (Figure 3.1), and were sensitive to phosphatase treatment (Figure 3.2A), making us suspect that this antibody recognized a phosphorylation modification on MCPyV LT. This cross-reaction seemed to be localized to the C-terminal half of the protein (Figure 3.1). Alanine substitutions of candidate serines and threonines further identified S816 as the target of phospho-Chk1 S345 cross-reaction (Figure 3.2B).

Our previous studies demonstrated that MCPyV LT activates the host DDR proteins, which are recruited to actively replicating viral genomes (14,49). The cross-reactive phospho-Chk1 S345 antibody was generated against Chk1 phosphorylated at serine 345, an ATR kinase phosphorylation site. We therefore asked whether the DDR kinases were responsible for the phosphorylation of MCPyV LT at S816. Activation of ATM kinase with etoposide caused dramatic stimulation of MCPyV LT phosphorylation. On the other hand, UV treatment, which predominantly activates the ATR pathway, had little stimulating effect on MCPyV LT S816 phosphorylation (Figure 3.3A). A screen with multiple DDR kinase inhibitors further supported the hypothesis that ATM kinase was the predominant member of the DDR pathways responsible for this modification (Figure 3.3B). *In vitro* phosphorylation of MCPyV LT with immunopurified ATM and ATR confirmed that ATM phosphorylates MCPyV LT at S816, but ATR cannot (Figure 3.4A). Additional pull-down experiments suggested that ATM and LT can indeed interact (Figure 3.4B). Together with our published results (14,49), this present study suggests that MCPyV is not only able to induce DDR in cells but can also take advantage

of this DDR activity and recruit a cellular DDR kinase, ATM, to phosphorylate its own LT at S816.

We next sought to understand the physiological role of this phosphorylation mark. Although S816 lies C-terminal to the helicase domain, no effects were seen on viral genome replication or transcription (data not shown). We therefore asked whether LT S816 phosphorylation contributes to the growth inhibitory activity that was localized to the final 100 residues of this protein (13). Interestingly, the growth inhibitory effect seen with wild type LT was partially reversed with LT S816A in a clonogenic assay (Figure 3.5). The cellular proliferation phenotype was supported by an analysis of apoptosis during LT expression. Annexin V staining and Western blot analyses of Caspase-3 and PARP1 cleavage showed that S816A LT induced less apoptosis in transfected cells (Figure 3.6). These results demonstrated that the ATM-mediated phosphorylation of MCPyV LT at S816 contributes to a mechanism that inhibits cellular proliferation by inducing cellular death.

Although this study establishes a direct functional interaction between ATM kinase and MCPyV LT, the precise role for this interaction remains elusive. ATM is a serine/threonine protein kinase that is recruited to and activated by DNA double-strand breaks to phosphorylate several key cellular proteins that initiate the activation of the DNA damage checkpoint (137-139). This checkpoint activation results in the phosphorylation and activation of p53, which in turn up-regulates the expression of key cellular factors involved in cell cycle arrest, DNA repair, and apoptosis (137-139). The

cell proliferation effects reported here when MCPyV LT is expressed could therefore be partially due to ATM activity and represent a host response to foreign DNA replication; indeed, the effects of blocking MCPyV LT S816 phosphorylation on cell proliferation are modest and S816A LT was unable to fully rescue the proliferative defect in C33A cells stably expressing LT (Figure 3.5), indicating that S816 phosphorylation-independent mechanisms are at play.

Our previous report and current study show that transfected LT only induces a very low level of ATM activation (Figure 3.3A and (14)). In contrast to transfected LT alone, infection with MCPyV virions or transfection of viral genomes robustly activates ATM (14); additionally, LT protein levels increase over time in these settings (data not shown). During true infection, therefore, the ATM-mediated MCPyV LT S816 phosphorylation may lead to a more robust cell-cycle arrest and apoptotic phenotype, which may be advantageous in dispersing newly formed virions late in infection. Alternatively, this ATM-mediated MCPyV LT S816 phosphorylation and associated apoptotic activities may represent a host antiviral defense mechanism for eliminating MCPyV infected cells.

It is also important to note that our study only examined LT when it is expressed alone. Whether LT phosphorylation is altered or temporally regulated when co-expressed with other viral proteins like sT, 57kT, or ALTO remains to be explored. Our previous study established the DDR machinery as critical for LT mediated viral replication (49). This study further establishes an intimate interaction between MCPyV infection and the

host DDR, revealing how activation of a host DDR by MCPyV is then utilized by the virus to carefully orchestrate key events in host cells. Future studies will investigate the downstream events of MCPyV LT S816 phosphorylation by identifying the cellular proteins that may recognize this phosphorylation event. The identification of the S816 phosphorylation site and the commercial availability of an antibody recognizing this modification provide valuable tools for advancing our understanding of MCPyV-host interactions.

3.5: FIGURES

FIGURE 3.1: Anti phospho-Chk1 S345 antibody cross-reacts with MCPyV LT. (A) U2OS cells were transfected with pcDNA4C (Vector), pcDNA4C encoding Xpress tagged MCPyV LT molecules as indicated, or pTIH encoding SV40 LT. At 36 hours post transfection, cells were lysed and immunoblotted with the indicated antibodies. Arrows indicate cross-reactive bands corresponding to the molecular weight of the transfected LT molecule. **(B)** U2OS cells were transfected with pEGFPC1 (Vector), or pEGFPC1 encoding MCPyV LT molecules as indicated. At 36 hours post transfection, cells were lysed and immunoblotted with the indicated antibodies. Arrows denote cross-reactive bands matching the molecular weight of the transfected LT molecules as indicated in (A). Asterisks (*) indicate an additional cross-reactive band present in U2OS cells regardless of LT expression.

FIGURE 3.2

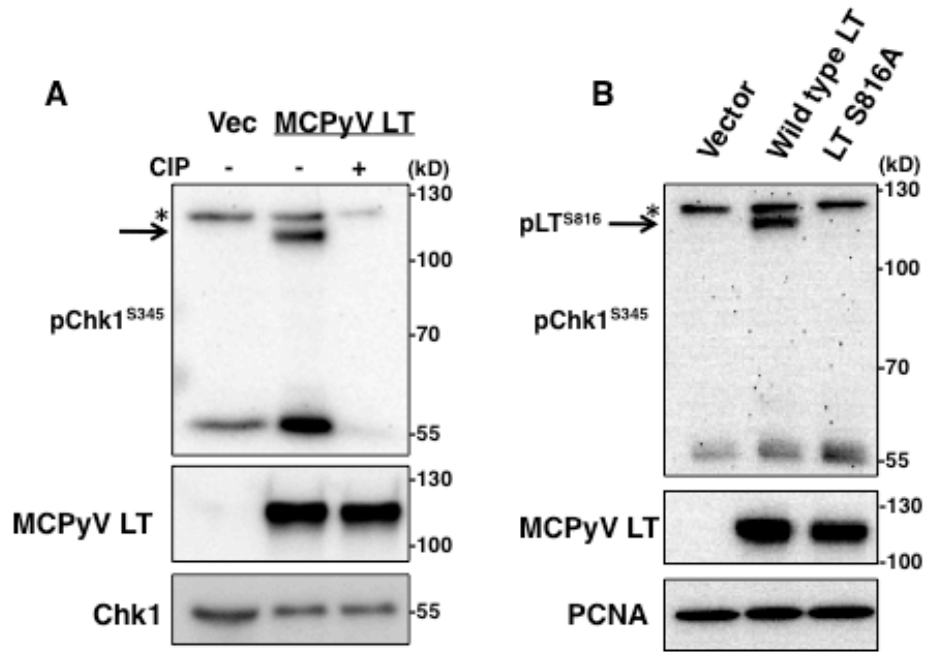


FIGURE 3.2: MCPyV LT is phosphorylated at S816. (A) U2OS cells were transfected with pcDNA4C vector (Vec) or pcDNA4C-MCPyV LT. Forty-eight hours post transfection, cells were treated with or without Calf-intestinal alkaline phosphatase (CIP) and analyzed by Western blot. Asterisk and arrow indicate cross-reactive bands as described in Figure 3.1. (B) U2OS cells were transfected with pcDNA4C (Vector), pcDNA4C-MCPyV LT1-817 (wild type LT), or pcDNA4C-MCPyV LT 1-817 S816A (LT S816A). Forty-eight hours post transfection, cells were harvested and proteins were analyzed by Western blot with the indicated antibodies. Asterisk and arrow indicate cross-reactive bands as described in Figure 3.1.

FIGURE 3.3

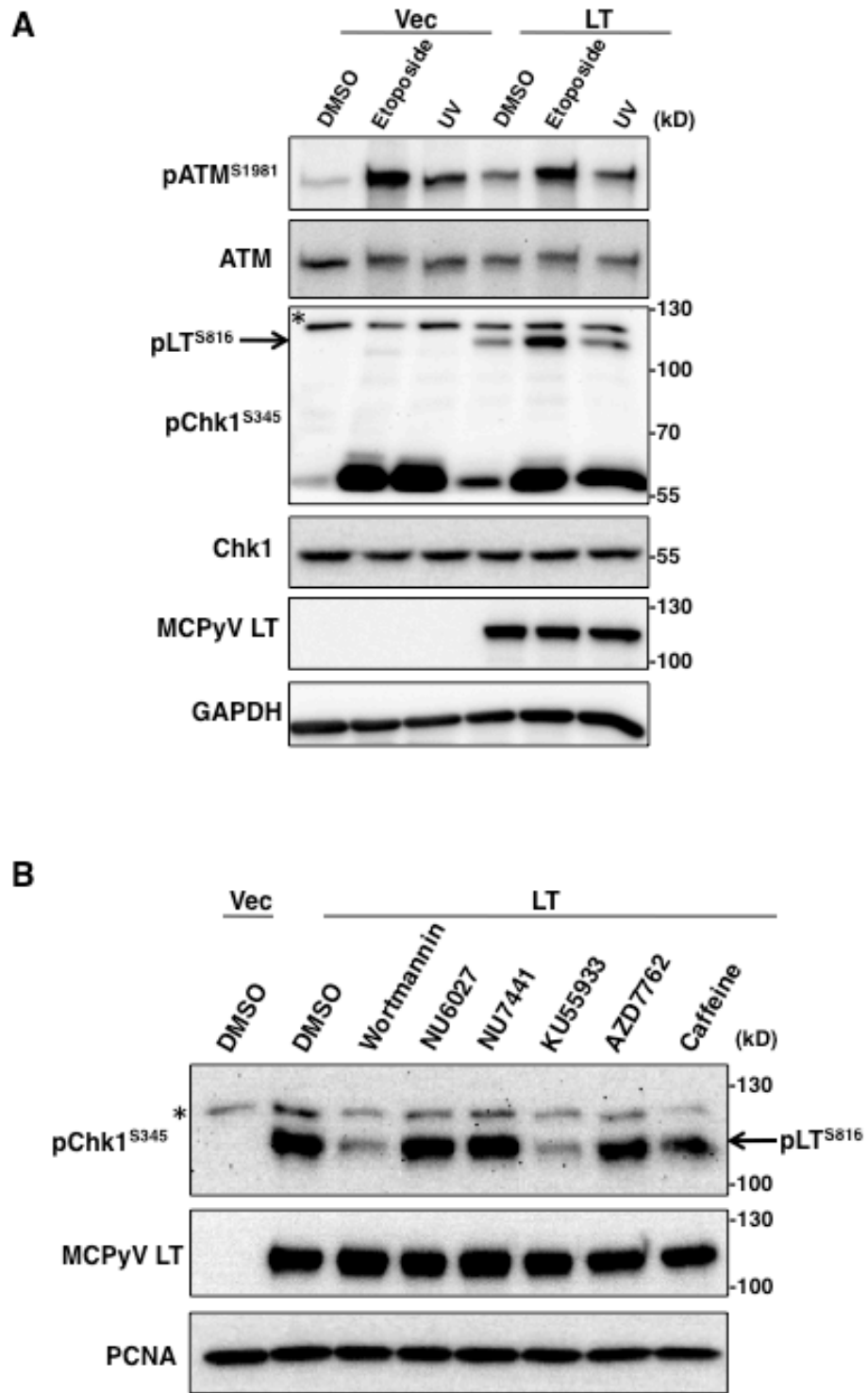


FIGURE 3.3: ATM kinase phosphorylates MCPyV LT at S816. (A) U2OS cells were transfected with pcDNA4C vector (Vec) or pcDNA4C-MCPyV LT (LT). At forty-four hours post transfection, cells were treated with 4 μ M etoposide for 4 hours or 10J UVC light. Cells were then harvested and analyzed by Western blot with the indicated antibodies. Asterisk and arrow indicate cross-reactive bands as described in Figure 3.1. **(B)** U2OS cells were transfected with pcDNA4C (Vec), or pcDNA4C-MCPyV LT1-817 (LT). At 44 hours post-transfection, cells were treated with DMSO, 20 μ M Wortmannin, 20 μ M NU6027, 1 μ M NU7441, 10 μ M KU55933, 10 nM AZD7762, or 10 mM Caffeine for 6 hours. Then cells were harvested and proteins were analyzed by Western blot with indicated antibodies. Asterisk and arrow indicate cross-reactive bands as described in Figure 3.1.

FIGURE 3.4

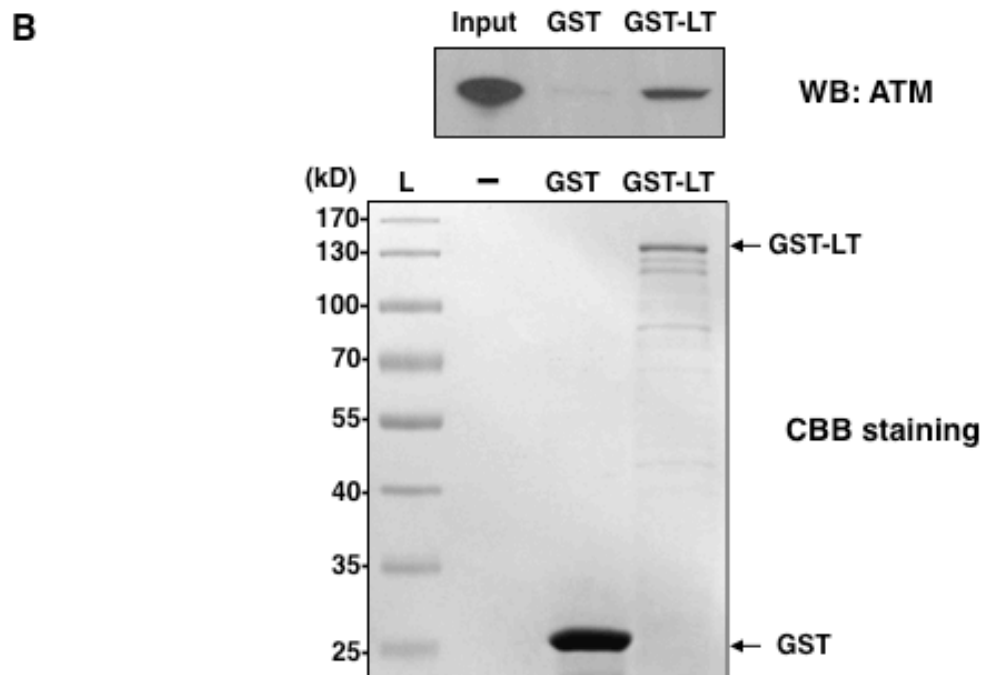
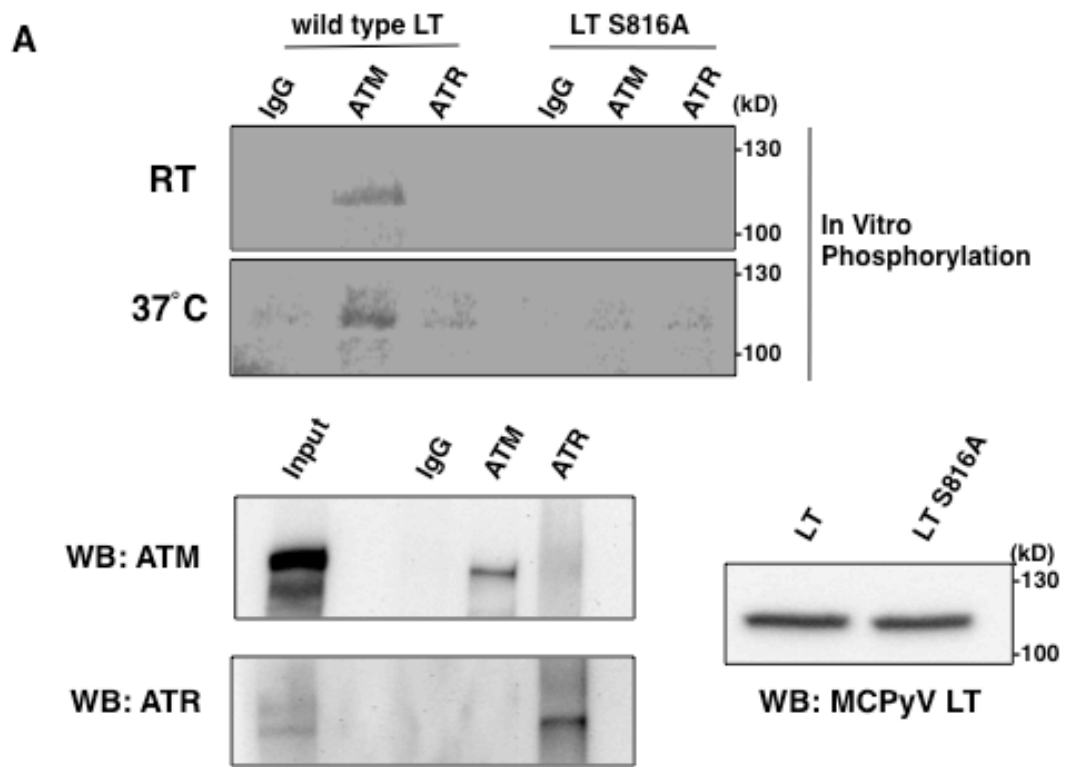


FIGURE 3.4: ATM can bind and phosphorylate LT *in vitro*. (A) *In Vitro* phosphorylation of MCPyV LT S816 by ATM. Affinity-tagged MCPyV LT or MCPyV LT S816A was purified from 293 cells and treated with CIP. ATM and ATR proteins were immunoprecipitated from U2OS cells which had been treated with 4 μ M etoposide for 4hr. Purified LT was then incubated with purified ATM or ATR in kinase reaction buffer supplemented with [γ - 32 P] ATP. Reactions were performed either at room temperature (RT) or 37°C for 30min. Reactions were separated by SDS-PAGE and then either dried and exposed for autoradiography (top) or Western blotted for MCPyV LT (bottom, right). Immunopurified ATM and ATR proteins were Western blotted with the indicated antibodies (bottom, left). (B) GST-LT pull-down of ATM. U2OS nuclear extracts were mixed with either immobilized, bacterially-derived GST or GST-LT protein. Input nuclear extract and pull-down samples were immunoblotted with anti ATM antibody (top). GST or GST-LT eluted from the glutathione resin was separated by SDS-PAGE and stained with Coomassie Brilliant Blue (CBB) (bottom). “L” – molecular weight ladder. “–” – empty lane.

FIGURE 3.5

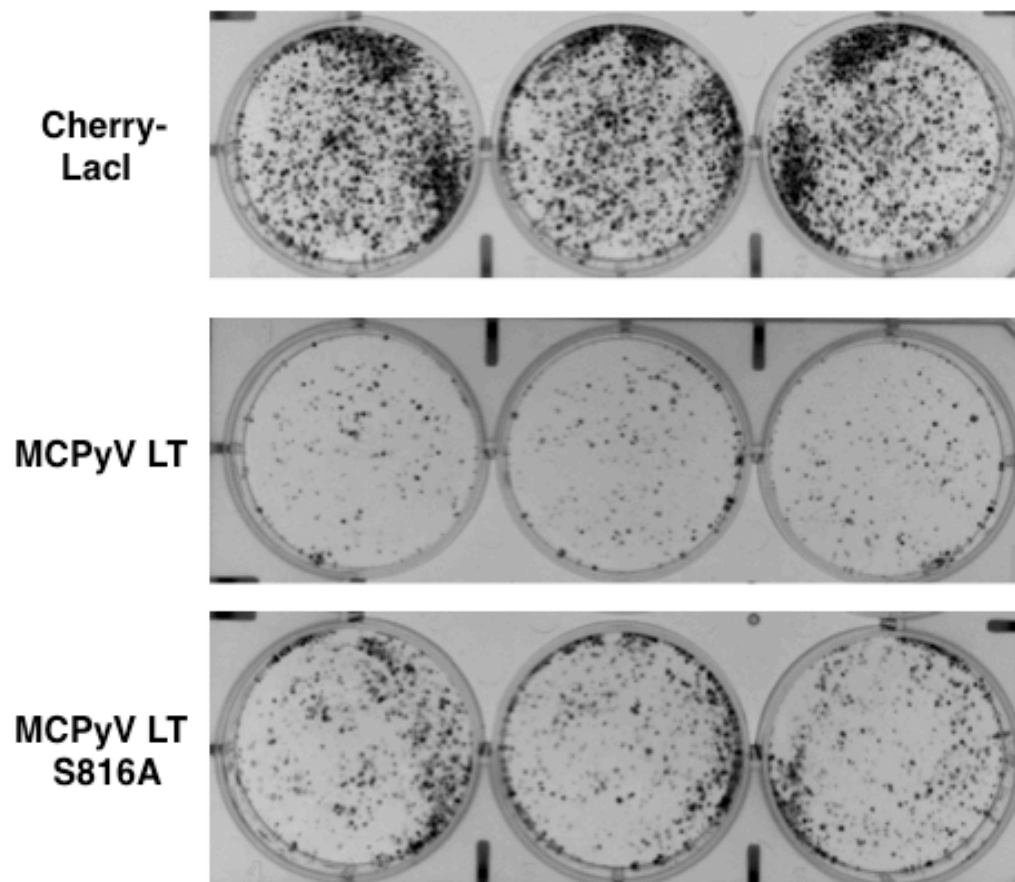


FIGURE 3.5: C33A cells stably expressing MCPyV LT S816A form more colonies than cells stably expressing wild-type LT. C33A cells stably expressing Cherry-LacI, MCPyV LT or MCPyV LT S816A were seeded at 5000 cells/well in a 6 well plate. Cells were cultured for 10 days with 0.625 µg/ml puromycin. Colonies were then fixed with methanol and stained with methylene blue. Data shown are representative of at least three experiments.

FIGURE 3.6

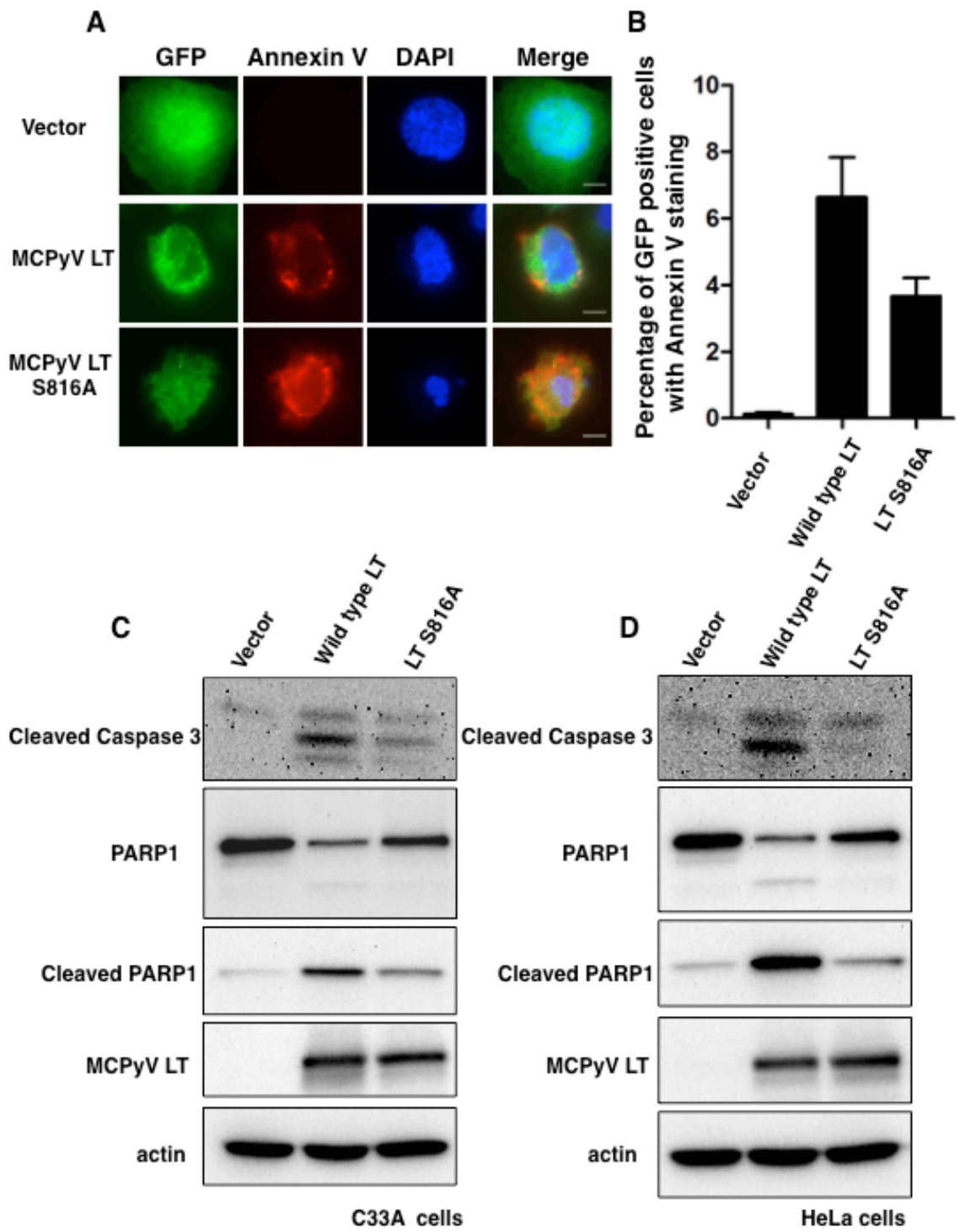


FIGURE 3.6: MCPyV LT induces more apoptosis than LT S816A. (A) C33A cells were transfected with pEGFPC1 (Vector), pEGFPC1-MCPyV LT, or pEGFPC1-MCPyV LT S816A. Twenty-four hours later, cells were stained with Annexin V-PE and DAPI. Images are representative of at least three experiments. Bar, 10 μ m. (B) The percent of GFP positive cells with Annexin V staining was quantified from approximately 100 cells. The mean and standard deviation (SD) was calculated from three cover slips. (C and D) C33A (C) and HeLa (D) cells were transfected with pcDNA4C (Vector), pcDNA4C-MCPyV LT, or pcDNA4C-MCPyV LT S816A. Cells were harvested at thirty hours post transfection and cell lysates were analyzed by Western blot with the indicated antibodies.

**CHAPTER 4: MERKEL CELL POLYOMAVIRUS LT AND ST
COOPERATIVELY REGULATE THE VIRAL LATE PROMOTER**

This chapter presents preliminary work elucidating how the MCPyV late promoter is regulated by both LT and sT. I am the primary investigator and performed all of the experiments. The NCCR reporter plasmids used in Figures 4.2 – 4.5 were constructed by Dr. Jing Li.

A preliminary manuscript of this work is in preparation.

4.1 SUMMARY

The work presented in Chapter 2 identified a threonine phosphorylation at T271 of MCPyV LT, but established that T271 phosphorylation was not important for viral replication. To test whether T271 phosphorylation is important for regulation of MCPyV promoters, transcriptional reporter constructs were generated by fusing the MCPyV NCCR to a luciferase gene such that protein expression would be controlled by the native early or late promoter. Preliminary results using these NCCR reporter constructs showed that the wild-type LT could stimulate luciferase expression from the late promoter, but only when sT was also expressed. The T271A mutant behaved identically to wild-type LT. Interestingly, sT expression activated both Early and Late NCCR reporter constructs to a small degree. The dependence of LT on sT co-expression for late promoter activation has not been previously reported in other polyomaviruses. Follow up experiments showed that sT's ability to stabilize LT expression did not play a major role in this co-operative activation phenotype. These NCCR constructs can presumably be replicated by LT as they retain the viral Ori (see Chapter 2); therefore, increased luciferase activity could be explained by an increase in reporter copy number. To address this concern, I examined two phosphomutant LTs (T297A and T299A, see Chapter 2) as well as an NCCR construct with a defective origin (Ori350, previously reported in (10)). The T297A mutant, which exhibits robust replication from the viral Ori, stimulated transcription just as well as wild-type LT. The T299A LT mutant, which has an abrogated replication phenotype, and the Ori350 NCCR mutant, which also supports very low levels of replication, had attenuated transcriptional activation. These results established that MCPyV replication and/or binding of the NCCR by LT is important for

stimulating the Late promoter. Finally, examination of the isolated Late promoter with the rest of the NCCR, including the Ori, removed showed that LT expression actually represses this promoter, highlighting the importance of an intact MCPyV Ori sequence for LT-mediated stimulation of the late promoter. These results present a model where LT expression negatively regulates the Late promoter prior to replication, and then robustly stimulates this promoter after binding to the NCCR and initiating replication. Interestingly, this post-replication activation by LT requires sT co-expression, revealing a synergistic interaction not exhibited by other polyomaviruses.

4.2 INTRODUCTION

MCPyV is associated with a large majority of MCC, a rare and highly aggressive cancer of the dermis (3,6,8,23). MCPyV-associated tumors exhibit a dependence on the expression of the viral oncogenes LT and sT; knockdown of these proteins cause MCC tumors to be rapidly cleared in a mouse xenograph model (32,33). MCPyV associated cancers are therefore similar to papillomavirus associated cancers, where high expression of oncogenic viral proteins drive tumor progression (11,12). Unlike papillomaviruses, however, the regulation of MCPyV oncogenes has not been well studied, either in a natural infection setting or in MCC cell lines. Similarly, MCPyV research has faced the difficulty of finding cell lines that can efficiently propagate the virus; this difficulty largely stems from a lack of knowledge of the cellular environment that supports activation of either the early genes, which are necessary for replication of the viral genome, or the late genes, which consist of the viral capsid proteins required for generating new virions. To date, the mechanisms by which the MCPyV early and late

genes are regulated have not been elucidated. Increasing our knowledge of viral transcription from both of these promoters will help us better understand MCPyV associated oncogenesis, and may also provide clues or even tools for more efficiently propagating fully functional virus for better studies of natural infection.

Like other polyomaviruses, MCPyV consists of a circular, doublestranded DNA genome of about 5.3kb that is packaged into virions comprised of VP1 and VP2 capsid proteins. The genome is bisected into an early region and a late region by a central non-coding control region (NCCR) which contains the viral origin of replication (Ori) and promoter sequences. The early promoter regulates the expression of the Tumor antigen locus; this open reading frame is multiply spliced into various gene products, including LT, sT, 57kT, and ALTO. The late promoter controls the expression of the viral capsid proteins, VP1 and VP2 (23).

The polyomavirus LT protein is a highly multifunctional protein that both manipulates the host cell cycle and initiates replication of the viral genome. The N-terminal region of LT contains conserved binding sites for various cellular proteins, including DnaJ heatshock protein family members and pRb, which serve to drive the host cell into a proliferative state. The C-terminal half of the protein contains functional domains required for initiating the replication of the viral genome, including a viral origin binding domain (OBD) that allows LT to bind directly to the Ori within the viral NCCR, and a helicase domain which is required for unwinding of the viral DNA (8,23). In SV40, LT also plays a major role in regulating both the early and late promoters (140-

148). The early promoter is activated by a variety of cellular transcription factors, including Sp1, Sp2, and NFAT, which drive initial activation of the T-antigen locus (84-86). As SV40 LT protein accumulates, it silences the early promoter and begins initiating replication of the viral genome. After replication, the accumulated LT is then able to efficiently stimulate the late promoter, which drives expression of the viral capsid proteins (87,149,150). Whether MCPyV LT can similarly regulate either the early or late viral promoters has not yet been investigated.

MCPyV sT has been shown to play an important role in both viral replication and MCPyV associated cancers. MCPyV sT stabilizes LT expression and enhances LT-mediated replication of the viral DNA (10,40). Additionally, sT uses its C-terminal PP2A binding domain to manipulate the host cell in a variety of ways to induce cellular proliferation and transformation. Some of these functions include instigating hyperphosphorylation of 4E-BP1 which consequently induces high levels of cap-dependent translation (27). MCPyV sT can also transform primary rat cells, and has been repeatedly shown to be necessary for maintaining the transformed phenotype of many MCPyV-associated MCC tumors (27,33,34). Interestingly, sT has been shown to inhibit NF- κ B signaling through its association with certain PP2A subunits and the NEMO adaptor protein (38). No report has thus far demonstrated a role for sT in regulating either of the viral promoters. In SV40 polyomavirus, sT plays a much less prominent role in both cellular transformation and the normal viral life cycle. Additionally, it does not regulate either of the two viral promoters, although one report showed that SV40 sT

expression could complement a low-level of LT expression to activate the Late promoter in a cooperative fashion (89).

We sought to better understand how the viral promoters are regulated by both LT and sT during MCPyV infection. Using a luciferase reporter, we investigated the potential role(s) of both MCPyV LT and sT in the regulation of both the native MCPyV NCCR as well as the early and late promoters in isolation. Our results exhibit a surprising departure from what has been known for SV40 promoter regulation. While replication does seem to play a critical role in triggering the activation of the late promoter, LT requires sT co-expression to robustly activate the late promoter in the context of the native NCCR. Interestingly, reducing the binding affinity of LT for the viral Ori, through mutation of either the viral Ori sequence itself or with LT phosphomutants described in Chapter 2, diminishes LT's ability to stimulate the late promoter, even in the context of sT co-expression. Surprisingly, LT showed an inhibitory effect on the late promoter when this sequence is isolated from the rest of the NCCR, even in the context of sT co-expression. These results highlight the importance of the Ori sequence for directing LT to the viral DNA, providing yet another example of MCPyV sT's more prominent role in the viral life cycle as compared to those of other polyomaviruses studied thus far.

4.3 RESULTS

4.3.1 The MCPyV Late Promoter is Activated by Coexpression of Both LT and sT in the Context of an Intact NCCR

Our previous studies of phosphorylation modification of MCPyV LT identified four sites: T271, T297, T299, and S816 (see Chapters 2 and 3). Of those four sites, the functional relevance of T271 has not yet been established, despite being identified with high confidence (see Figure 2.1). An important viral process not yet tested with the T271A LT mutant was regulation of MCPyV transcription, an activity which in SV40 is largely dependent on LT expression. To this end, reporter constructs were generated by fusing the NCCR of MCPyV to a luciferase reporter plasmid such that luciferase expression would be driven by either the Early or Late promoter regions (see Figure 4.1). These two reporter constructs (NCCR Early and NCCR Late) were then co-expressed with MCPyV LT and sT. LT expression had little effect on the early promoter, but had a robust activating effect on the late promoter only in the context of sT coexpression (Figure 4.2A and data not shown). The T271A mutant behaved identically to wild-type LT in all cases, precluding further study of this mutant (data not shown). Interestingly, sT expression alone was able to moderately but reproducibly activate both the early and late constructs approximately two-fold at all time points tested with the most robust activation seen on the late promoter when LT and sT were co-expressed (Figure 4.2A and data not shown).

To rule out whether LT and/or sT could act as a global activator of transcription, we tested whether these proteins could affect an interferon-sensitive response element (ISRE). MCPyV proteins were co-transfected with a luciferase reporter under the control of an ISRE. Cells were then treated with or without recombinant IFN- α . Luciferase activity was greatly stimulated by IFN treatment as would be expected. Expression of the

MCPyV proteins did not activate this protein in the absence of IFN. Interestingly, expression of LT and especially sT severely attenuated the activation induced by IFN treatment, showing that these proteins can actually repress this promoter (Figure 4.2B). This finding is supported by a study showing that MCPyV sT can negatively regulate NF- κ B signaling (38). These results established that the activation of the viral promoters was due to a specific interaction with MCPyV LT and sT, and not due to a more global activation of cellular transcription.

4.3.2 Increased LT Expression Alone Does Not Account for Activation of the Late Promoter

The observation that MCPyV LT required sT co-expression to activate the NCCR Late reporter was surprising to us (Figure 4.2A); in SV40, LT is able to activate the late promoter by itself following replication (87,148-150). To our knowledge, there is only one report showing that SV40 sT could complement LT activation of the late promoter, but only in situations where LT expression was “sub-optimal” (89). It has been well established by our lab and others that sT expression can stabilize LT expression (data not shown and (10,40)). We therefore asked whether LT’s robust activation of the late promoter when sT was co-expressed was due to an increase in LT stabilization mediated by sT. Cells were transfected with the NCCR Late reporter construct and an increasing amount of LT expression construct either alone or with sT co-expression. Lysates were immunoblotted for LT and sT expression to assess the extent of LT stabilization (Figure 4.3).

Interestingly, LT was able to robustly activate the late promoter at any given expression level, but only in the context of sT co-expression (Figure 4.3A). Western blot analysis showed that co-expression of sT did in fact stabilize LT expression (Figure 4.3B, compare LT expression of a given level when sT is absent or present). The expression level of LT alone, however, did not explain the activation of the late promoter. For example, the overall LT expression level was similar between the 2xLT/sT and 5xLT samples; however, the late promoter was only robustly activated in the 2xLT/sT condition (Figure 4.3B). Furthermore, the LT expression level of 5xLT is well above that seen for 1xLT/sT, yet it is only in the latter condition that the late promoter is robustly activated (Figure 4.3B). These observations indicate that sT expression has enhancing activity on the late promoter independent of its ability to stabilize LT expression. It is important to note that this activation phenotype was somewhat reduced in the 5xLT/sT setting; it is possible that LT might saturate whatever helper function sT might have when expressed at this level, although additional experiments will have to be performed to more clearly define this phenomenon.

4.3.3 Replication of the NCCR Reporter Partially Contributes to Late Promoter Activation

Polyomaviruses commonly exhibit robust late promoter activation following replication. The NCCR reporter constructs used in this study retain an intact Ori which would presumably be targeted by LT for replication. In addition to MCPyV LT and sT acting as molecular switches for late promoter activation, increasing numbers of reporter plasmid could artificially inflate the reporter signal due to an increase in reporter copy

number. Additionally, sT's stabilization of LT is known to stimulate LT's ability to replicate the viral Ori (10). The results in Figures 4.2 and 4.3 could therefore be solely due to an increase in copy number of the NCCR reporter.

To begin addressing this question, we introduced the previously reported Ori350 mutation into the NCCR reporter construct (10,49,151). This mutation was derived from an MCC tumor and introduces a single nucleotide substitution in pentanucleotide 7 of the MCPyV Ori (Figure 4.1), which severely abrogates LT-mediated replication from this Ori (10). We then used quantitative PCR to measure the amount of either wild-type or Ori350 mutated NCCR reporter plasmids in the presence and absence of MCPyV LT and sT after four days of expression (Figure 4.4A).

As expected, the wild-type NCCR Late reporter replicated to a high degree (about two-fold) in the presence of both LT and sT; expression of just LT induced a modest increase in reporter number. The Ori350 NCCR Late reporter also replicated to a small degree when LT and sT were co-expressed, but this replication was severely abrogated compared to the wild-type NCCR Late reporter (Figure 4.4A). Interestingly, examination of luciferase activity in this setting shows that copy number only partially contributes to the observed increase in luciferase activity driven by the NCCR Late reporter (Figure 4.4B). The luciferase activity of the WT NCCR Late reporter was stimulated approximately eight-fold when LT and sT were co-expressed (Figure 4.4B), even though the total copy number only increased two-fold in this setting (Figure 4.4A). Additionally, even though the Ori350 NCCR Late reporter did replicate to a small but measurable

degree when LT and sT were co-expressed, this construct failed to exhibit luciferase activity over vector control. A previous report showed by CHIP analysis that LT binding to Ori350 is greatly reduced, presumably because this mutation disrupts a key LT binding site (10). It is possible, therefore, that LT binding to the Ori is required for its ability to activate the late promoter. These data suggest that the combined effect of LT binding to the viral NCCR and sT expression, rather than NCCR plasmid copy number alone, contribute to the observed increase in NCCR Late luciferase activity.

4.3.4 A Phosphomutant LT With a Defective Replication Phenotype Still Robustly Activates the Late Promoter

In a previous chapter, I described two LT phosphomutants (T297A and T299A) which exhibited altered replication phenotypes (see Chapter 2). The T297A mutant exhibits enhanced replication of MCPyV Ori plasmids, likely because it can bind the Ori with greater affinity than wild-type LT; conversely, the T299A mutant, which exhibits reduced binding to the viral Ori, fails to replicate MCPyV Ori plasmids (Figures 2.3, 2.5 and 2.6). To further probe whether replication plays a role in activating the late promoter, I tested these mutants for their ability to stimulate NCCR Late promoter driven luciferase activity in the presence or absence of sT (Figure 4.5). Southern blot analysis confirmed that the T297A mutant could replicate to a high degree, and that this activity was greatly stimulated by co-expression of sT; T299A on the other hand failed to replicate plasmids with or without sT co-expression (data not shown). Surprisingly, all LT mutants behaved similarly to wild-type LT: they were all able to activate the NCCR Late reporter, but only when co-expressed with sT. Interestingly, the activation of the

NCCR Late reporter was slightly attenuated with the T299A mutant, which has reduced binding affinity to the MCPyV Ori (Figure 2.6). This is in agreement with the Ori350 NCCR Late promoter reporter data presented in Figure 4.4, where reduced MCPyV LT binding to the NCCR Late promoter reporter prevented activation of the promoter despite a small level of observed replication (see section 4.3.3). Together, these results rule out replication of these plasmids as a major contributing factor for the increased luciferase activity, and suggest that LT binding to the Ori in the presence of sT expression is critical for NCCR Late reporter activation.

4.3.5 MCPyV LT Silences the Late Promoter in the Absence of Ori Sequences

The experiments presented thus far have been in the context of a native NCCR, which includes both promoter sequences and the viral Ori. Data presented in Figures 4.4 and 4.5 suggest that binding of the Ori sequences and/or replication in the presence of sT may play a major role in LT's ability to activate the late promoter. We asked how LT and sT might act on the Late promoter when the Ori was no longer present. The isolated Late promoter (highlighted in green in Figure 4.1) was cloned into the same luciferase reporter vector and assessed for activation by LT and sT. sT was still able to activate the isolated Late reporter when expressed alone; however, LT expression actually reduced activation of the isolated Late reporter below vector control levels. Co-expression of sT and LT showed activity similar to vector (figure 4.6A). We were surprised to see LT show such a robust silencing effect; we therefore tested whether scaling down the dose of LT would relieve this repression. Interestingly, LT showed a robust silencing effect at all

doses tested; expression of sT was not able to overcome this silencing effect, although it still activated the late promoter when expressed alone (data not shown).

4.4 DISCUSSION

Thus far, little research has been done to understand how MCPyV gene expression is regulated. Knowledge of viral gene regulation is important not just for understanding natural infection, but also in the case of MCPyV associated cancers, where high expression of the viral oncogenes is necessary for tumorigenesis. This work represents a preliminary investigation of the regulation of the MCPyV promoters through the lens of the viral protein products themselves. Polyomaviruses generally utilize the LT protein as a major regulator of both early and late gene transcription (87,148-150). MCPyV sT has also shown itself to be a critical protein involved in various MCPyV activities (10,27,34,38,40), so both of these proteins were tested for their ability to regulate the early and late viral promoters.

Reporter constructs were first generated utilizing the entire NCCR of MCPyV to keep the early and late promoters close to their native configurations (Figure 4.1). An initial look at promoter activation by both LT and sT showed that sT could surprisingly activate both promoters at a small but reproducible level (two-fold, Figure 4.2A and data not shown). This was independent of time-point or promoter (data not shown). Interestingly, expression of LT alone showed little activity, in some cases even repressing the late promoter (Figure 4.2A, Day 3). At four days post transfection, however, LT was able to robustly activate the late promoter, but only in the context of sT co-expression.

This is in contrast to SV40 where LT expression alone is able to stimulate late gene expression.

The stimulation of the viral promoters was not due to a global effect on transcription: analysis of an interferon-sensitive response element showed that LT and especially sT actually repressed transcription from these reporters upon interferon stimulation (Figure 4.2B). sT's cooperative activity with LT to activate the late promoter could partially be explained by a dramatically increased level of LT expression when sT is coexpressed, as sT is able to stabilize LT protein expression (40); however, higher LT expression alone was not able to stimulate the NCCR Late promoter (Figure 4.3). Even with a five-fold increase in transfected LT, sT was required for robust activation of the NCCR Late promoter (Figure 4.3).

The observed increase in the NCCR Late reporter luciferase activity could also be explained by the replication of this reporter in the context of LT expression. These reporter constructs contain the native MCPyV NCCR, which includes the viral Ori. LT binds to the viral Ori to initiate replication (See Chapter 2) and could presumably replicate these reporter constructs as well; the observed increase in the NCCR Late reporter luciferase activity could be due to an increase in reporter copy number after four days of LT expression. To address this issue, we measured the copy number of NCCR plasmids in cells after four days with or without LT or sT expression. While a two-fold increase in plasmid number was evident when LT and sT were co-expressed, the increase in NCCR Late promoter activation (> 8 fold) far exceeded this increase in plasmid count

(Figure 4.4). We also examined an NCCR with a point mutation in a LT binding site located in the viral Ori (termed Ori350, Figure 4.1), which has previously been shown to have reduced replication and LT binding (10,49). This mutant NCCR was still able to replicate to a very small degree when LT and sT were co-expressed, but the NCCR Late promoter failed to be activated from this construct (Figure 4.4). Additionally, expression of phosphomutant LT proteins which either exhibit enhanced (T297A) or abrogated (T299A) replication were still able to activate the NCCR Late promoter, again only in the context of sT co-expression (Figure 4.5). These results indicate that the promoter activation phenomenon is not likely due solely to an increase in reporter copy number.

Interestingly, when the Ori and Early promoter are removed, LT appears to suppress the isolated late promoter, even when sT is co-expressed (Figure 4.6). A similar phenomenon can be noted in the NCCR construct at day 3 (Figure 4.2, Day 3 data). This isolated Late promoter construct represents an artificial setting that demonstrates what might happen at this promoter prior to replication. In the greater scheme of the viral life cycle, it makes sense for the late promoter to be repressed prior to genome amplification.

Polyomaviruses have traditionally used replication as a major switch towards activating the late promoter. The data presented here supports the notion that the viral Ori is critical for efficient activation of the late promoter. Both an NCCR mutated with the Ori350 LT binding site mutation and a LT mutant with decreased affinity for the viral Ori (T299A, see Figure 2.6) showed attenuated activation of the late promoter, albeit to different degrees. Removal of the Ori revealed LT's ability to strongly repress the late

promoter (Figure 4.6). These data suggest that LT binding to the Ori is required for efficient activation of the late promoter. The molecular mechanisms by which Ori binding stimulates Late promoter activation, and only in the context of sT co-expression, are not clear. It is possible that replication of the viral genome causes physical changes to the viral chromatin structure that allow access to cellular transcription factors. MCPyV LT is known to recruit the host cellular chromatin factor Brd4 to viral replication foci; it is possible that Brd4 not only recruits RFC1 to help stimulate replication, but also occupies newly formed viral genomes to then recruit P-TEFb and stimulate transcription (50). Additionally, other factors left over after replication, such as PCNA, may signal or recruit transcription factors, or interact with LT or sT in some way as to stimulate late promoter activation. All of these factors represent exciting areas of research that should be pursued to increase our understanding of the activation of late gene expression and virion assembly. Finally, it is interesting to note that sT was only able to co-activate the late promoter in the context of an intact NCCR: although sT alone was able to activate the Isolated Late reporter modestly, it was unable to counteract LT's repressive activity (Figure 4.6). This may indicate that sT activity is somehow tied to LT binding to the Ori, although the molecular mechanisms of this interaction remain largely speculative at this point.

The studies presented in this chapter focus exclusively on the regulation of the late promoter. The early promoter was similarly studied, both in the context of the native NCCR, as well as in isolation. Results from these experiments were much more variable and inconsistent, although in general sT expression was able to stimulate both the early

and late promoters at almost all time points (data not shown). This stimulation was consistently modest (two-fold) but extremely reproducible. It is likely that sT exhibits some activity that somehow primes the host cell for transcription from the viral genome, likely through its PP2A binding activity. It would be interesting to test whether PP2A binding mutants show differential activity on either promoter, or on sT's ability to co-activate the late promoter with LT.

Ultimately, without a robust infection system, the data presented here represent a somewhat artificial look at MCPyV transcription; a true infection system with a natural host cell will greatly advance our understanding of MCPyV virology. It would similarly be interesting to examine the MCPyV gene expression dynamics of both the early and late promoters in the context of Merkel cell infection, as this may provide clues towards understanding the early events of oncogenesis. Unfortunately, cells lines of either human Merkel cells or even MCPyV-negative MCC cells do not currently exist, further hampering progress towards better understanding this important tumor virus.

Even with these limitations, however, this preliminary study sheds some light on MCPyV late promoter activation, and once again highlights how MCPyV is distinct from other polyomaviruses. Whereas SV40 LT is largely sufficient on its own to regulate viral gene expression and transform infected cells, MCPyV has shown a greater dependence on sT function for both tumorigenesis and, in this study, promoter activation. Ultimately, a better understanding of viral gene expression, both in the context of natural infection

and in Merkel cells, will help advance our understanding of MCPyV pathogenesis and cancer progression.

4.5 FIGURES

FIGURE 4.1

MCPyV NCCR



FIGURE 4.1: The MCPyV Non-coding Regulatory Region. The regulatory region of the MCPyV R17b isolate was used to generate the NCCR Early and NCCR Late reporters. Perfect LT binding sites (GAGGC pentanucleotides) are highlighted in red, while inverted complementary sequences (CTCCG) are highlighted in blue. Imperfect repeats are noted in orange and light blue. The Ori350 mutant is a C→A substitution in pentanucleotide 7 which abrogates replication (asterisk, (10)). The location of the early and late regions of MCPyV are noted. The isolated Late Promoter used in this study is highlighted in green.

FIGURE 4.2

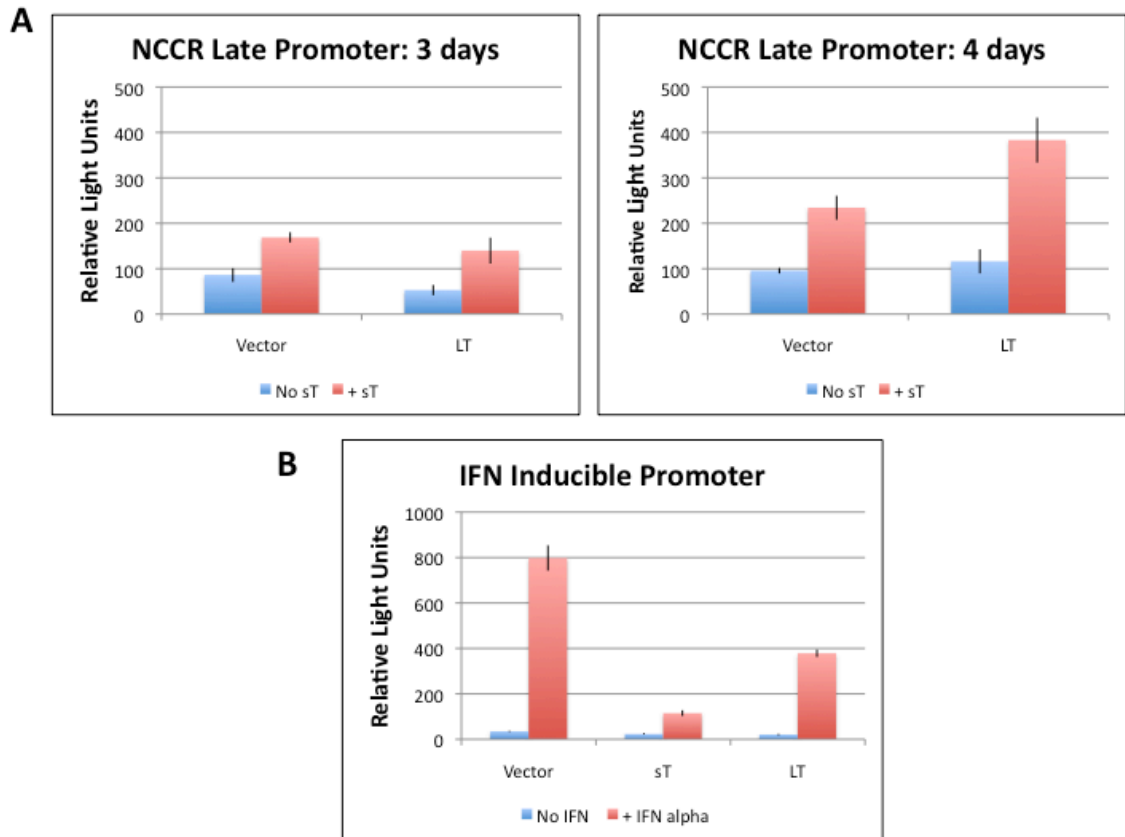


FIGURE 4.2: MCPyV LT and sT cooperate within the NCCR to activate the late promoter. **(A)** 293 cells were co-transfected with NCCR Late Luciferase Reporter and various combinations of MCPyV LT and sT expression constructs. Cells were collected at the indicated times post transfection. Luciferase activity was normalized to protein content. Graphs show the mean of a triplicate transfection; error bars represent the standard deviation from the mean. Data are representative of three independent experiments. **(B)** 293 cells were co-transfected with an Interferon-Sensitive Response Element reporter plasmid and the indicated MCPyV gene construct. Twenty-four hours post-transfection, cells were stimulated with recombinant IFN- α or PBS. Forty-eight hours post-transfection, cells were collected. Luciferase activity was normalized to protein content. Graphs show the mean of a triplicate transfection; error bars represent the standard deviation from the mean. Data are representative of three independent experiments.

FIGURE 4.3

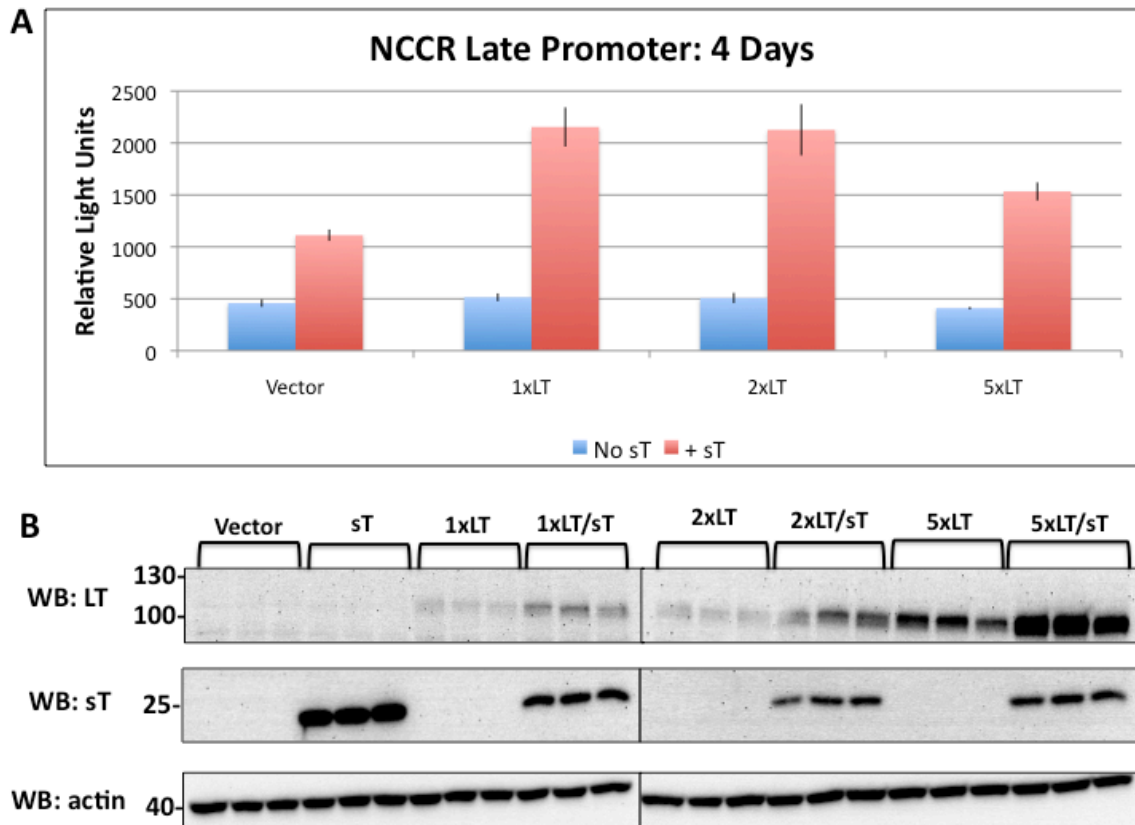


FIGURE 4.3: LT protein level alone does not explain late promoter activation. 293 cells were co-transfected with the NCCR Late Luciferase reporter and increasing amounts of LT expression plasmid with or without a constant amount of sT expression plasmid. Cells were collected four days post-transfection. **(A)** Luciferase activity was normalized to protein content. Graphs show the mean of a triplicate transfection; error bars represent the standard deviation from the mean. **(B)** Lysates were separated by SDS-PAGE and immunoblotted for the indicated proteins. Data are representative of three independent experiments.

FIGURE 4.4

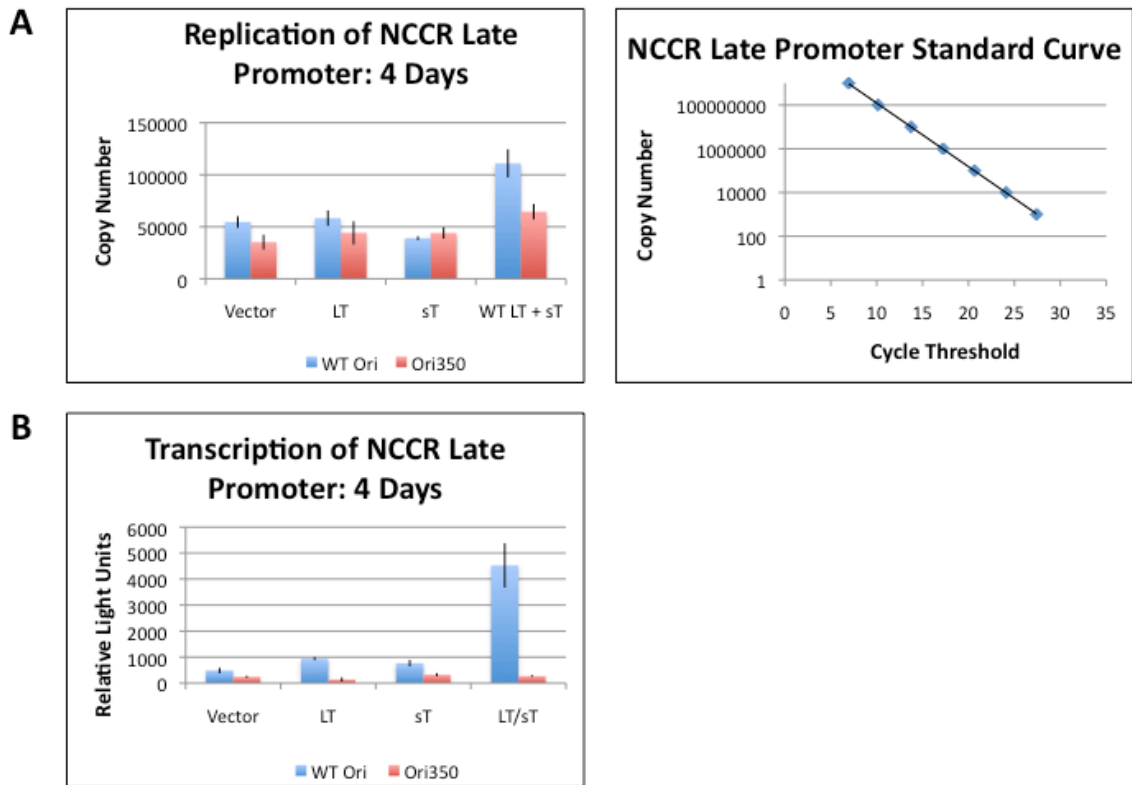


FIGURE 4.4: An intact origin of replication is required for late promoter activation.

(A) 293 cells were transfected with the indicated MCPyV proteins and either WT NCCR Late or the replication-defective Ori350 NCCR Late Luciferase reporter. Whole-genomic DNA was extracted from cells collected four days post-transfection. NCCR plasmids were measured by qPCR (calculated against a standard curve, depicted on the right, with an R^2 value of 0.99988) and normalized to GAPDH. **(B)** 293 cells were transfected as in (A) and collected four days-post transfection. Luciferase activity was normalized against protein content. Graphs show the mean of a triplicate transfection; error bars represent the standard deviation from the mean. Data are representative of three independent experiments.

FIGURE 4.5

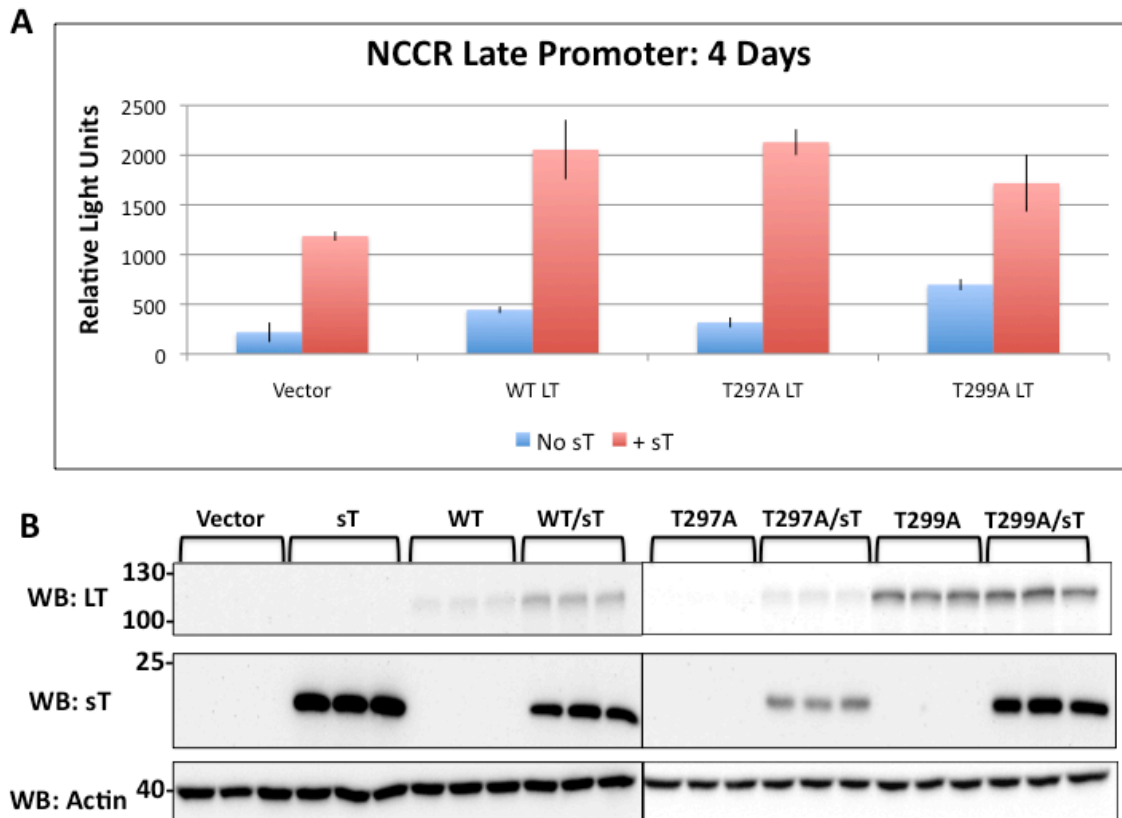


FIGURE 4.5: A MCPyV LT replication-defective mutant can still activate the late promoter. 293 cells were co-transfected with the NCCR Late Luciferase reporter and the indicated LT expression plasmid with or without sT expression plasmid. Cells were collected four days post-transfection. **(A)** Luciferase activity was normalized protein content. Graphs show the mean of a triplicate transfection; error bars represent the standard deviation from the mean. **(B)** Lysates were separated by SDS-PAGE and immunoblotted for the indicated proteins. Data are representative of three independent experiments.

FIGURE 4.6

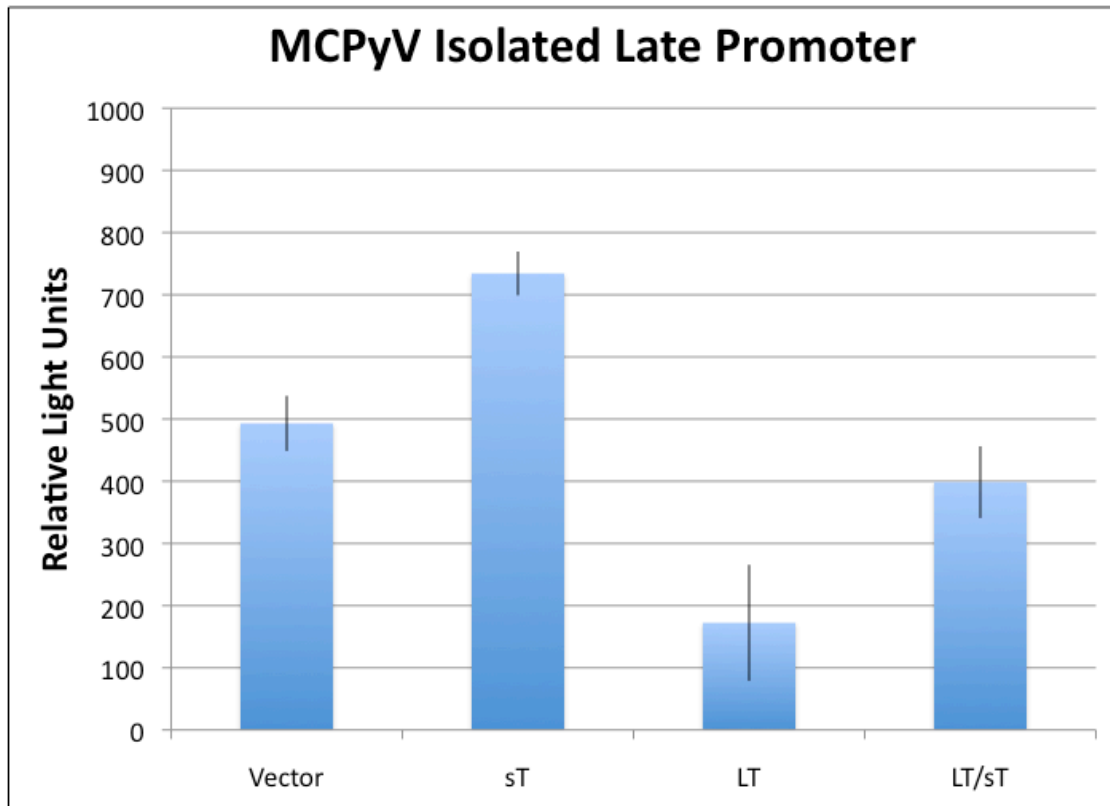


FIGURE 4.6: MCPyV LT represses the late promoter when the viral origin is absent. 293 cells were transfected with the MCPyV isolated Late Luciferase reporter with or without sT co-expression. Two-days post-transfection, cells were collected, and luciferase activity was normalized to protein concentration. Graphs show the mean of a triplicate transfection; error bars represent the standard deviation from the mean. Data are representative of four independent experiments.

CHAPTER 5: CONCLUSIONS AND FUTURE DIRECTIONS

5.1: Regulation of MCPyV LT Function by Phosphorylation

5.1.1: Regulation of Protein Function by Phosphorylation

A majority of my thesis work has centered around a fundamental question: how are the myriad of functions of a complex viral protein like MCPyV LT regulated to allow for the exquisitely coordinated progression of viral infection? The LT protein of polyomaviruses is involved in almost every facet of the viral life cycle, including manipulating the host cell cycle to favor proliferation, initiating replication of the viral genome, and (usually) controlling the expression of early and late genes such that T-antigens are expressed first to manipulate the cell, and capsid proteins are expressed only when it is convenient to produce new virions. Understanding how LT protein function is regulated is the heart of elucidating how polyomaviruses coordinate their life cycle in host cells.

Polyomavirus LT proteins were readily identified as highly phosphorylated, and the functional relevance for many of these modifications remain a mystery even for SV40, arguably one of the best studied viruses in the world. Phosphorylation is a versatile post-translational modification, as it is readily added and removed from substrates by kinases and phosphatases, respectively, allowing for a dynamic regulation of protein function in response to an ever changing cellular environment. In addition to acting as a molecular mark whose presence or absence can be recognized by other proteins, the negative charge inherent to the phosphate moiety can be utilized to alter protein structure or interaction with other proteins.

The work presented here represents a first look at how phosphorylation regulates MCPyV LT function, and provides many avenues of research worth pursuing to better understand the basic life cycle of this important tumor virus.

5.1.2: Regulation of MCPyV Replication by Phosphorylation of LT T297 and T299

The work presented in Chapter 2 identified three threonine phosphorylation sites on MCPyV LT (Figure 2.1). Ultimately, two of them (T297 and T299) proved to be important regulators of LT-mediated replication. Identification of T299 as a phospho-site was encouraging to me because of its homology to a well-described regulatory threonine in SV40 LT, providing confidence in the validity of my mass spectrometry data. Its homology to T124 in SV40 LT naturally led me to ask whether this mutant abrogates replication; this hypothesis ultimately proved to be correct (Figures 2.3 and 2.5). To my surprise, T297 was identified as being equally important, if in an opposite fashion; the T297A mutant actually showed enhanced replication, well over that seen for wild-type LT (Figures 2.3 and 2.5). This finding was completely unexpected to me, and led me to generate models to better understand the underlying molecular mechanisms.

Modeling of the LT OBD suggested that T297 faces the LT/DNA interaction interface (Figure 2.2); electrostatic theory would predict that a phosphate moiety at this site would be repelled by the negatively charged phosphate backbone of DNA; therefore, the alanine mutant would have this repulsive interaction abrogated. In line with this reasoning, electromobility shift assays showed that the T297A mutant had enhanced affinity for the viral Ori, while the T299A mutant showed reduced Ori binding. To test

the hypothesis that electrostatic interactions drive T297's regulation of replication, I could test whether a T297D or T297E mutant evidence reduced binding. The functional consequence of T299 phosphorylation is not as clear. In the homologous site on SV40 LT, the major outcome of phosphorylation at this site is stimulation of interactions between adjacent hexameric LT complexes assembled at the viral origin. Using an elegant series of DNA probes, Barbaro and colleagues were able to show this double-hexamer interaction and its dependence on T124 phosphorylation in SV40 by splitting the SV40 Ori in half, retaining two of the four LT binding sites in both probes (73). The SV40 Ori is largely symmetrical, with opposing pairs of GAGGC repeats for recruiting LT flanked by A/T rich or palindromic sequences (see Figure 1.2). In contrast, the MCPyV Ori has an asymmetric organization, with as many as ten potential LT binding sites separated by a large A/T rich tract; a second A/T rich track caps the late end of the Ori (10,28). Due to this unique nature of the MCPyV origin, as well as technical difficulties with my own hands, I was unable to recapitulate this finding in MCPyV LT, although I would predict that T299 phosphorylation behaves very similarly to T124 in SV40. A more rigorous demonstration of this remains to be seen.

These data suggest a model where phosphorylation at T299 enhances LT-mediated replication, presumably by stimulating hexamer-hexamer interactions, while T297 phosphorylation would act as a brake to prevent unscheduled genome replication by reducing the affinity of LT for the viral Ori. Unfortunately it is currently impossible to begin probing the temporal dynamics of phosphorylation at these sites during the viral life cycle – we lack both the specific antibodies required for assessing phosphorylation at

these sites, and a relevant cell culture system that recapitulates a “natural infection.” Additionally, we have little clues as to the kinase(s) and potentially phosphatase(s) involved in adding or removing phosphates from these two critical threonines. Phosphorylation of T124 in SV40 LT is mediated by a cyclin dependent kinase *in vitro* (71); while this has not been definitively proven *in vivo*, the virus would likely want to initiate replication only when the host cell has transitioned into S-phase, when the DNA synthesis machinery has been primed.

Phosphorylation of T297 could follow a myriad of routes, depending on whether it functions to prevent premature initiation of replication, to put a brake on replication after amplification of the viral genomes, or both. T297 lies within a region of LT which in SV40 is commonly found phosphorylated early in infection, albeit at serine residues; these phosphorylation marks similarly reduce SV40 LT’s capacity to replicate the viral genome (77,79,93). Interestingly, it is believed that PP2A phosphatases might be involved in removing these marks as infection transitions to amplification of the viral genome (76,78). Given sT’s ability to interact with PP2A proteins, it is interesting to speculate whether an additional layer of regulation of LT phosphorylation exists with this accessory protein. Thus far, MCPyV sT has proven to be a major player in the MCPyV life cycle, quite contrary to SV40 in which it plays a largely supporting role; it would not be surprising, therefore, to discover that sT plays a major role in regulating LT-mediated transcription not just by stabilizing the LT protein but also by regulating the dephosphorylation of key inhibitory phosphates, like T297 phosphorylation.

5.1.3: Phosphorylation of MCPyV LT by ATM Kinase at S816

The interaction between DNA viruses and the host DDR has been an emerging field of interest in the past decade. That DNA viruses must contend with the DDR machinery – either to subvert unwanted activities or co-opt these pathways for their own replication – has now become a major theme in DNA virology. In the case of MCPyV, our lab showed that LT expression alone induces activation of a host DDR response (14). Our more recent work demonstrated that components of the DDR machinery are actively recruited to viral replication centers, and disruption of this machinery had a negative impact on viral replication (49). It is clear that MCPyV interacts with the host DDR, but precisely how, and for what reason, has remained an open question.

Our identification of a cross-reactive activity with an antibody specific for serine 345 phosphorylation of a key DDR protein, Chk1, leading to the discovery yet another phosphorylation site on LT: serine 816. We immediately hypothesized that some DDR kinase might be responsible for this phosphorylation, as the epitope recognized by the cross-reactive antibody represented a classic “S/T-Q” site recognized by both ATM and ATR kinases, and we already knew that the DDR machinery was activated by LT and recruited to viral replication centers, as already outline above. Using *in vitro* techniques, we were able to show that, indeed, ATM kinase is able to interact with LT and mediate phosphorylation at S816 (Figure 3.2, 3.3 and 3.4). We then attempted to uncover the functional relevance of MCPyV LT phosphorylation at S816. MCPyV LT expression has a well-documented growth-inhibitory property that had been localized by our lab and others to the C-terminal half of the protein (13,14). We therefore asked whether

phosphorylation at S816 was involved in this growth inhibition. Clonogenic assays and screens of molecular markers of apoptosis seem to lend some support for this hypothesis, but the effects are modest, at best (Figure 3.5 and 3.6). It is unclear whether other MCPyV LT function(s) are regulated by the phosphorylation of S816; even if its only function was indeed to arrest the host cell, it is not clear whether this activity is a strategy employed by MCPyV to maintain the cell in a pseudo-S-phase/G2 state, or if this represents a host anti-viral strategy to eliminate virally infected cells. More rigorous exploration of other potential functions of S816 phosphorylation is necessary to better understand how MCPyV might subvert – or be victim to – the host DDR machinery.

It is interesting to note that 57kT retains the C-terminal 100 amino acids of LT, and presumably shares this phosphorylation site. Although we currently do not have much information about 57kT's function during infection, it would be interesting to test whether this protein is indeed phosphorylated at the same site, and whether this has a more obvious phenotype on this smaller tumor antigen.

5.1.4: Uncovering the Function of MCPyV LT T271 Phosphorylation

One of the more fascinating aspects of MCPyV LT is the presence of a 200 amino acid stretch flanking the “LXCXE” pRb binding site, which is unique to MCPyV LT and does not exist in any other polyomavirus LT discovered thus far. This region has been termed the MUR and has generated a lot of curiosity and interest, although currently no functional data have surfaced apart from one report showing a vacuolar sorting protein binds LT in this region (24). MCPyV has thus far proven to behave very differently from

its more well studied SV40 counterpart, and it has been thought that understanding the function of the MUR may help us better understand what unique functions MCPyV LT has acquired.

Of particular interest to me was the identification of T271 phosphorylation. Of the three sites identified in Chapter 2, the phosphorylated T271 peptide was most frequently captured in both the standard and titanium oxide purification schemes, providing high confidence that this site is likely phosphorylated during LT expression (Figure 2.1). Despite this, I have been unable to find any functional phenotype for a T271A mutant in relation to transcription, replication, or cell cycle control. Of all the work presented here, this phosphorylation site remains a major area of potential new research and represents a key clue into uncovering novel functions acquired by the MCPyV LT unique region. It is again interesting to note that 57kT retains the amino acid sequence for this phosphorylation site, and therefore it may be more relevant in that protein than in full length LT.

5.2: Regulation of Viral Transcription

I began my work on viral transcription primarily as a means of screening the T271A LT mutant for a potential phenotype. To my surprise, contrary to what had been reported for SV40, MCPyV LT was unable to activate the late promoter on its own in the context of the native NCCR; it required sT co-expression (Figure 4.2). I also uncovered a dependence on viral replication and/or binding of LT to the MCPyV Ori for robust activation of the late promoter (Figure 4.4 and 4.5), although this phenomenon has

already been described for polyomaviruses (146,147). Unfortunately, difficulty in getting consistent results with the early promoter constructs, coupled with the fact that MCPyV LT can negatively regulate a number of control reporter constructs used in various reporter assays, has made progress in studying transcription preliminary at best. Developing a more robust transcription assay system with better transfection controls will help solidify the data I have already generated and hopefully lead to new discoveries with the early promoter as well.

A better understanding of the regulation of the early and late promoter is critical for advancing our knowledge of both MCPyV natural infection and its associated oncogenesis. Our current lack of a viable cell-culture model for propagating virus is due, in part, to a lack of a tissue culture system for stimulation of the early and late promoters. A greater understanding of the requirements for efficient activation of these promoters can help us identify a more natural host cell, or engineer new tools to make propagation and infection with virions much less laborious. Additionally, understanding how the early promoter in particular is regulated will be key for understanding how this regulation is altered in MCC, in which sT and LT can both be expressed and are often required for maintaining the cancer phenotype (9,33,34).

5.3: Current Obstacles in Basic MCPyV Research

The major obstacle, by far, facing the field is the lack of a viable cell culture system for propagating virus. Any research into the basic life cycle of MCPyV thus far has largely been done using overexpression of viral proteins in isolation or sometimes in

combination. Re-ligated genomes or molecular clones of MCPyV have offered more relevant systems for exploring viral infection, but the delivery systems for these genomes are still artificial. Once a viable cell culture model has been established, much of the work that has been performed to understand MCPyV replication, transcription, and cell cycle manipulation will have to be repeated. A viable and physiologically relevant system might also allow us to finally uncover the function of a variety of unique aspects of MCPyV that have thus far eluded us, such as the function of the MCPyV LT MUR or the contribution of 57kT.

5.4: Concluding Remarks

My thesis work has explored basic aspects of early MCPyV activities, focusing on the LT protein. In addition to tying key post-translational modifications of LT to its various functions in cells, my work also highlights how MCPyV is unique among polyomaviruses in its greater dependence on sT; further exploration of how the phosphorylation sites I identified are regulated will likely uncover even more unique ways in which MCPyV has adapted to its host. The eventual development of a viable and physiologically relevant cell culture system will pave the way to an explosion of new knowledge for this critically important human tumor virus.

CHAPTER 6: MATERIALS AND METHODS

6.1: Cell Lines, Cell Culture and Transfection

HEK 293, HEK 293T, HeLa and C33A cell lines were maintained in Dulbecco's Modified Eagle Medium (DMEM; Invitrogen) supplemented with 10% fetal bovine serum (Hyclone). HEK 293TT cells, a gift from Chris Buck (NCI), were generated by stably transfecting 293T cells with an SV40 LT expression plasmid, pTIH, which also contains a Hygromycin resistance cassette (152). 293TT cells were maintained in DMEM supplemented with 10% fetal bovine serum and 250 µg/mL Hygromycin B (Clontech). U2OS cells were maintained in McCoy's 5A medium (Invitrogen) containing 10% fetal bovine serum (Hyclone, Logan, UT, USA). FuGENE6 transfection reagent (Roche Applied Science), or Lipofectamine 2000 (Invitrogen) reagents were used to transfect 293TT, U2OS, C33A, or HeLa cells per the manufacturer's instructions in the work presented in Chapter 3. HEK 293, 293T and C33A cells were transfected using the calcium phosphate method as described previously (50).

6.2: Recombinant Plasmids

Construction of the pcDNA4c-MCPyV LT, pcDNA-MCPyV LT 1-211, pcDNA4C-MCPyV LT 212-440, pcDNA4C-MCPyV LT 1-440, pcDNA4C-MCPyV LT 212-817, pcDNA4C-MCPyV LT 1-817, pEGFPC1-MCPyV LT 1-440, pEGFPC1-MCPyV LT 441-817, pEGFPC1-MCPyV LT 1-817, pcDNA4C-IIT-MCPyV LT 1-817, pLPCX-Cherry-LacI, pLPCX-MCPyV LT 1-817, pGEX-MCPyV LT and pcDNA4c-MCPyV Ori plasmids have been described previously (14,50). For the phospho-mutant

constructs T271A, T297A and T299A, Quik-Change Site-Directed Mutagenesis (Stratagene) was performed. Briefly, synthetic oligonucleotides containing the desired mutation were annealed with denatured template plasmid pcDNA4c-MCPyV LT and extended with *Pfu Turbo* polymerase (Agilent Technologies) following the manufacturer's instructions. Unmutated plasmid DNA templates were removed by DpnI digestion, and the remaining DNA was used to transform DH5 α competent cells. To generate IIT affinity-tagged constructs, a DNA sequence encoding two IgG binding domains of *Staphylococcus aureus* protein A and a TEV protease cleavage site was fused in frame to the N terminus of MCPyV LT constructs using the KpnI site of the pcDNA4c-MCPyV LT expression construct.

The NCCR reporter constructs were generated by PCR amplifying the NCCR of the pMoHF construct (derived from the MCPyV R17b isolate, a gift from Chris Buck, NCI) and subcloning into the KpnI site of pGL4-Basic (Promega). The primers used were (MCPyV NCCR 1: 5' – CGGGGTACCTGAAAATAAATAAGG – 3'; MCPyV NCCR 2: 5' – CGGGGTACCTTGTCTATATGCAGAAG – 3'). The NCCR Ori350 constructs were generated by introducing the C \rightarrow A mutation in pentanucleotide 7 of the MCPyV Ori sequence of pGL4-NCCR constructs using QuikChange Site-Directed mutagenesis (Stratagene). The Isolated Late Reporter was generated by PCR amplifying the late promoter of pMoHF and cloning it into the KpnI and XhoI sites of pGL4-Basic. The primers used were Isolated Late For: 5' – TAGGTACCAGGCAGCCAAGTTGTGG – 3' and Isolated Late Rev: 5' – TACTCGAGTGAAAATAAATAAGG – 3'.

The pELU-ISRE reporter plasmid for assessing Type 1 Interferon signaling was a gift from Dr. Susan Weiss, University of Pennsylvania. The pTIH construct expressing SV40 LT, as well as the expression constructs for MCPyV sT, pMono-Blast, pWM, pMtBs and pMtW, were gifts from Chris Buck, NCI. All constructs were confirmed by DNA sequencing.

6.3: Antibodies and Chemicals

The following antibodies were used for immunofluorescent staining: mouse anti-Xpress (R910-25, Invitrogen), rabbit anti-RFC1 (H-300, Santa Cruz), rabbit anti-RPA70 (2267, Cell Signaling), Alexa Fluor 594 goat anti-rabbit IgG (A11012, Invitrogen), and Alexa Fluor 488 goat anti-mouse IgG (A11001, Invitrogen). The polyclonal rabbit anti-Brd4CA recognizes aa 1313–1362 (83). The rabbit polyclonal antiserum raised against MCPyV VP1 was a gift from Chris Buck, NCI (17).

Antibodies used for western blotting include: mouse anti-MCPyV LT (sc-136172, CM2B4, Santa Cruz), mouse 2t2 (recognizes the common N-terminal domain of MCPyV sT and LT; gift from Chris Buck, NCI), mouse anti-glyceraldehyde 3-phosphate-dehydrogenase (GAPDH) (G8140-01, US Biological), mouse anti-Xpress (R910-25, Invitrogen), rabbit anti-phosphorylated ATM Ser1981 (ab-81292, Abcam), rabbit anti-ATM (2873s, Cell Signaling), rabbit anti-ATR (ab-2905, Abcam), mouse anti-PCNA (ab-2426, Abcam), rabbit anti-phosphorylated Chk1 Ser345 (2348s, Cell Signaling), mouse

anti-actin (MAB 1501M, Chemicon), HRP conjugated goat anti-mouse (7076s, Cell Signaling), and HRP conjugated goat anti-rabbit (7074s, Cell Signaling).

Mouse anti-ATM (2873S, Cell Signaling), rabbit anti-ATR (ab-2905, Abcam), normal rabbit IgG (12-370, Millipore), and normal mouse IgG (12-371, Millipore) were used for immunoprecipitations.

Etoposide, wortmannin, NU 6027, caffeine and puromycin were purchased from Sigma. NU 7441 was purchased from TOCRIS Bioscience. KU 55933 was purchased from EMD Millipore. AZD 7762 was purchased from Selleck Chemicals. Calf-intestinal alkaline phosphatase (CIP) was purchased from New England Biolabs. Annexin V-PE was purchased from BioVision. AcTEV protease was obtained from Invitrogen. Western Lightning Plus-ECL solution was purchased from Perkin Elmer (NEL).

6.4: Sample Preparation for Mass Spectrometry Analysis

HEK 293 cells were transfected with IIT-tagged pcDNA4c-MCPyV LT using the calcium phosphate method (50). Forty-eight hours post-transfection, nuclear extracts were prepared. Briefly, cells were resuspended in Buffer A supplemented with phosphatase inhibitors (10mM HEPES [pH 7.9], 10mM KCl, 0.1mM EDTA, 30mM NaF, 1mM Na₃VO₄, 40mM β-glycerophosphate, 0.2 mM PMSF and protease inhibitors). Cells were swollen on ice for 10 min before NP-40 was added to a final concentration of 6% and then vortexed for 10 sec. Nuclei were pelleted by centrifugation at 1200g at 4°C for 5 min. Nuclei were resuspended in Buffer B supplemented with phosphatase inhibitors

(20mM HEPES [pH 7.9], 400mM NaCl, 1mM EDTA, 30mM NaF, 1mM Na₃VO₄, 40mM β-glycerophosphate, 0.2mM PMSF and protease inhibitors) and lysed by passing through a 22-gauge needle 10 times. Lysates were incubated at 4°C for 1 hr and clarified at 20,000g at 4°C for 15 min. The supernatant was then immunopurified with IgG-Sepharose 6 Fast Flow beads (GE Healthcare, Pittsburgh, PA, USA), pre-blocked with 1% BSA, for 2 hr at 4°C. Bound immune complexes were washed twice with IP wash buffer with phosphatase inhibitors (10mM Tris-HCl [pH 8.0], 150mM NaCl, 0.1% NP-40, 30mM NaF, 1mM Na₃VO₄, and 40mM β-glycerophosphate), once with IP wash buffer without phosphatase inhibitors, and finally once with cleavage buffer (10mM Tris-HCl [pH 8.0], 150mM NaCl, 0.1% NP-40, 0.5mM EDTA, 0.5mM EGTA, and 1mM DTT). Bound proteins were then cleaved with TEV protease (Invitrogen) in cleavage buffer for 2 hr at room temperature. Beads were spun down and the supernatant was boiled in sample buffer and resolved by SDS-PAGE. The gel was stained with Coomassie Brilliant blue. The band corresponding to MCPyV LT was excised and analyzed by mass spectrometry.

6.5: Mass Spectrometry Analysis

The mass spectrometry analysis was provided by the Proteomics Core Facility, University of Pennsylvania. Protein samples were digested with trypsin as described by Strader *et al.* (153). Digested peptides were then purified by liquid chromatography using standard purification techniques or with a titanium oxide column (GE Healthcare Biosciences, Pittsburgh, PA, USA). Peptides were analyzed by nanoLC/MS/MS with a LTQ Mass Spectrometer (Thermo Scientific, Waltham, MA, USA) equipped with a nano

LC-2D HPLC system (Eksigent, Framingham, MA, USA). The data were analyzed with Sequest and Scaffold software.

6.6: Sequence Alignment of Polyomavirus LT Proteins

Clone Manager 9 software was used to align the amino acid sequences of various polyomavirus LT proteins. Amino acid sequences were aligned using the Mult-Way view and BLOSUM 62 scoring matrix. Polyomavirus LT sequences and their NCBI accession numbers are as follows: Merkel Cell Polyomavirus LT, R17a isolate (HM011555.1); Murine Polyomavirus LT (NC_001515.1); African Green Monkey Polyomavirus LT (NC_004763.2); WU Polyomavirus LT (NC_009539.1); KI Polyomavirus LT (NC_009238.1); BK Polyomavirus LT (NC_001538.1); JC Polyomavirus LT (NC_001699.1); SV40 LT (NC_001669.1).

6.7: Phyre2 Modeling of MCPyV LT Fragments

We modeled MCPyV LT amino acids 290–433 using Phyre2 software's intensive mode (154). The PDB file was then visualized using PyMOL software (155). The model was oriented using the origin binding domain crystal structure reported by Harrison and colleagues as a reference (28).

6.8: Immunofluorescent (IF) Staining

Cells were fixed with 3% paraformaldehyde in PBS for 20 min at 4 °C. Cells were incubated in blocking/permeabilization buffer (0.5% Triton X-100 and 3% BSA in PBS) for 10 min at room temperature and stained with specific primary antibodies (as

described in the figure legends) at room temperature for 60 min. After incubation, the cells were washed three times with blocking/permeabilization buffer and incubated with Alexa Fluor 594 goat anti-rabbit IgG and 488 goat anti-mouse IgG (Invitrogen, Molecular Probes, Ashburn, VA, USA) for an additional 60 min. After incubation with the secondary antibodies, cells were counterstained with DAPI (4',6'-diamidino-2-phenylindol) and examined with an Olympus IX81 inverted fluorescence microscope.

6.9: Microscopy and Image Analysis

All immunofluorescent images were collected using an inverted fluorescence microscope (Olympus IX81) connected to a high-resolution charge-coupled device camera (QImaging, FAST1394). Images were analyzed and presented using SlideBook 5.0 software (Intelligent Imaging Innovations, Inc., Denver, CO, USA). The scale bars were added using ImageJ software.

6.10: Southern Blotting

Replication assays were performed as described previously (49). Briefly, MCPyV LT constructs were transfected into C33A cells using the calcium phosphate method (50). Forty-eight hours post-transfection, whole genomic DNA was extracted. Genomic DNA (15 µg) was digested with BamHI, treated with or without DpnI at 37 °C overnight, and separated on a 0.7% agarose gel. DNA was transferred to a Hybond-N+ nitrocellulose membrane (Amersham, Piscataway, NJ, USA) and hybridized with a pcDNA4c-MCPyV Ori probe labeled with [α -³²P] dCTP using Prime-It II random primer labeling kit (Agilent Technologies) per the manufacturer's instructions. The results were analyzed

using a Phosphorimager (Typhoon 9400; GE Healthcare).

6.11: Western Blotting

For the work presented in chapter 2, cells were lysed in hypertonic lysis buffer (10mM HEPES [pH 7.9], 500mM NaCl, 3mM MgCl₂, 1mM dithiothreitol, 1mM phenylmethylsulfonyl fluoride, and protease inhibitors) by passage through a 22-gauge needle 10 times. After a 20-min incubation on ice, the soluble and insoluble fractions were separated by centrifugation at 5,000rpm for 10 min at 4°C. The supernatants (20 µg) were resolved on a SDS-PAGE gel and transferred to PVDF membrane. Membranes were blocked in 5% PBST-milk (5% w/v milk, 0.1% Tween in Phosphate-buffered Saline, [PBS]) for 1 hr at room temperature and incubated in PBST-milk containing primary antibodies at room temperature for 1 hr. After washing three times with PBST, membranes were then incubated with HRP-conjugated secondary antibodies in PBST-milk for 1 hr at room temperature. Western blots were developed using ECL solution and images were captured using a Fuji imaging system.

For immunoblotting with phosphospecific antibodies in chapter 3, cells were collected thirty-six hours post transfection in lysis buffer (10mM HEPES [pH 7.9], 300mM NaCl, 3mM MgCl₂, 1mM DTT, 1mM PMSF, 3mM sodium butyrate, 1mM PMSF, 1mM NaF, 100µM Na₃VO₄, supplemented with protease inhibitor cocktails (Roche) and S/T protein phosphatase inhibitor cocktails (Sigma)) and lysed by passing through a 26-gauge needle 10 times. After a 20 min incubation on ice with occasional vortexing, the soluble and insoluble fractions were separated by centrifugation at 5,000

rpm for 5 min at 4°C. The supernatant (20µg) was resolved by SDS-PAGE. Phosphatase inhibitors (1 mM NaF and 100 µM Na₃VO₄) were added to electrophoresis buffer and transfer buffer. Membranes were blocked in 5% TBST-milk (5% w/v milk, 0.1% Tween in Tris-Buffered Saline [TBS]) for 1 hour at room temperature and incubated in TBST-milk containing primary antibodies at 4°C overnight. For anti-phospho protein antibodies, TBST-BSA was used instead of TBST-milk. Membranes were then incubated with HRP conjugated secondary antibodies in TBST-milk for 1 hour at room temperature.

For immunoblots in Chapter 4, lysates generated for the luciferase assay using the Reporter Lysis system (Promega) were separated (25µL lysate) by SDS-PAGE and blotted with the antibodies indicated in the figure legends.

Western blots were developed using ECL solution and images were captured using a Fuji imaging system.

6.12: Affinity Purification of MCPyV LT

HEK 293 cells were transfected with constructs expressing IIT-tagged MCPyV LT (wild-type or mutant) using the calcium phosphate method. Forty-eight hours post-transfection, nuclear extracts were prepared. Briefly, cells were resuspended in Buffer A (10mM HEPES [pH 7.9], 10mM KCl, 0.1mM EDTA, 0.2mM PMSF, and protease inhibitors). Cells were swollen on ice for 10 min before NP-40 was added to a final concentration of 6% and then vortexed for 10 sec. Nuclei were pelleted by centrifugation

at 1200g at 4°C for 5 min. Nuclei were resuspended in Buffer B (20mM HEPE [pH 7.9], 400mM NaCl, 20% glycerol, 1mM EDTA, 0.2mM PMSF and protease inhibitors) and lysed by passing through a 22-gauge needle 10 times. Lysates were clarified at 20,000g at 4°C for 15 min. The supernatant was then immunopurified with IgG-Sepharose 6 Fast Flow beads (GE Healthcare) pre-blocked with 1% BSA for 2 hr at 4°C. Bound immune complexes were washed three times with IP 150 buffer (10mM Tris-HCl [pH 8.0], 150mM NaCl, 0.1% NP-40) and once with TEV cleavage buffer (50mM Tris-HCl [pH 8.0], 6% glycerol, 0.5mM EDTA, 0.5mM DTT, 1mM PMSF). Bound proteins were then cleaved with TEV protease (Invitrogen) in TEV cleavage buffer, overnight at 4°C. The beads were spun down and the supernatant collected for further biochemical analysis.

6.13: Electromobility Shift Assays (EMSA)

The EMSA probe was generated by PCR amplifying a portion of pcDNA4c-MCPyV Ori (Forward Primer: TTG GCA GAG GCT TGG GGC TCC, Reverse Primer: GCG GAA TTC TAA GCC TCT TAA GCC TC). The PCR product was purified using a Qiagen PCR Purification Kit (Cat# 28104) following the manufacturer's instructions. The purified probe (100 ng) was then 5' labeled with [³²P-γ] ATP with T4 Polynucleotide Kinase (New England Biolabs, Ipswich, MA, USA) following the manufacturer's instructions. The labeled probe was then diluted 1:50 before being used in the EMSA.

Binding reactions (20 μL) were assembled on ice. Various amounts of affinity purified MCPyV LT was mixed with 40 fmol labeled probe in binding buffer (30mM Tris-HCl [pH 8.0], 10% glycerol, 0.5μg BSA, 10ng poly d(I-C), 40ng Sonicated Salmon

Sperm DNA, 5mM AMP-PNP, 1mM DTT, and 1mM PMSF). Reactions were incubated at room temperature for 25 min and then separated on a 4% non-denaturing polyacrylamide gel in $0.5 \times$ TBE (Tris-Borate-EDTA) at 120V for 3 hr. The gel was dried and subjected to autoradiography. The non-hydrolyzable ATP analogue, adenylyl imidodiphosphate (AMP-PNP) was obtained from Sigma (St. Louis, MO, USA, Cat# A2647).

6.14: Unwinding Assay

The probe was generated by annealing two oligos (80ng each) spanning the central portion of the MCPyV Ori sequence (Figure 2.7 A) (Top Strand Oligo: GTG ACT TTT TTT TTT CAA GTT GGC AGA GGC TTG GGG CTC CTA GCC TCC GAG GCC TCT GGA AAA AAA AGA GAG AGG CC; Bottom Strand Oligo: CAG AGG CCT CTC TCT TTT TTT TCC AGA GGC CTC GGA GGC TAG GAG CCC CAA GCC TCT GCC AAC TTG AAA AAA AAA AGT CAC). The four-nucleotide overhang was filled in using Klenow DNA Polymerase (New England Biolabs) by mixing the duplexed probe in a reaction containing 0.1mM dTTP, dGTP, and [32 P- α] dCTP and incubating at room temperature for 20 min. After adding dATP to a final concentration of 0.1mM, reactions were incubated for another 20 min at room temperature.

Various amounts of purified MCPyV LT were combined with 60pg of labeled probe in 20 μ L unwinding reaction buffer (30mM HEPES [pH 8.0], 0.1mg/mL BSA, 7mM MgCl₂, 4mM ATP, 40mM creatine phosphate, 25 μ g/mL creatine phosphate kinase). Reactions were carried out at room temperature for 1 hr. Reactions were stopped

by adding 5 μ L 5 \times Stop Buffer (2.5% SDS, and 100mM EDTA). Loading dye (bromophenol blue, 4% sucrose and 1XTBE) was added and samples were separated on an 11% non-denaturing PAGE in 0.5XTBE. Gels were dried and analyzed using autoradiography.

6.15: Helicase Assay

The helicase assay was performed as previously described with minor modification (14). Wild-type or mutant MCPyV LT fused to an IIT tag was expressed in HEK 293 cells and purified using IgG Sepharose 6 Fast Flow beads (GE Healthcare), which were preblocked with 1% BSA in PBS at 4 °C for >1 hr. Beads with bound LT were split into two equal fractions for SDS-PAGE/Coomassie brilliant blue staining and helicase assays, respectively. To label the helicase assay substrate, 35ng of a 31-mer oligo (5'-CCA GGG TTT TCC CAG TCA CGA CGT TGT AAA C-3') was annealed to 1 μ g of M13mp18 DNA (New England BioLabs). The primer was then elongated using Klenow polymerase (New England BioLabs) in a 50 μ L reaction containing 0.1mM dCTP, dGTP, and [α -³²P] dATP. After 20 min of incubation at room temperature, 0.1mM dATP was added and the reaction incubated for another 20 min. Then, 0.5 μ L of labeled substrate was used in each reaction. LT purified on IgG Sepharose was incubated with the substrate in helicase assay buffer (20mM Tris-HCl [pH 7.5], 10mM MgCl₂, 1mM DTT, 0.1mg/mL BSA, and 5mM ATP) at 37°C for 30 min. The reaction was stopped by adding SDS to a final concentration of 0.2% and EDTA to 50mM. Total reaction mixtures were resolved by electrophoresis on 11% non-denaturing polyacrylamide gels. The gels were dried and subjected to autoradiography.

6.16: Calf-intestinal Alkaline Phosphatase (CIP) Assay

Forty-eight hours post transfection, cells were lysed in lysis buffer (50mM Tris-HCl, pH 8.0, 150mM NaCl, 10% Glycerol, 1% NP-40, 5mM MgCl₂, 1mM DTT, and protease inhibitors) and passed through a 26-gauge needle 5 times. Lysates were incubated on ice for 20 min with occasional vortexing. Lysates were then spun down at 5,000rpm for 5 min at 4°C. Cleared supernatants were collected. A Bradford assay was performed to determine protein concentration and lysates were then diluted to 1mg/ml with lysis buffer. A 100µg aliquot of lysate was used for CIP treatment: NEB buffer 3 was added to the lysate to a final concentration of 1X Buffer, and the solution was incubated at 37°C for 5 min. The samples were then treated with 50 units of CIP for 30 min at 37°C. Samples were boiled in sample buffer and immunoblotted.

6.17: Annexin V Staining

C33A cells were transfected with pEGFPC1, pEGFPC1-MCPyV LT, or pEGFPC1-MCPyV LT S816A. 24 hours post transfection, cells were washed with binding buffer (10mM HEPES [pH 7.4], 140mM NaCl, 2.5mM CaCl₂), stained with Annexin V-PE for 10 min, washed once more with binding buffer, and fixed with 3% paraformaldehyde for 20 min. Nuclei were counterstained with DAPI.

6.18: Retrovirus Production and Stable Cell Line Construction

293T cells were cultured in 10 cm dishes to reach 95%-100% confluency. pLPCX-based plasmids (pLPCX-Cherry-LacI, pLPCX-MCPyV LT 1-817, and pLPCX-MCPyV LT 1-817 S816A), pVSVG, and pMD-gagpol were co-transfected into 293T

using Lipofectamine 2000 transfection reagent. After 48 hours, the packaged retroviruses in the supernatant were harvested and filtered through a 0.45 μ m filter before transducing C33A and HeLa cells. At 48 hours post-infection, the transduced cells were selected using 0.625 μ g/ml or 1 μ g/ml puromycin, respectively, for 4 days. Expression of MCPyV LT was confirmed by immunofluorescent staining and western blotting, and the selected cells were maintained as stable cell lines in DMEM supplemented with puromycin.

6.19: In Vitro phosphorylation Assay

To activate ATM and ATR, U2OS cells were treated for 4 hr with 4 μ M etoposide, which induces double-strand DNA breaks. Treated cells were harvested and re-suspended in buffer A [10mM HEPES [pH 7.9], 10mM KCl, 0.1mM EDTA, 0.1mM EGTA, 1mM DTT, 0.2mM PMSF, 3mM sodium butyrate, 1mM NaF, and 100 μ M Na₃VO₄, supplemented with protease inhibitor cocktails (Roche) and S/T protein phosphatase inhibitor cocktails (Sigma)], and incubated on ice for 10 min. NP-40 was added to a final concentration of 0.02% and cells were vortexed for 10 seconds. Nuclei were separated by centrifugation at 4,000rpm, 10 min, 4°C. Isolated nuclei were lysed in buffer B [20mM HEPES [pH 7.9], 0.5M NaCl, 1mM EDTA, 1mM EGTA, 1mM DTT, 0.2mM PMSF, 3mM sodium butyrate, 1mM NaF, and 100 μ M Na₃VO₄, supplemented with protease inhibitor cocktails (Roche) and S/T protein phosphatase inhibitor cocktails (Sigma)] by passing through a 22-gauge needle 10 times, followed by rotation at 4°C for 1 hour. Nuclear extracts were isolated by centrifugation at 14,000rpm, 10 min, 4°C.

Nuclear extracts (500 μ g) were mixed with 10 μ g rabbit anti-ATM, 10 μ g mouse anti-ATR, or 10 μ g normal rabbit IgG together with 10 μ g normal mouse IgG. Nuclear extracts and antibody mixture was rotated at 4°C for 2 hours, and then 10 μ l protein G agarose beads (Invitrogen) were added. Mixtures were rotated for another hour at 4°C. Proteins bound to the resin were washed four times with KCl buffer (20mM Tris [pH 8.0], 10% Glycerol, 5mM MgCl₂, 0.1% Tween-20, 150mM KCl, 0.1mM PMSF, 3mM sodium butyrate, 1mM NaF, and 100 μ M Na₃VO₄, supplemented with protease inhibitor cocktails (Roche) and S/T protein phosphatase inhibitor cocktails (Sigma)). Resin was then equilibrated once with kinase buffer (20mM HEPES [pH 7.6], 50mM NaCl, 10mM MgCl₂, 1mM DTT, 20mM MnCl₂ and 1mM NaF). IIT-MCPyV LT was purified as previously described (14) and treated with CIP as described in Section 6.16. MCPyV LT was cleaved by AcTEV protease (Invitrogen) following the manufacturer's instructions.

Equilibrated resin (10 μ L) with purified ATM or ATR proteins was mixed with 30 μ l kinase buffer, 1 μ g purified MCPyV LT, 200 μ M ATP, and 0.5 μ l of 3,000Ci/mmol [γ -³²P] ATP. Kinase assay was performed at room temperature or 37°C for 30 min. Proteins were separated by SDS-PAGE, and the gel was subsequently dried at 80°C for 30 min. Autoradiography was performed as previously described (50).

6.20: Glutathione S-Transferase Pull-Down Assay

BL21(DE3)pLysS *E. coli* were transformed with pGEX-MCPyV LT or pGEX vector. Bacteria were lysed with lysis buffer (10mM Tris-HCl [pH 8.0], 50mM NaCl, 0.4mg/ml lysozyme, 2mM DTT, 0.1mM EDTA, supplemented with protease inhibitors)

before running through Q-sepharose (Sigma) and SP-sepharose (Sigma) columns. The SP-sepharose column was washed with buffer (50mM Tris-HCl [pH 8.0], 150mM NaCl, 2mM DTT, 0.1mM EDTA, supplemented with protease inhibitors) before elution with the same buffer containing 400mM NaCl. Elution was then incubated with GSH-agarose (Sigma) at 4°C for 2 hr. GSH-agarose was washed five times with wash buffer (20mM Tris-HCl [pH 8.0], 5mM MgCl₂, 0.1% Tween-20, 100mM KCl, supplemented with protease inhibitors). Bound proteins were used for GST pull-down assay. Briefly, U2OS nuclear extracts was prepared as previously described (156) and incubated with beads bound with GST or GST-LT at 4°C overnight. The beads were washed three times with 0.5ml of 0.1 M KCl buffer and eluted with 30ul of SDS-PAGE sample buffer.

6.21: Clonogenic Assay

C33A cells stably expressing Cherry-LacI, LT 1-817 or LT 1-817 S816A were plated in triplicate at 5×10^3 cells/well in a 6-well plate, and cultured in DMEM medium with 10% FBS and 0.625µg/ml puromycin for 10 days. The cells were then fixed with methanol and stained with 0.5% methylene blue.

6.22: Luciferase Assay

293 cells were plated in triplicate at 2×10^3 cells/well in a 6-well plate and cultured in DMEM with 10% FBS. Cells were co-transfected with the luciferase reporter plasmid and viral protein expression constructs indicated in the figure legends using the calcium phosphate method (50). Cells were collected at the indicated time points using the Reporter Lysis system (Promega) following the manufacturer's instructions. Protein

concentration was measured by NanoDrop. Luciferase activity was measured using the Luciferase Assay System (Promega) according to the manufacturer's instructions and normalized to protein concentration. For ISRE activation in Figure 4.2, cells were stimulated 24 hrs post transfection with 1,000units/per well recombinant IFN- α , and collected 48 hrs post transfection.

6.23: Statistical Analyses

Prism software was used to perform a one-way ANOVA test. A $p < 0.05$ was considered statistically significant.

REFERENCES

1. Toker, C. (1972) Trabecular carcinoma of the skin. *Arch Dermatol* **105**, 107-110
2. Lucarz, A., and Brand, G. (2007) Current considerations about Merkel cells. *Eur J Cell Biol* **86**, 243-251
3. Chang, Y., and Moore, P. S. (2011) Merkel cell carcinoma: a virus-induced human cancer. *Annu Rev Pathol* **7**, 123-144
4. Heath, M., Jaimes, N., Lemos, B., Mostaghimi, A., Wang, L. C., Penas, P. F., and Nghiem, P. (2008) Clinical characteristics of Merkel cell carcinoma at diagnosis in 195 patients: the AEIOU features. *J Am Acad Dermatol* **58**, 375-381
5. Hodgson, N. C. (2005) Merkel cell carcinoma: changing incidence trends. *J Surg Oncol* **89**, 1-4
6. Feng, H., Shuda, M., Chang, Y., and Moore, P. S. (2008) Clonal integration of a polyomavirus in human Merkel cell carcinoma. *Science* **319**, 1096-1100
7. Rodig, S. J., Cheng, J., Wardzala, J., DoRosario, A., Scanlon, J. J., Laga, A. C., Martinez-Fernandez, A., Barletta, J. A., Bellizzi, A. M., Sadasivam, S., Holloway, D. T., Cooper, D. J., Kupper, T. S., Wang, L. C., and DeCaprio, J. A. (2012) Improved detection suggests all Merkel cell carcinomas harbor Merkel polyomavirus. *J Clin Invest* **122**, 4645-4653
8. Gjoerup, O., and Chang, Y. (2010) Update on human polyomaviruses and cancer. *Adv Cancer Res* **106**, 1-51
9. Shuda, M., Feng, H., Kwun, H. J., Rosen, S. T., Gjoerup, O., Moore, P. S., and Chang, Y. (2008) T antigen mutations are a human tumor-specific signature for Merkel cell polyomavirus. *Proc Natl Acad Sci U S A* **105**, 16272-16277
10. Kwun, H. J., Guastafierro, A., Shuda, M., Meinke, G., Bohm, A., Moore, P. S., and Chang, Y. (2009) The minimum replication origin of merkel cell polyomavirus has a unique large T-antigen loading architecture and requires small T-antigen expression for optimal replication. *J Virol* **83**, 12118-12128
11. Doorbar, J. (2006) Molecular biology of human papillomavirus infection and cervical cancer. *Clin Sci (Lond)* **110**, 525-541
12. Doorbar, J., Quint, W., Banks, L., Bravo, I. G., Stoler, M., Broker, T. R., and Stanley, M. A. (2012) The biology and life-cycle of human papillomaviruses. *Vaccine* **30 Suppl 5**, F55-70
13. Cheng, J., Rozenblatt-Rosen, O., Paulson, K. G., Nghiem, P., and DeCaprio, J. A. (2013) Merkel cell polyomavirus large T antigen has growth-promoting and inhibitory activities. *J Virol* **87**, 6118-6126
14. Li, J., Wang, X., Diaz, J., Tsang, S. H., Buck, C. B., and You, J. (2013) Merkel cell polyomavirus large T antigen disrupts host genomic integrity and inhibits cellular proliferation. *J Virol* **87**, 9173-9188
15. Carter, J. J., Paulson, K. G., Wipf, G. C., Miranda, D., Madeleine, M. M., Johnson, L. G., Lemos, B. D., Lee, S., Warcola, A. H., Iyer, J. G., Nghiem, P., and Galloway, D. A. (2009) Association of Merkel cell polyomavirus-specific antibodies with Merkel cell carcinoma. *J Natl Cancer Inst* **101**, 1510-1522
16. Kean, J. M., Rao, S., Wang, M., and Garcea, R. L. (2009) Seroepidemiology of human polyomaviruses. *PLoS Pathog* **5**, e1000363

17. Pastrana, D. V., Tolstov, Y. L., Becker, J. C., Moore, P. S., Chang, Y., and Buck, C. B. (2009) Quantitation of human seroresponsiveness to Merkel cell polyomavirus. *PLoS Pathog* **5**, e1000578
18. Tolstov, Y. L., Knauer, A., Chen, J. G., Kensler, T. W., Kingsley, L. A., Moore, P. S., and Chang, Y. (2011) Asymptomatic primary Merkel cell polyomavirus infection among adults. *Emerg Infect Dis* **17**, 1371-1380
19. Tolstov, Y. L., Pastrana, D. V., Feng, H., Becker, J. C., Jenkins, F. J., Moschos, S., Chang, Y., Buck, C. B., and Moore, P. S. (2009) Human Merkel cell polyomavirus infection II. MCV is a common human infection that can be detected by conformational capsid epitope immunoassays. *Int J Cancer* **125**, 1250-1256
20. Touze, A., Gaitan, J., Arnold, F., Cazal, R., Fleury, M. J., Combelas, N., Sizaret, P. Y., Guyetant, S., Maruani, A., Baay, M., Tognon, M., and Coursaget, P. (2010) Generation of Merkel cell polyomavirus (MCV)-like particles and their application to detection of MCV antibodies. *J Clin Microbiol* **48**, 1767-1770
21. Foulongne, V., Sauvage, V., Hebert, C., Dereure, O., Cheval, J., Gouilh, M. A., Pariente, K., Segondy, M., Burguiere, A., Manuguerra, J. C., Caro, V., and Eloit, M. (2012) Human skin microbiota: high diversity of DNA viruses identified on the human skin by high throughput sequencing. *PLoS One* **7**, e38499
22. Schowalter, R. M., Pastrana, D. V., Pumphrey, K. A., Moyer, A. L., and Buck, C. B. (2010) Merkel cell polyomavirus and two previously unknown polyomaviruses are chronically shed from human skin. *Cell Host Microbe* **7**, 509-515
23. Spurgeon, M. E., and Lambert, P. F. (2013) Merkel cell polyomavirus: a newly discovered human virus with oncogenic potential. *Virology* **435**, 118-130
24. Liu, X., Hein, J., Richardson, S. C., Basse, P. H., Toptan, T., Moore, P. S., Gjoerup, O. V., and Chang, Y. (2010) Merkel cell polyomavirus large T antigen disrupts lysosome clustering by translocating human Vam6p from the cytoplasm to the nucleus. *J Biol Chem* **286**, 17079-17090
25. Houben, R., Angermeyer, S., Haferkamp, S., Aue, A., Goebeler, M., Schrama, D., and Hesbacher, S. (2014) Characterization of functional domains in the Merkel cell polyoma virus Large T antigen. *Int J Cancer*
26. Borchert, S., Czech-Sioli, M., Neumann, F., Schmidt, C., Wimmer, P., Dobner, T., Grundhoff, A., and Fischer, N. (2014) High-Affinity Rb Binding, p53 Inhibition, Subcellular Localization, and Transformation by Wild-Type or Tumor-Derived Shortened Merkel Cell Polyomavirus Large T Antigens. *J Virol* **88**, 3144-3160
27. Shuda, M., Kwun, H. J., Feng, H., Chang, Y., and Moore, P. S. (2011) Human Merkel cell polyomavirus small T antigen is an oncoprotein targeting the 4E-BP1 translation regulator. *J Clin Invest* **121**, 3623-3634
28. Harrison, C. J., Meinke, G., Kwun, H. J., Rogalin, H., Phelan, P. J., Bullock, P. A., Chang, Y., Moore, P. S., and Bohm, A. (2011) Asymmetric assembly of Merkel cell polyomavirus large T-antigen origin binding domains at the viral origin. *J Mol Biol* **409**, 529-542
29. Collot-Teixeira, S., Bass, J., Denis, F., and Ranger-Rogez, S. (2004) Human tumor suppressor p53 and DNA viruses. *Rev Med Virol* **14**, 301-319

30. Ahuja, D., Saenz-Robles, M. T., and Pipas, J. M. (2005) SV40 large T antigen targets multiple cellular pathways to elicit cellular transformation. *Oncogene* **24**, 7729-7745
31. Cheng, J., DeCaprio, J. A., Fluck, M. M., and Schaffhausen, B. S. (2009) Cellular transformation by Simian Virus 40 and Murine Polyoma Virus T antigens. *Semin Cancer Biol* **19**, 218-228
32. Houben, R., Adam, C., Baeurle, A., Hesbacher, S., Grimm, J., Angermeyer, S., Henzel, K., Hauser, S., Elling, R., Brocker, E. B., Gaubatz, S., Becker, J. C., and Schrama, D. (2012) An intact retinoblastoma protein-binding site in Merkel cell polyomavirus large T antigen is required for promoting growth of Merkel cell carcinoma cells. *Int J Cancer* **130**, 847-856
33. Houben, R., Shuda, M., Weinkam, R., Schrama, D., Feng, H., Chang, Y., Moore, P. S., and Becker, J. C. (2010) Merkel cell polyomavirus-infected Merkel cell carcinoma cells require expression of viral T antigens. *J Virol* **84**, 7064-7072
34. Shuda, M., Chang, Y., and Moore, P. S. (2013) Merkel Cell Polyomavirus-Positive Merkel Cell Carcinoma Requires Viral Small T-Antigen for Cell Proliferation. *J Invest Dermatol*
35. Pallas, D. C., Shahrik, L. K., Martin, B. L., Jaspers, S., Miller, T. B., Brautigan, D. L., and Roberts, T. M. (1990) Polyoma small and middle T antigens and SV40 small t antigen form stable complexes with protein phosphatase 2A. *Cell* **60**, 167-176
36. Sontag, E., Fedorov, S., Kamibayashi, C., Robbins, D., Cobb, M., and Mumby, M. (1993) The interaction of SV40 small tumor antigen with protein phosphatase 2A stimulates the map kinase pathway and induces cell proliferation. *Cell* **75**, 887-897
37. Rodriguez-Viciana, P., Collins, C., and Fried, M. (2006) Polyoma and SV40 proteins differentially regulate PP2A to activate distinct cellular signaling pathways involved in growth control. *Proc Natl Acad Sci U S A* **103**, 19290-19295
38. Griffiths, D. A., Abdul-Sada, H., Knight, L. M., Jackson, B. R., Richards, K., Prescott, E. L., Peach, A. H., Blair, G. E., Macdonald, A., and Whitehouse, A. (2013) Merkel cell polyomavirus small T antigen targets the NEMO adaptor protein to disrupt inflammatory signaling. *J Virol* **87**, 13853-13867
39. Knight, L. M., Stakaityte, G., Wood, J. J., Abdul-Sada, H., Griffiths, D. A., Howell, G. J., Wheat, R., Blair, G. E., Steven, N. M., Macdonald, A., Blackburn, D. J., and Whitehouse, A. (2014) Merkel cell polyomavirus small T antigen mediates microtubule destabilisation to promote cell motility and migration. *J Virol*
40. Kwun, H. J., Shuda, M., Feng, H., Camacho, C. J., Moore, P. S., and Chang, Y. (2013) Merkel cell polyomavirus small T antigen controls viral replication and oncoprotein expression by targeting the cellular ubiquitin ligase SCFFbw7. *Cell Host Microbe* **14**, 125-135
41. Feng, H., Kwun, H. J., Liu, X., Gjoerup, O., Stolz, D. B., Chang, Y., and Moore, P. S. (2011) Cellular and viral factors regulating Merkel cell polyomavirus replication. *PLoS One* **6**, e22468

42. Boyapati, A., Wilson, M., Yu, J., and Rundell, K. (2003) SV40 17KT antigen complements dnaJ mutations in large T antigen to restore transformation of primary human fibroblasts. *Virology* **315**, 148-158
43. Zerrahn, J., Knippschild, U., Winkler, T., and Deppert, W. (1993) Independent expression of the transforming amino-terminal domain of SV40 large I antigen from an alternatively spliced third SV40 early mRNA. *EMBO J* **12**, 4739-4746
44. Carter, J. J., Daugherty, M. D., Qi, X., Bheda-Malge, A., Wipf, G. C., Robinson, K., Roman, A., Malik, H. S., and Galloway, D. A. (2013) Identification of an overprinting gene in Merkel cell polyomavirus provides evolutionary insight into the birth of viral genes. *Proc Natl Acad Sci U S A* **110**, 12744-12749
45. Neumann, F., Borchert, S., Schmidt, C., Reimer, R., Hohenberg, H., Fischer, N., and Grundhoff, A. (2011) Replication, gene expression and particle production by a consensus Merkel Cell Polyomavirus (MCPyV) genome. *PLoS One* **6**, e29112
46. Schowalter, R. M., Pastrana, D. V., and Buck, C. B. (2011) Glycosaminoglycans and sialylated glycans sequentially facilitate Merkel cell polyomavirus infectious entry. *PLoS Pathog* **7**, e1002161
47. Erickson, K. D., Garcea, R. L., and Tsai, B. (2009) Ganglioside GT1b is a putative host cell receptor for the Merkel cell polyomavirus. *J Virol* **83**, 10275-10279
48. Neu, U., Hengel, H., Blaum, B. S., Schowalter, R. M., Macejak, D., Gilbert, M., Wakarchuk, W. W., Imamura, A., Ando, H., Kiso, M., Arnberg, N., Garcea, R. L., Peters, T., Buck, C. B., and Stehle, T. (2012) Structures of Merkel cell polyomavirus VP1 complexes define a sialic acid binding site required for infection. *PLoS Pathog* **8**, e1002738
49. Tsang, S. H., Wang, X., Li, J., Buck, C. B., and You, J. (2014) Host DNA damage response factors localize to merkel cell polyomavirus DNA replication sites to support efficient viral DNA replication. *J Virol* **88**, 3285-3297
50. Wang, X., Li, J., Schowalter, R. M., Jiao, J., Buck, C. B., and You, J. (2012) Bromodomain protein Brd4 plays a key role in Merkel cell polyomavirus DNA replication. *PLoS Pathog* **8**, e1003021
51. Fanning, E., and Zhao, K. (2009) SV40 DNA replication: from the A gene to a nanomachine. *Virology* **384**, 352-359
52. Borowiec, J. A., Dean, F. B., Bullock, P. A., and Hurwitz, J. (1990) Binding and unwinding--how T antigen engages the SV40 origin of DNA replication. *Cell* **60**, 181-184
53. Meinke, G., Bullock, P. A., and Bohm, A. (2006) Crystal structure of the simian virus 40 large T-antigen origin-binding domain. *J Virol* **80**, 4304-4312
54. Cole, C. N., Tornow, J., Clark, R., and Tjian, R. (1986) Properties of the simian virus 40 (SV40) large T antigens encoded by SV40 mutants with deletions in gene A. *J Virol* **57**, 539-546
55. Giacherio, D., and Hager, L. P. (1979) A poly(dT)-stimulated ATPase activity associated with simian virus 40 large T antigen. *J Biol Chem* **254**, 8113-8116
56. Spillman, T., Giacherio, D., and Hager, L. P. (1979) Single strand DNA binding of simian virus 40 tumor antigen. *J Biol Chem* **254**, 3100-3104

57. Stenlund, A. (2003) Initiation of DNA replication: lessons from viral initiator proteins. *Nat Rev Mol Cell Biol* **4**, 777-785
58. Parsons, R. E., Stenger, J. E., Ray, S., Welker, R., Anderson, M. E., and Tegtmeyer, P. (1991) Cooperative assembly of simian virus 40 T-antigen hexamers on functional halves of the replication origin. *J Virol* **65**, 2798-2806
59. Cuesta, I., Nunez-Ramirez, R., Scheres, S. H., Gai, D., Chen, X. S., Fanning, E., and Carazo, J. M. (2010) Conformational rearrangements of SV40 large T antigen during early replication events. *J Mol Biol* **397**, 1276-1286
60. Foster, E. C., and Simmons, D. T. (2010) The SV40 large T-antigen origin binding domain directly participates in DNA unwinding. *Biochemistry* **49**, 2087-2096
61. Mastrangelo, I. A., Hough, P. V., Wall, J. S., Dodson, M., Dean, F. B., and Hurwitz, J. (1989) ATP-dependent assembly of double hexamers of SV40 T antigen at the viral origin of DNA replication. *Nature* **338**, 658-662
62. Reynisdottir, I., Lorimer, H. E., Friedman, P. N., Wang, E. H., and Prives, C. (1993) Phosphorylation and active ATP hydrolysis are not required for SV40 T antigen hexamer formation. *J Biol Chem* **268**, 24647-24654
63. San Martin, M. C., Gruss, C., and Carazo, J. M. (1997) Six molecules of SV40 large T antigen assemble in a propeller-shaped particle around a channel. *J Mol Biol* **268**, 15-20
64. Smelkova, N. V., and Borowiec, J. A. (1997) Dimerization of simian virus 40 T-antigen hexamers activates T-antigen DNA helicase activity. *J Virol* **71**, 8766-8773
65. Valle, M., Chen, X. S., Donate, L. E., Fanning, E., and Carazo, J. M. (2006) Structural basis for the cooperative assembly of large T antigen on the origin of replication. *J Mol Biol* **357**, 1295-1305
66. VanLoock, M. S., Alexandrov, A., Yu, X., Cozzarelli, N. R., and Egelman, E. H. (2002) SV40 large T antigen hexamer structure: domain organization and DNA-induced conformational changes. *Curr Biol* **12**, 472-476
67. Weisshart, K., Friedl, S., Taneja, P., Nasheuer, H. P., Schlott, B., Grosse, F., and Fanning, E. (2004) Partial proteolysis of simian virus 40 T antigen reveals intramolecular contacts between domains and conformation changes upon hexamer assembly. *J Biol Chem* **279**, 38943-38951
68. Weisshart, K., Taneja, P., Jenne, A., Herbig, U., Simmons, D. T., and Fanning, E. (1999) Two regions of simian virus 40 T antigen determine cooperativity of double-hexamer assembly on the viral origin of DNA replication and promote hexamer interactions during bidirectional origin DNA unwinding. *J Virol* **73**, 2201-2211
69. Wessel, R., Schweizer, J., and Stahl, H. (1992) Simian virus 40 T-antigen DNA helicase is a hexamer which forms a binary complex during bidirectional unwinding from the viral origin of DNA replication. *J Virol* **66**, 804-815
70. Yardimci, H., Wang, X., Loveland, A. B., Tappin, I., Rudner, D. Z., Hurwitz, J., van Oijen, A. M., and Walter, J. C. (2012) Bypass of a protein barrier by a replicative DNA helicase. *Nature* **492**, 205-209

71. McVey, D., Brizuela, L., Mohr, I., Marshak, D. R., Gluzman, Y., and Beach, D. (1989) Phosphorylation of large tumour antigen by cdc2 stimulates SV40 DNA replication. *Nature* **341**, 503-507
72. McVey, D., Woelker, B., and Tegtmeyer, P. (1996) Mechanisms of simian virus 40 T-antigen activation by phosphorylation of threonine 124. *J Virol* **70**, 3887-3893
73. Barbaro, B. A., Sreekumar, K. R., Winters, D. R., Prack, A. E., and Bullock, P. A. (2000) Phosphorylation of simian virus 40 T antigen on Thr 124 selectively promotes double-hexamer formation on subfragments of the viral core origin. *J Virol* **74**, 8601-8613
74. Cegielska, A., Moarefi, I., Fanning, E., and Virshup, D. M. (1994) T-antigen kinase inhibits simian virus 40 DNA replication by phosphorylation of intact T antigen on serines 120 and 123. *J Virol* **68**, 269-275
75. Cegielska, A., Shaffer, S., Derua, R., Goris, J., and Virshup, D. M. (1994) Different oligomeric forms of protein phosphatase 2A activate and inhibit simian virus 40 DNA replication. *Mol Cell Biol* **14**, 4616-4623
76. Scheidtmann, K. H., Mumby, M. C., Rundell, K., and Walter, G. (1991) Dephosphorylation of simian virus 40 large-T antigen and p53 protein by protein phosphatase 2A: inhibition by small-t antigen. *Mol Cell Biol* **11**, 1996-2003
77. Umphress, J. L., Tuazon, P. T., Chen, C. J., and Traugh, J. A. (1992) Determinants on simian virus 40 large T antigen are important for recognition and phosphorylation by casein kinase I. *Eur J Biochem* **203**, 239-243
78. Virshup, D. M., Kauffman, M. G., and Kelly, T. J. (1989) Activation of SV40 DNA replication in vitro by cellular protein phosphatase 2A. *EMBO J* **8**, 3891-3898
79. Xiao, C. Y., Hubner, S., and Jans, D. A. (1997) SV40 large tumor antigen nuclear import is regulated by the double-stranded DNA-dependent protein kinase site (serine 120) flanking the nuclear localization sequence. *J Biol Chem* **272**, 22191-22198
80. Zhao, X., Madden-Fuentes, R. J., Lou, B. X., Pipas, J. M., Gerhardt, J., Rigell, C. J., and Fanning, E. (2008) Ataxia telangiectasia-mutated damage-signaling kinase- and proteasome-dependent destruction of Mre11-Rad50-Nbs1 subunits in Simian virus 40-infected primate cells. *J Virol* **82**, 5316-5328
81. Shi, Y., Dodson, G. E., Shaikh, S., Rundell, K., and Tibbetts, R. S. (2005) Ataxia-telangiectasia-mutated (ATM) is a T-antigen kinase that controls SV40 viral replication in vivo. *J Biol Chem* **280**, 40195-40200
82. Harrison, C., Jiang, T., Banerjee, P., Meinke, G., D'Abramo, C. M., Schaffhausen, B., and Bohm, A. (2013) Polyomavirus large T antigen binds symmetrical repeats at the viral origin in an asymmetrical manner. *J Virol* **87**, 13751-13759
83. Wang, X., Helfer, C. M., Pancholi, N., Bradner, J. E., and You, J. (2013) Recruitment of Brd4 to the human papillomavirus type 16 DNA replication complex is essential for replication of viral DNA. *J Virol* **87**, 3871-3884
84. Dynan, W. S., and Tjian, R. (1983) The promoter-specific transcription factor Sp1 binds to upstream sequences in the SV40 early promoter. *Cell* **35**, 79-87

85. Dynan, W. S., and Tjian, R. (1983) Isolation of transcription factors that discriminate between different promoters recognized by RNA polymerase II. *Cell* **32**, 669-680
86. Manley, K., O'Hara, B. A., and Atwood, W. J. (2008) Nuclear factor of activated T-cells (NFAT) plays a role in SV40 infection. *Virology* **372**, 48-55
87. White, M. K., Safak, M., and Khalili, K. (2009) Regulation of gene expression in primate polyomaviruses. *J Virol* **83**, 10846-10856
88. Mathis, D. J., and Chambon, P. (1981) The SV40 early region TATA box is required for accurate in vitro initiation of transcription. *Nature* **290**, 310-315
89. Bikel, I., and Loeken, M. R. (1992) Involvement of simian virus 40 (SV40) small t antigen in trans activation of SV40 early and late promoters. *J Virol* **66**, 1489-1494
90. Schowalter, R. M., Reinhold, W. C., and Buck, C. B. (2012) Entry tropism of BK and Merkel cell polyomaviruses in cell culture. *PLoS One* **7**, e42181
91. Shuda, M., Arora, R., Kwun, H. J., Feng, H., Sarid, R., Fernandez-Figueras, M. T., Tolstov, Y., Gjoerup, O., Mansukhani, M. M., Swerdlow, S. H., Chaudhary, P. M., Kirkwood, J. M., Nalesnik, M. A., Kant, J. A., Weiss, L. M., Moore, P. S., and Chang, Y. (2009) Human Merkel cell polyomavirus infection I. MCV T antigen expression in Merkel cell carcinoma, lymphoid tissues and lymphoid tumors. *Int J Cancer* **125**, 1243-1249
92. Tsang, S. H., Wang, X., Li, J., Buck, C. B., and You, J. (2014) Host DNA Damage Response Factors Localize to Merkel Cell Polyomavirus DNA Replication Sites to Support Efficient Viral DNA Replication. *J Virol*
93. Fanning, E. (1994) Control of SV40 DNA replication by protein phosphorylation: a model for cellular DNA replication? *Trends Cell Biol* **4**, 250-255
94. Moarefi, I. F., Small, D., Gilbert, I., Hopfner, M., Randall, S. K., Schneider, C., Russo, A. A., Ramsperger, U., Arthur, A. K., Stahl, H., and et al. (1993) Mutation of the cyclin-dependent kinase phosphorylation site in simian virus 40 (SV40) large T antigen specifically blocks SV40 origin DNA unwinding. *J Virol* **67**, 4992-5002
95. Mohr, I. J., Stillman, B., and Gluzman, Y. (1987) Regulation of SV40 DNA replication by phosphorylation of T antigen. *EMBO J* **6**, 153-160
96. Montenarh, M., and Muller, D. (1987) The phosphorylation at Thr 124 of simian virus 40 large T antigen is crucial for its oligomerization. *FEBS Lett* **221**, 199-204
97. Simmons, D. T. (1984) Stepwise phosphorylation of the NH₂-terminal region of the simian virus 40 large T antigen. *J Biol Chem* **259**, 8633-8640
98. Harrison, C., Jiang, T., Banerjee, P., Meinke, G., D'Abramo, C. M., Schaffhausen, B., and Bohm, A. (2011) Polyomavirus large T antigen binds symmetrical repeats at the viral origin in an asymmetrical manner. *J Virol* **87**, 13751-13759
99. Schneider, J., and Fanning, E. (1988) Mutations in the phosphorylation sites of simian virus 40 (SV40) T antigen alter its origin DNA-binding specificity for sites I or II and affect SV40 DNA replication activity. *J Virol* **62**, 1598-1605
100. Stahl, H., Droge, P., and Knippers, R. (1986) DNA helicase activity of SV40 large tumor antigen. *EMBO J* **5**, 1939-1944

101. Moreno, S., and Nurse, P. (1990) Substrates for p34cdc2: in vivo veritas? *Cell* **61**, 549-551
102. Gotz, C., Koenig, M. G., Issinger, O. G., and Montenarh, M. (1995) A casein-kinase-2-related protein kinase is tightly associated with the large T antigen of simian virus 40. *Eur J Biochem* **233**, 327-334
103. Hubner, S., Xiao, C. Y., and Jans, D. A. (1997) The protein kinase CK2 site (Ser111/112) enhances recognition of the simian virus 40 large T-antigen nuclear localization sequence by importin. *J Biol Chem* **272**, 17191-17195
104. Jans, D. A., and Jans, P. (1994) Negative charge at the casein kinase II site flanking the nuclear localization signal of the SV40 large T-antigen is mechanistically important for enhanced nuclear import. *Oncogene* **9**, 2961-2968
105. Xiao, C. Y., Jans, P., and Jans, D. A. (1998) Negative charge at the protein kinase CK2 site enhances recognition of the SV40 large T-antigen NLS by importin: effect of conformation. *FEBS Lett* **440**, 297-301
106. Kassem, A., Schopflin, A., Diaz, C., Weyers, W., Stickeler, E., Werner, M., and Zur Hausen, A. (2008) Frequent detection of Merkel cell polyomavirus in human Merkel cell carcinomas and identification of a unique deletion in the VP1 gene. *Cancer Res* **68**, 5009-5013
107. Lemos, B., and Nghiem, P. (2007) Merkel cell carcinoma: more deaths but still no pathway to blame. *J Invest Dermatol* **127**, 2100-2103
108. Agelli, M., and Clegg, L. X. (2003) Epidemiology of primary Merkel cell carcinoma in the United States. *J Am Acad Dermatol* **49**, 832-841
109. Bichakjian, C. K., Lowe, L., Lao, C. D., Sandler, H. M., Bradford, C. R., Johnson, T. M., and Wong, S. L. (2007) Merkel cell carcinoma: critical review with guidelines for multidisciplinary management. *Cancer* **110**, 1-12
110. Schrama, D., Ugurel, S., and Becker, J. C. (2012) Merkel cell carcinoma: recent insights and new treatment options. *Curr Opin Oncol* **24**, 141-149
111. Demetriou, S. K., Ona-Vu, K., Sullivan, E. M., Dong, T. K., Hsu, S. W., and Oh, D. H. (2012) Defective DNA repair and cell cycle arrest in cells expressing Merkel cell polyomavirus T antigen. *Int J Cancer* **131**, 1818-1827
112. Hahn, W. C., Counter, C. M., Lundberg, A. S., Beijersbergen, R. L., Brooks, M. W., and Weinberg, R. A. (1999) Creation of human tumour cells with defined genetic elements. *Nature* **400**, 464-468
113. Harris, K. F., Christensen, J. B., and Imperiale, M. J. (1996) BK virus large T antigen: interactions with the retinoblastoma family of tumor suppressor proteins and effects on cellular growth control. *J Virol* **70**, 2378-2386
114. Shivakumar, C. V., and Das, G. C. (1996) Interaction of human polyomavirus BK with the tumor-suppressor protein p53. *Oncogene* **13**, 323-332
115. Bollag, B., Prins, C., Snyder, E. L., and Frisque, R. J. (2000) Purified JC virus T and T' proteins differentially interact with the retinoblastoma family of tumor suppressor proteins. *Virology* **274**, 165-178
116. Poulin, D. L., Kung, A. L., and DeCaprio, J. A. (2004) p53 targets simian virus 40 large T antigen for acetylation by CBP. *J Virol* **78**, 8245-8253
117. Grasser, F. A., Scheidtmann, K. H., Tuazon, P. T., Traugh, J. A., and Walter, G. (1988) In vitro phosphorylation of SV40 large T antigen. *Virology* **165**, 13-22

118. Prives, C. (1990) The replication functions of SV40 T antigen are regulated by phosphorylation. *Cell* **61**, 735-738
119. Shimazu, T., Komatsu, Y., Nakayama, K. I., Fukazawa, H., Horinouchi, S., and Yoshida, M. (2006) Regulation of SV40 large T-antigen stability by reversible acetylation. *Oncogene* **25**, 7391-7400
120. Ciccio, A., and Elledge, S. J. (2010) The DNA Damage Response: Making It Safe to Play with Knives. *Molecular Cell* **40**, 179-204
121. Yang, J., Yu, Y., Hamrick, H. E., and Duerksen-Hughes, P. J. (2003) ATM, ATR and DNA-PK: initiators of the cellular genotoxic stress responses. *Carcinogenesis* **24**, 1571-1580
122. Brown, E. J., and Baltimore, D. (2003) Essential and dispensable roles of ATR in cell cycle arrest and genome maintenance. *Genes Dev* **17**, 615-628
123. Cimprich, K. A., and Cortez, D. (2008) ATR: an essential regulator of genome integrity. *Nat Rev Mol Cell Biol* **9**, 616-627
124. Cuadrado, M., Martinez-Pastor, B., Murga, M., Toledo, L. I., Gutierrez-Martinez, P., Lopez, E., and Fernandez-Capetillo, O. (2006) ATM regulates ATR chromatin loading in response to DNA double-strand breaks. *J Exp Med* **203**, 297-303
125. Koopman, G., Reutelingsperger, C. P., Kuijten, G. A., Keehnen, R. M., Pals, S. T., and van Oers, M. H. (1994) Annexin V for flow cytometric detection of phosphatidylserine expression on B cells undergoing apoptosis. *Blood* **84**, 1415-1420
126. Salvesen, G. S. (2002) Caspases: opening the boxes and interpreting the arrows. *Cell Death Differ* **9**, 3-5
127. Ghavami, S., Hashemi, M., Ande, S. R., Yeganeh, B., Xiao, W., Eshraghi, M., Bus, C. J., Kadkhoda, K., Wiechec, E., Halayko, A. J., and Los, M. (2009) Apoptosis and cancer: mutations within caspase genes. *J Med Genet* **46**, 497-510
128. Porter, A. G., and Janicke, R. U. (1999) Emerging roles of caspase-3 in apoptosis. *Cell Death Differ* **6**, 99-104
129. Katunuma, N., Matsui, A., Le, Q. T., Utsumi, K., Salvesen, G., and Ohashi, A. (2001) Novel procaspase-3 activating cascade mediated by lysoapoptases and its biological significances in apoptosis. *Adv Enzyme Regul* **41**, 237-250
130. Li, P., Nijhawan, D., and Wang, X. (2004) Mitochondrial activation of apoptosis. *Cell* **116**, S57-59, 52 p following S59
131. Chaitanya, G. V., Steven, A. J., and Babu, P. P. (2010) PARP-1 cleavage fragments: signatures of cell-death proteases in neurodegeneration. *Cell Commun Signal* **8**, 31
132. D'Amours, D., Sallmann, F. R., Dixit, V. M., and Poirier, G. G. (2001) Gain-of-function of poly(ADP-ribose) polymerase-1 upon cleavage by apoptotic proteases: implications for apoptosis. *J Cell Sci* **114**, 3771-3778
133. Kaufmann, S. H., Desnoyers, S., Ottaviano, Y., Davidson, N. E., and Poirier, G. G. (1993) Specific proteolytic cleavage of poly(ADP-ribose) polymerase: an early marker of chemotherapy-induced apoptosis. *Cancer Res* **53**, 3976-3985
134. Tewari, M., Quan, L. T., O'Rourke, K., Desnoyers, S., Zeng, Z., Beidler, D. R., Poirier, G. G., Salvesen, G. S., and Dixit, V. M. (1995) Yama/CPP32 beta, a

- mammalian homolog of CED-3, is a CrmA-inhibitable protease that cleaves the death substrate poly(ADP-ribose) polymerase. *Cell* **81**, 801-809
135. Diaz, J., Wang, X., Tsang, S. H., Jiao, J., and You, J. (2014) Phosphorylation of large T antigen regulates merkel cell polyomavirus replication. *Cancers (In Press)*
 136. Fradet-Turcotte, A., Vincent, C., Joubert, S., Bullock, P. A., and Archambault, J. (2007) Quantitative analysis of the binding of simian virus 40 large T antigen to DNA. *J Virol* **81**, 9162-9174
 137. Barlow, C., Brown, K. D., Deng, C. X., Tagle, D. A., and Wynshaw-Boris, A. (1997) Atm selectively regulates distinct p53-dependent cell-cycle checkpoint and apoptotic pathways. *Nat Genet* **17**, 453-456
 138. Abraham, R. T. (2001) Cell cycle checkpoint signaling through the ATM and ATR kinases. *Genes Dev* **15**, 2177-2196
 139. Zhou, B. B., and Elledge, S. J. (2000) The DNA damage response: putting checkpoints in perspective. *Nature* **408**, 433-439
 140. Tegtmeyer, P., Schwartz, M., Collins, J. K., and Rundell, K. (1975) Regulation of tumor antigen synthesis by simian virus 40 gene A. *J Virol* **16**, 168-178
 141. Reed, S. I., Stark, G. R., and Alwine, J. C. (1976) Autoregulation of simian virus 40 gene A by T antigen. *Proc Natl Acad Sci U S A* **73**, 3083-3087
 142. Khoury, G., and May, E. (1977) Regulation of early and late simian virus 40 transcription: overproduction of early viral RNA in the absence of a functional T-antigen. *J Virol* **23**, 167-176
 143. Alwine, J. C., Reed, S. I., and Stark, G. R. (1977) Characterization of the autoregulation of simian virus 40 gene A. *J Virol* **24**, 22-27
 144. Rio, D., Robbins, A., Myers, R., and Tjian, R. (1980) Regulation of simian virus 40 early transcription in vitro by a purified tumor antigen. *Proc Natl Acad Sci U S A* **77**, 5706-5710
 145. Hansen, U., Tenen, D. G., Livingston, D. M., and Sharp, P. A. (1981) T antigen repression of SV40 early transcription from two promoters. *Cell* **27**, 603-613
 146. Myers, R. M., Rio, D. C., Robbins, A. K., and Tjian, R. (1981) SV40 gene expression is modulated by the cooperative binding of T antigen to DNA. *Cell* **25**, 373-384
 147. Alwine, J. C., and Khoury, G. (1980) Effect of a tsA mutation of simian virus 40 late gene expression: variations between host cell lines. *J Virol* **33**, 920-925
 148. Keller, J. M., and Alwine, J. C. (1984) Activation of the SV40 late promoter: direct effects of T antigen in the absence of viral DNA replication. *Cell* **36**, 381-389
 149. Brady, J., Bolen, J. B., Radonovich, M., Salzman, N., and Khoury, G. (1984) Stimulation of simian virus 40 late gene expression by simian virus 40 tumor antigen. *Proc Natl Acad Sci U S A* **81**, 2040-2044
 150. Farmerie, W. G., and Folk, W. R. (1984) Regulation of polyomavirus transcription by large tumor antigen. *Proc Natl Acad Sci U S A* **81**, 6919-6923
 151. Diaz, J., Wang, X., Tsang, S. H., Jiao, J., and You, J. (2014) Phosphorylation of large T antigen regulates merkel cell polyomavirus replication. *Cancers* **6**, 1464-1486

152. Buck, C. B., Pastrana, D. V., Lowy, D. R., and Schiller, J. T. (2004) Efficient intracellular assembly of papillomaviral vectors. *J Virol* **78**, 751-757
153. Strader, M. B., Tabb, D. L., Hervey, W. J., Pan, C., and Hurst, G. B. (2006) Efficient and specific trypsin digestion of microgram to nanogram quantities of proteins in organic-aqueous solvent systems. *Anal Chem* **78**, 125-134
154. Kelley, L. A., and Sternberg, M. J. (2009) Protein structure prediction on the Web: a case study using the Phyre server. *Nat Protoc* **4**, 363-371
155. Schrodinger, LLC. (2010) The PyMOL Molecular Graphics System, Version 1.3r1.
156. Schreiber, E., Matthias, P., Muller, M. M., and Schaffner, W. (1989) Rapid detection of octamer binding proteins with 'mini-extracts', prepared from a small number of cells. *Nucleic Acids Res* **17**, 6419